# Technical University of Denmark

DTU

# First Clinical Investigations of New Ultrasound Techniques in Three Patient Groups: Patients with Liver Tumors, Arteriovenous Fistulas, and Arteriosclerotic Femoral Arteries

**Hansen, Peter Møller; Jensen, Jørgen Arendt; Bachmann Nielsen, Michael**

[Link back to DTU Orbit](#)

## DTU Library
Technical Information Center of Denmark

**Main supervisor**

**Michael Bachmann Nielsen**, M.D., Ph.D., Dr. Med., Professor

Department Of Radiology

Copenhagen University Hospital, Rigshospitalet, Denmark


**Project supervisor**

**Jørgen Arendt Jensen**, M.Sc., Ph.D., Dr. Techn., Professor

DTU Elektro, Center for Fast Ultrasound Imaging

Technical University of Denmark


**Evaluating Committee**


**Andreas Kjær**, M.D., Ph.D., Dr. Med., Professor

Department of Clinical Physiology, Nuclear Medicine and PET

Copenhagen University Hospital, Rigshospitalet, Denmark


**Hans Nygaard**, M.Sc., Dr. Med., Professor

The Faculty of Health Sciences, University of Aarhus

Department of Cardiothoracic and Vascular Surgery

Aarhus University Hospital, Skejby, Denmark


**Ola Björgell**, M.D., Ph.D., Docent

Department Of Radiology

Skåne University Hospital, Malmö, Sweden

*Front page illustration: Comparison of SASB and conventional ultrasound technique (left), arteriosclerotic stenosis in the SFA illustrated with a MATLAB script and angiography (right), and cross sectional area and longitudinal VFI flow of an arteriovenous fistula (bottom).*

# Contents

# Acknowledgements

# Dansk resumé

I dette PhD projekt er to nyere ultralydteknikker for første gang anvendt til klinisk brug på patienter med maligne levertumorer (studie I), hæmodialysefistler (studie II) og arteriosklerotiske stenoserede femoral arterier (studie III). Den samme kommercielle ultralydskanner blev anvendt i alle tre studier.

Studie I var et sammenlignende studie af B-mode ultralydbilleder optaget med konventionel teknik og den eksperimentielle teknik Synthetic Aperture Sequential Beamforming (SASB). SASB er en datareducerende version af teknikken "syntetisk apertur" som har potentiale til at frembringe ultralydbilleder af meget høj kvalitet med høj framerate. Desværre er syntetisk apertur særdeles resourcekrævende, og bruges derfor kun i eksperimentielle skannere. SASB reducerer datamængden med en faktor 64, og gør det derved muligt, at implementere teknikken på en kommerciel ultralydskanner, samt at foretage trådløs overførsel af data og senere udvikle for eksempel en trådløs ultralydtransducer. Nitten patienter med enten primær levercancer eller levermetastaser fra coloncancer blev ultralydskannet skannet dagen før de skulle have udført leverresektion. Patienterne blev skannet simultant med konventionel teknik og SASB, og optagelsernes billedkvalitet blev efterfølgende evalueret ud fra et klinisk perspektiv af fem radiologer med ultralyderfaring. Evalueringerne viste en beskeden (statistisk insignifikant) fordel til SASB, og studiet viste dermed, at SASB, på trods af den betydelige datareduktion, er egnet til klinisk brug.

I studie II blev 20 patienter med arteriovenøse fistler til hæmodialyse ultralydskannet direkte på den mest overfladiske og tilgængelige del af fistlen. Til dette blev den vinkeluafhængige vektorteknik "Vector Flow Imaging" (VFI) anvendt. VFI kan kvantitativt estimere den retning og hastighed som blodet strømmer i, uanset hvilken vinkel der er mellem ultralydstrålen og blodkarret. Konventionel Dopplerteknik til måling af blodets hastighed fungerer kun ved en vinkel mindre end 60-70° mellem ultralydstråle og blodkar, og er derfor særdeles svær at anvende på de helt overfladiske arteriovenøse fistler. Fistlerne blev skannet vinkelret på karret, hvorved tværsnitsarealet blev beregnet og blodets flow hastighed målt. Den gennemsnitlige flow hastighed blev beregnet og ganget med tværsnitsarealet, hvorved et volumenflow i fistlen blev beregnet. Dette blev sammenholdt med guldstandarden for volumen flow målinger (ultrasound dilution technique), og var 31 – 35 % lavere end guldstandarden, men udviste en væsentligt forbedret standard afvigelse. Studiet demonstrerede således en ny, direkte og

intuitiv måde at måle blodgennemstrømning i hæmodialysefistler på.

Studie III var også et flow studie hvor vektorteknikken VFI igen blev anvendt. Elleve patienter med arteriosklerotiske stenoser i *a. femoralis superficialis* blev ultralydskannet over karret umiddelbart inden de skulle have udført arteriografi af underekstremitetens arterier. De steder i karret hvor der med VFI blev konstateret turbulent/komplekst flow, og derved rejst mistanke om en flow forstyrrende arteriosklerotisk læsion, blev der foretaget optagelser. Optagelserne blev efterfølgende analyseret, og for hver optagelse blev blodets flow hastighed ved læsionen sammenholdt med flow hastigheden i et normalt arteriesegment umiddelbart ved siden af. Hvis hastigheden ved læsionen var højere end i det raske segment, blev det taget som et udtryk for en forsnævring. Ved sammenligning med den efterfølgende arteriografi blev der konstateret en stærk korrelation mellem de beregnede hastighedsforhold og de målte stenosegrader på arteriografien. Det er således muligt at vurdere stenosegraden kvantitativt ud fra VFI ultralydskanningen. Det blev desuden beregnet, at en fordobling af flow hastigheden indikerer en stenosegrad på 50 %, og dermed en behandlingskrævende stenose. Studiet er det første af sin art, hvor en vektorteknik anvendes til at beregne disse hastighedsforhold relateret til arteriosclerotiske stenoser, og de opnåede resultater stemmer overens med tidligere studier udført med konventionel Dopplerteknik. VFI er dog mere intuitiv i sin anvendelse, og kan muligvis bruges til at udføre en hurtigere og mere nøjagtig screening af disse patienter, før de eventuelt tilbydes arteriografi.

De tre studier demonstrerer den første anvendelse af de nye ultralydteknikker på udvalgte patientgrupper, og giver for alle tre studier håb om at teknikkerne indenfor en overskuelig periode kan finde vej til den kliniske hverdag til gavn for både patienter og personale.

# Project summary

In this PhD project two newer ultrasound techniques are for the first time used for clinical scans of patients with malignant liver tumors (Study I), arteriovenous fistulas for hemodialysis (Study II) and arteriosclerotic femoral arteries (Study III). The same commercial ultrasound scanner was used in all three studies.

Study I was a comparative study of B-mode ultrasound images obtained with conventional technique and the experimental technique Synthetic Aperture Sequential Beamforming (SASB). SASB is a data-reducing version of the technique synthetic aperture, which has the potential to produce ultrasound images of very high quality with high frame rate. Synthetic aperture is unfortunately very demanding computationally, and is therefore used only in experimental scanners. SASB reduces the data volume by a factor of 64, thereby making it possible to implement the technology on a commercial ultrasound scanner, to perform wireless data transfer and in the future to develop e.g. a wireless ultrasonic transducer. Nineteen patients with either primary liver cancer or liver metastases from colon cancer were ultrasound scanned the day before planned liver resection. Patients were scanned simultaneously with the conventional technique and SASB, and the image quality was subsequently evaluated from a clinical perspective by five radiologists with ultrasound experience. The evaluations showed a slight (statistically insignificant) advantage to SASB, and the study thereby showed that SASB, in spite of the significant data reduction, is suitable for clinical use.

In Study II, 20 patients with arteriovenous fistulas for hemodialysis were ultrasound scanned directly on the most superficial and accessible part of the fistula. The vector ultrasound technique Vector Flow Imaging (VFI) was used. VFI can quantitatively estimate the direction and velocity of the blood flow in a vessel, independently of the angle of insonation. Conventional Doppler technique is dependent on an angle of insonation < 60-70° when a quantitative estimation of flow is needed. It is therefore challenging to use on the very superficial arteriovenous fistulas. The fistulas were scanned perpendicular to the vessel, the cross-sectional area was calculated and blood flow velocity measured. The average flow velocity was calculated and multiplied by the cross sectional area, thereby calculating volume flow in the fistula. This was compared with the gold standard for volume flow measurements (ultrasound dilution technique), and was 31 – 35 % lower than the gold standard, but showed a

4

significantly improved standard deviation. The study thus demonstrated a new, direct and intuitive way to measure blood flow in arteriovenous fistulas.

Study III was also a flow study using VFI. Eleven patients with arteriosclerotic disease in the superficial femoral artery had an ultrasound scan of the vessel performed just before a planned angiography of the arteries. If turbulent/disturbed flow was identified with VFI, and suspicion of a flow disturbing arteriosclerotic lesion was raised, recordings of the flow were made. The recordings were subsequently analyzed, and for each recording blood flow velocity at the lesion was compared with the flow velocity in a healthy adjacent arterial segment. If the velocity at the lesion was higher than in the healthy segment, it was considered a stenosis. By comparison with the subsequent angiography a strong correlation was found between the calculated velocity ratios and the measured angiographic stenosis degrees. Thus, it was possible to assess stenosis degree quantitatively from the VFI ultrasound scan. Furthermore, it was calculated that a doubling of the flow velocity indicates a stenosis degree of 50 %, and thus a clinically significant stenosis requiring treatment. The study is the first of its kind where a vector ultrasound technique is used to calculate velocity ratios related to arteriosclerotic stenoses, and the obtained results are consistent with previous studies performed with conventional Doppler technique. Use of VFI is more intuitive, and may be used to perform faster and more accurate screening of these patients before they are referred to angiography.

The three studies demonstrate the first application of the new ultrasound techniques in selected groups of patients. For all three studies the results are promising, and hopefully the techniques will find their way into everyday clinical practice for the benefit of both patients and healthcare practitioners.

# List of papers

**Clinical Evaluation of Synthetic Aperture Sequential Beamforming Ultrasound in Patients with Liver Tumors**

Peter Møller Hansen, Martin Hemmsen, Andreas Brandt, Joachim Rasmussen, Theis Lange, Paul Suno Krohn, Lars Lönn, Jørgen Arendt Jensen, and Michael Bachmann Nielsen

*Ultrasound in Med. & Biol., Vol. 40, No. 12, pp. 2805–2810, 2014*

Included in appendix 1

**Volume Flow in Arteriovenous Fistulas using Vector Velocity Ultrasound**

Peter Møller Hansen, Jacob Bjerring Olesen, Michael Johannes Pihl, Theis Lange, Søren Heerwagen, Mads Møller Pedersen, Marianne Rix, Lars Lönn, Jørgen Arendt Jensen, and Michael Bachmann Nielsen

*Ultrasound in Med. & Biol., Vol. 40, No. 11, pp. 2707–2714, 2014*

Included in appendix 2

**Arteriosclerotic Lesions in the Superficial Femoral Artery (SFA) Characterized with Velocity Ratios using Vector Velocity Ultrasound**

Peter Møller Hansen, Kristoffer Lindskov Hansen, Mads Møller Pedersen, Lars Lönn, Jørgen Arendt Jensen, and Michael Bachmann Nielsen

*Manuscript*

Included in appendix 3

# Abbreviations

B-mode:      Brightness mode

CFU:        Center for Fast Ultrasound Imaging

IQap:        Image Quality assessment program

SASB:       Synthetic aperture sequential beamforming

SFA:        Superficial femoral artery

TO:         Transverse Oscillation

UDT:       Ultrasound dilution technique

VFI:        Vector Flow Imaging

# Introduction and background

This thesis is part of the continued collaboration between the Department of Radiology at Copenhagen University Hospital, Rigshospitalet and the Center for Fast Ultrasound Imaging (CFU) at the Technical University of Denmark. At CFU ultrasound techniques for both visualization of blood flow and B-mode imaging are developed, and at the Department of Radiology, the techniques are tested in a clinical setting. One of the three studies in this thesis is based on a synthetic aperture technique for B-mode imaging, and the remaining two studies are based on the vector ultrasound technique transverse oscillation (TO) used for blood flow visualization and estimation. Both experimental techniques are developed at CFU. Furthermore TO was implemented in a commercial ultrasound scanner in 2010 and FDA-approved in 2012, facilitating clinical studies on patients.

All scans in the three studies were performed on patients admitted to Rigshospitalet.

This introduction provides a brief overview of the different experimental and reference techniques used in the studies, as well as the patients subjected to the techniques.

# Ultrasound image formation

**Conventional technique**

A conventional ultrasound image is generated by a number of adjacent ultrasound beams emitted and received sequentially by a group of elements in the transducer. Each time an ultrasound beam is emitted and the echoes are received, the active group of elements is shifted a little to the side, and a new beam is emitted and received. Each beam is converted to an image line, and the process continues until the entire array has been swept through, and a complete image of the region of interest is formed. The frame rate of the imaging is therefore limited by the speed of sound in tissue, the scanning depth, and the number of image lines (1). Visualization of deep structures and organs and generation of high resolution ultrasound images, which require a high number of image lines, are thus performed at the expense of frame rate. Even though focus is dynamically adjusted during receive, there is typically only one focus point during emission/transmit, causing the final image to be optimally focused in one depth only. This can be alleviated using multiple transmit foci, but the frame rate is then reduced by the number of foci. These conditions limit the possibilities of performing high resolution dynamic examinations of e.g. the beating heart, a joint in motion, or internal organs moving due to breathing.

**Synthetic aperture ultrasound**

One way to obtain high resolution, high frame rate, and improved penetration is to apply a synthetic aperture technique. Synthetic aperture is inspired by radar technology (2), and the basic idea is to synthesize a large aperture, by stepwise movement of a smaller active aperture through the complete array. For each step a low resolution image of the entire desired region is generated from a single unfocused ultrasound wave, and these low resolution images are summed to produce a high resolution image with focus throughout the image (3,4). Several different implementations of synthetic aperture exist. The most simple version uses one array element at the time in both transmit and receive (5), similar to the typical radar setup, where a single radar antenna used for both transmit and receive is moved (i.e. on an airplane or satellite) to cover a large area. See figure 1.

Figure 1: A single radar antenna on an airplane covers a large ground area by movement of the antenna.
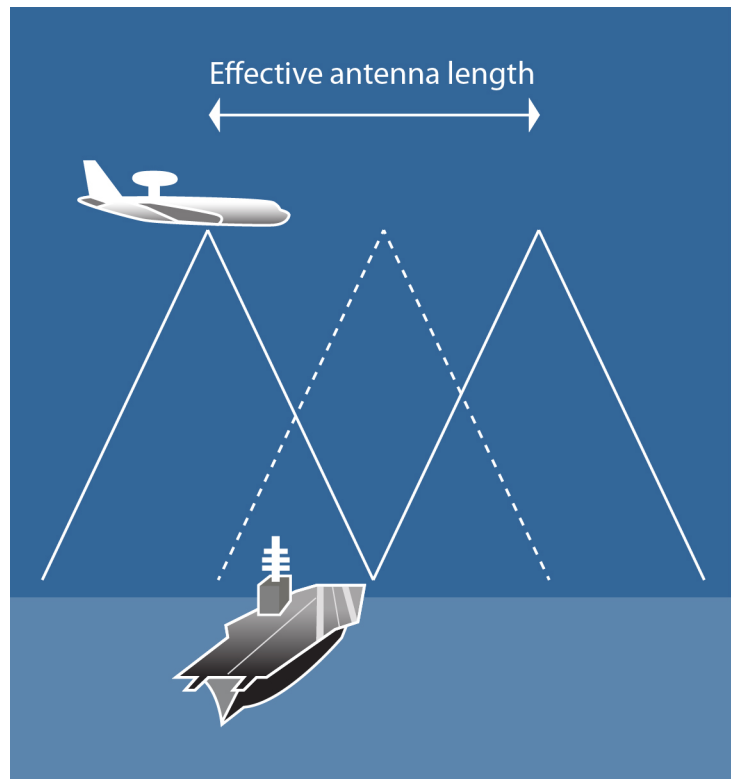


The most demanding versions of synthetic aperture use one or a small group of elements for transmitting and all of the elements for receiving (full synthetic aperture) (3,6). To implement full synthetic aperture, the scanner must have one channel for each element, and be able to control all channels individually. Synthetic aperture has previously been tested in-vivo with convincing results using an experimental ultrasound scanner (7). The technique is also investigated for 3-D scans (8,9) The disadvantage of synthetic aperture is high system requirements, due to the high number of low resolution images the scanner has to produce and process, and the high number of channels that must be available. See figure 2.
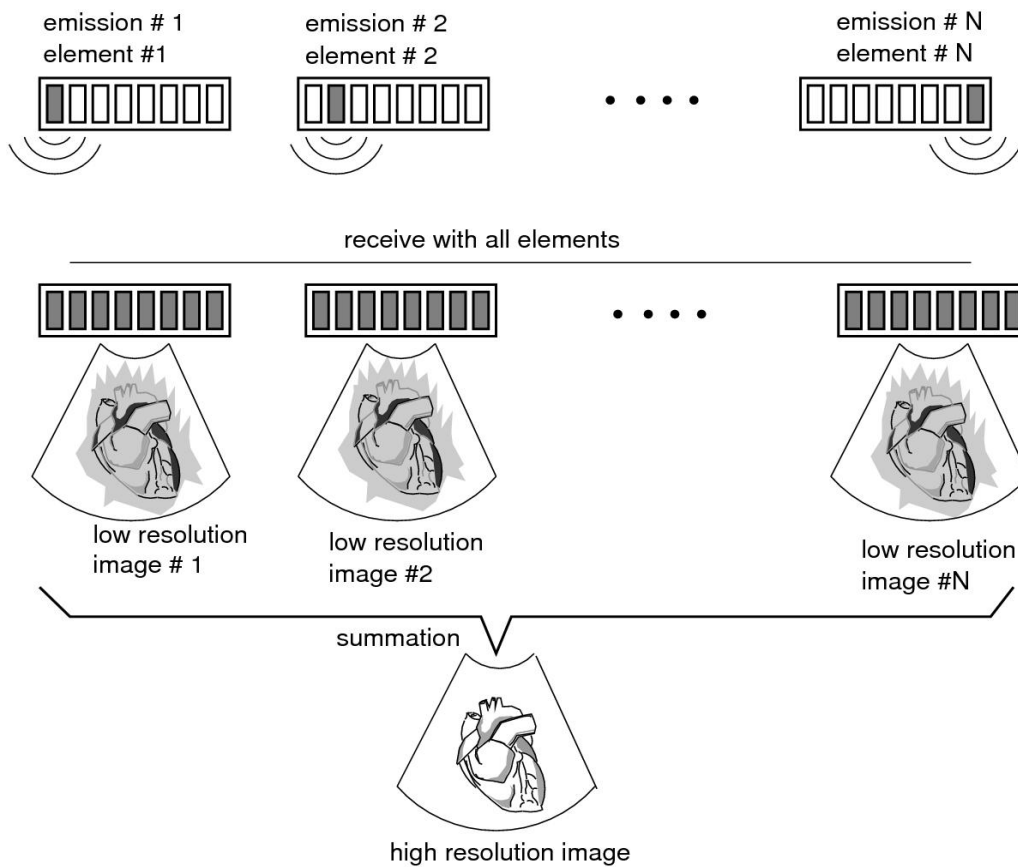
Figure 2: Schematic illustration of full synthetic aperture. One transducer element at the time emits a spherical ultrasound wave and all elements receive, generating a low resolution image for each emission. All low resolution images are finally summed to produce the high resolution image. In medical ultrasound it is necessary to emit with several transducer elements at the same time to increase the emitted energy and obtain sufficient image quality. The image is used by permission (4).

**Synthetic aperture sequential beamforming ultrasound**

To decrease the system requirements and implement synthetic aperture on a more modest system, i.e. a conventional ultrasound scanner, the concept of synthetic aperture sequential beamforming (SASB) was proposed (10). Using synthetic aperture as multi element synthetic aperture, where a group of elements transmits and receives (11), reduces the number of channels needed in the system. Further combining it with a dual stage procedure for beamforming, using two separate beamformers, leads to a substantial data reduction. In the current setup, the amount of data is reduced by a factor of 64. See figure 3. SASB has previously been evaluated *in-vivo* on healthy volunteers using a set-up consisting of

a conventional scanner connected to a PC, and in spite of the data reduction, the image quality of SASB was rated better than conventional ultrasound (12)
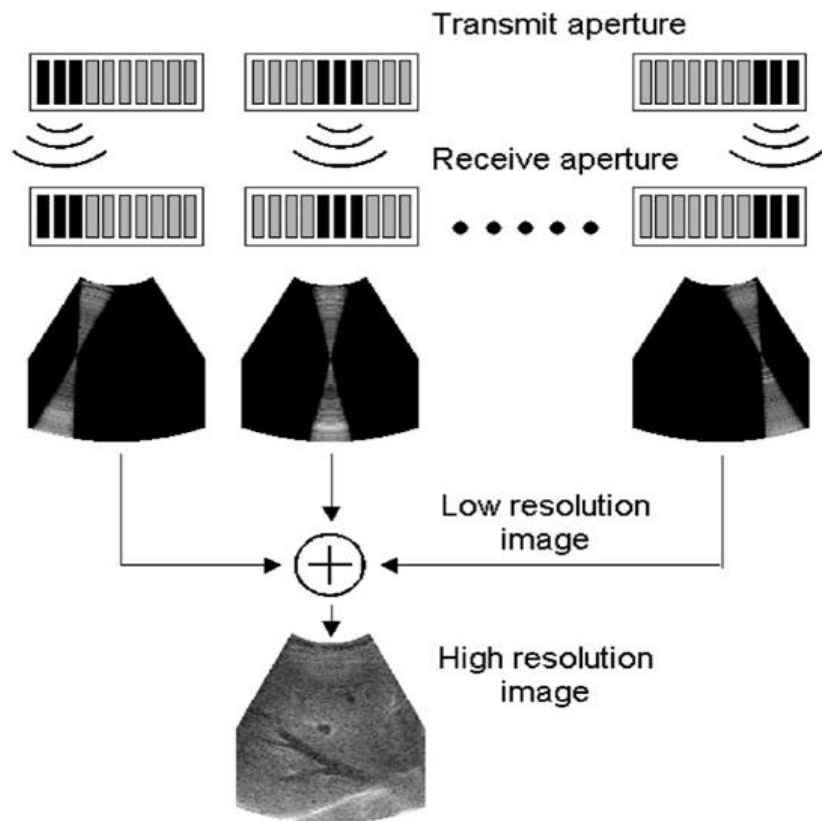


Figure 3: Schematic illustration of ultrasound imaging using SASB. The same group of elements is used for transmit and receive for each emission, and a number of fixed-focused beams are emitted and received for generating the basic data. Each beam is seen as a virtual ultrasound source emitting from the beam focal point. All the received beams are then combined in a second stage beamformer to yield a dynamically focused image in both transmit and receive from the second stage focusing. The image is used by permission (12)

# Clinical evaluation of a new ultrasound technique

**From product development to clinical evaluation**

Prior to the actual clinical evaluation, a longer development phase was undergone. To reach the point where the experimental technique (SASB) was ready for the clinical evaluation (Study I), we went through the following steps as set up by Hemmsen (13):

- **Demonstration of a prototype:** Cooperation between the developer and operator where all parameters are optimized to achieve the ultimate experimental set-up, leading to demonstration of a few *in-vivo* recordings.
- **Preclinical trials:** During the preclinical trials the clinical protocol is developed via scanning of a larger number of healthy volunteers and evaluation of the recordings. Furthermore the number of patients needed for the clinical trial is decided. The scanning set-up is finalized, allowing the operator to scan and record data without any influence from the developer. The evaluation process is also finalized and performed by assessors independent of both operator and developer (12).
- **Clinical trials:** The final step is where the experimental technique is tested on patients in a clinical setting. The developer is not involved in any part of the process, and the evaluation is performed independently of the operator. (See appendix 1)

**Scan setup**

To perform a structured and fair comparison of the experimental and reference technique, it is essential to keep all factors not related to the actual image generating technique identical, i.e. use the same transducer, scanner, region of interest, recording time, etc, and the reference technique shall of course be adjusted to best possible performance. Furthermore it is important to obtain a sufficient amount of recordings under realistic operating conditions, within a reasonable period of time. When ultrasound scanning in a clinical environment, i.e. at a hospital, a conventional ultrasound scanner is desirable. Using a robust medical device allows for easy transportation of the equipment with less risk of

malfunction. All scans in study I were performed using the same setup consisting of a conventional ultrasound scanner connected to a PC via a research interface (14–16). This setup makes it possible to adjust the scan sequences as required to obtain the needed recordings, and is described more detailed in appendix 1.

**Choosing clinical region of interest**

For both the demonstration of the prototype, the preclinical trials, and the clinical trial the liver was chosen as the primary region of interest. The organ is large and it is therefore possible to produce ultrasound images where all of the image contains relevant motive, including the most superficial and deepest parts of the image. The liver contains large blood vessels, providing areas with pronounced contrast, and a large surface, especially against the adjacent right kidney providing a significant organ interface/boundary. Furthermore the liver has a very distinct and recognizable speckle pattern. See figure 4. The above stated of course also applies in the pathological cases from the clinical trial, and with a significant number of liver cancers/metastases each year (17), the necessary number of patients are obtained within reasonable time.

**Image evaluation setup**

Evaluation of the visual quality of a medical ultrasound image is challenging. Objective quality assessment techniques are based on mathematical algorithms, and provide a swift and quantitative evaluation of the image quality. Unfortunately, the objective visual quality may not be equal to the clinical visual quality, since the clinical/diagnostic quality of an ultrasound image is multifaceted beyond what the present objective quality assessment algorithms are capable of handling. Therefore the subjective quality assessment, where a person (medical expert) evaluates the image based on his own perception, is preferred when the clinical/diagnostic image quality is evaluated, even though it may be impractical and time consuming (18)**.** Since the scans in study I were performed on patients (opposed to ultrasound phantoms), radiologists with ultrasound experience were selected to perform the subjective quality assessments.

The recorded ultrasound sequences in study I were evaluated using the in-house coded "Image Quality Assessment Program" (IQap) (14). Using this program evaluations were performed as double-blinded,

side-by-side comparisons of matching real time sequence pairs in random order. Each sequence pair consisted of the interleaved frames recorded with SASB and conventional technique. This way the radiologists evaluated the two techniques, by directly comparing two ultrasound sequences, displaying the same anatomical location. The actual evaluation was performed on a visual analog scale underneath the displayed sequence. See figure 4.
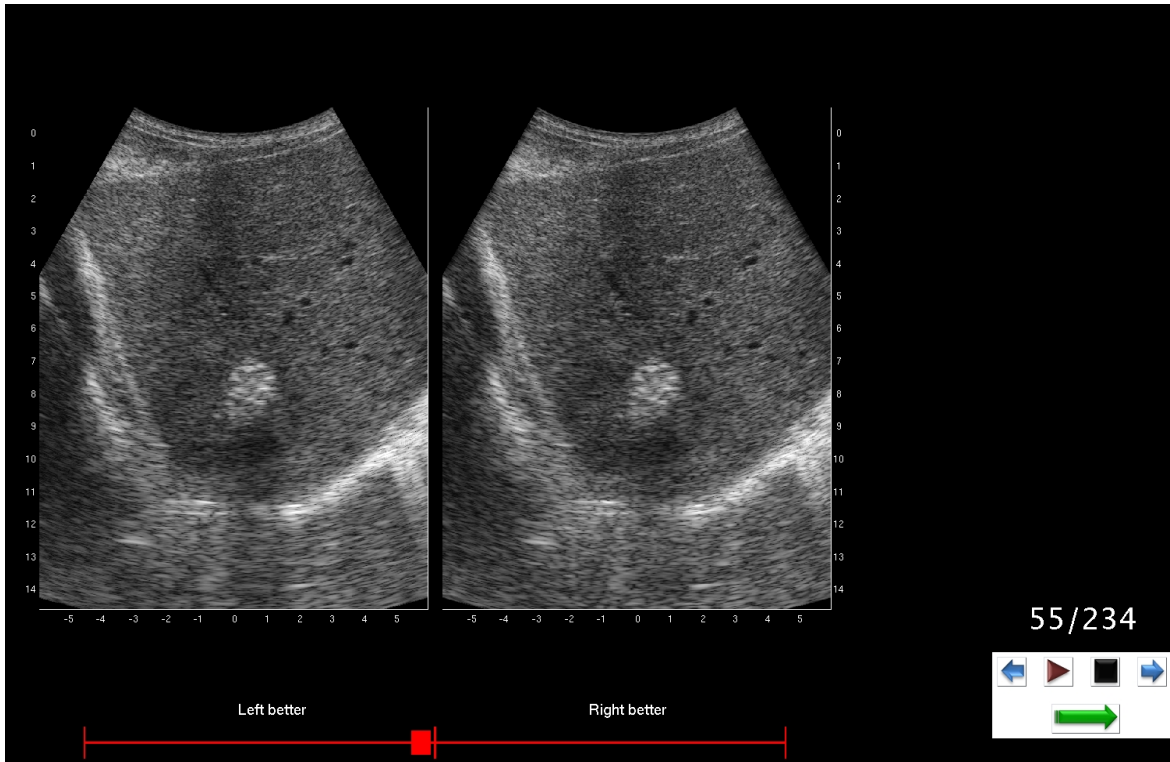


Figure 4: Image from IQap showing a colorectal liver metastasis. The visual analog scale is seen, and in the lower right corner the controls for navigating the sequences are seen.

# Flow estimation

**Conventional ultrasound flow estimation**

Measurements of blood flow direction and velocity are widely used clinically to diagnose and assess severity of hemodynamic (and other) diseases. Examples include arterial stenoses, valve diseases, restrictive liver conditions, and pulmonary hypertension (19–23).

The clinical choice for real time estimation of blood flow is Doppler ultrasound. The technique is easily accessible, provides instantaneous results, the ultrasound scanner is highly mobile and relatively inexpensive.

Doppler ultrasound estimates the blood flow only in the direction of the emitted ultrasound beam, i.e. in the axial direction (1), but in most, if not all cases blood is flowing with an angle other than zero to the ultrasound beam direction. The technique is therefore not able to provide a correct velocity estimate *per se.* As long as a qualitative visualization of blood flow is sufficient, color Doppler/color flow mapping provides a swift overview, see figure 5.



Figure 5: Color Doppler of the common carotid artery illustrating flow. The blue color indicates a flow direction away from the transducer
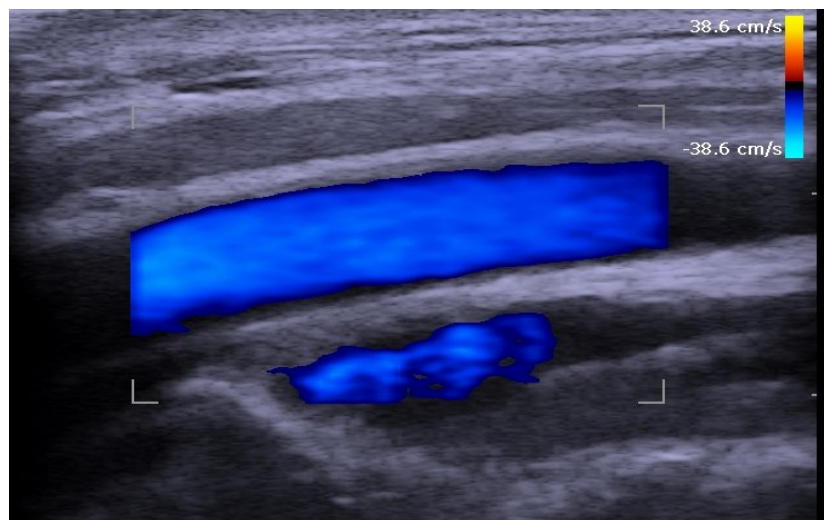
When a quantitative estimation of blood flow velocity is needed, spectral Doppler allows the operator to provide an educated guess of flow direction and perform angle correction of the axial velocity to calculate the true velocity. The velocity is measured within the range gate, which is manually positioned by the operator (Figure 6), and it is necessary to assume that blood flow in the vessel is laminar at all times.

Figure 6: Spectral Doppler measurement of flow in the common carotid artery. Flow velocity is illustrated with the spectrogram. The ultrasound beam is electronically steered to obtain an acute angle of insonation less than 60º. Flow velocity is only measured within the range gate positioned in the middle of the vessel.
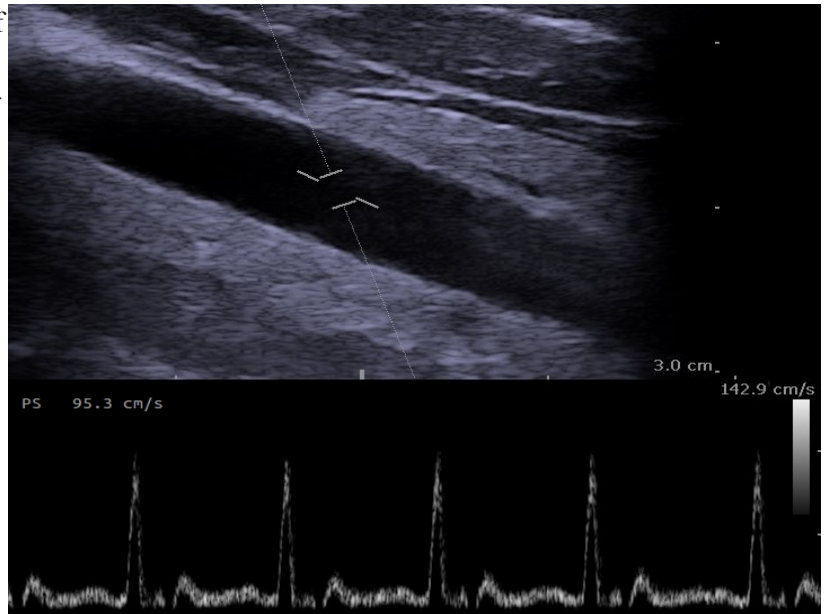
The relationship between axial velocity $v_z$, true velocity $v$, and angle of insonation $\theta$ is given by

$$v = v_z / cos\ \theta. \tag{1}$$

From (1) it is seen that a velocity estimate can not be calculated at an angle of 90º because $cos(90) = 0$. Due to the nature of the cosine function it is required to obtain an angle $\leq 60º$, since a small angle measurement error at angles $> 60º$ will lead to a disproportionate larger velocity estimation error. It is important to emphasize that even under ideal circumstances, the spectral Doppler technique only provides flow velocity within the very restricted area of the range gate, and the velocity estimate is completely dependent on the operators ability to guess the flow direction and perform the angle correction accordingly.

**Vector flow ultrasound**

The ambition to overcome the angle (and operator) dependency of conventional Doppler has led to development of several different ultrasound techniques able to provide the 2-D vector velocity. Examples are speckle tracking (19,20), two crossed ultrasound beams (26), synthetic aperture flow imaging (3,27), and plane wave vector Doppler (28).

One promising vector velocity technique is transverse oscillation suggested by Jensen and Munk (29,30). Transverse oscillation provides simultaneously the axial and transverse velocity components of the blood flow. A conventional ultrasound pulse for flow estimation is transmitted, and the axial velocity component is estimated as in conventional Doppler. An estimator for the transverse velocity

17

component is generated by manipulating the apodization function during receive beamforming, and both velocity components is thus estimated from the same ultrasound emission. By combining the two velocity components the 2-D vector velocity is obtained.

**Clinical use of transverse oscillation**

Transverse oscillation was in 2010 implemented in a commercial ultrasound scanner as "Vector Flow Imaging" (VFI). VFI provides 2-D images of the blood flow where each colored pixel contains quantitative information about direction and velocity. To improve visualization of the flow, the scanner can superimpose arrows in real-time on the color-coded pixels. The arrows indicate flow direction and the length of the arrows indicate velocity magnitude. It is therefore possible to immediately and intuitively assess the flow conditions at any given point of the vessel (Fig. 7). VFI is so far only operational with linear transducers, and the penetration is thus limited to approximately 5 cm.

In 2012 the technique was FDA-approved for clinical scanning. The approval does not include the quantitative estimation of flow velocity, since a sufficiently large clinical study of flow velocities has not yet been conducted. From previous investigations on flow velocities conducted on a flow phantom and in clinical studies (31,32) a negative bias of approximately - 10 % is indicated. This is caused by a bias in the estimation scheme, and an optimized scheme is already developed (33), but unfortunately not yet implemented in the scanner.



Figure 7: Bidirectional flow in the common carotid artery (lower vessel) and the jugular vein (upper vessel) at an angle of 90º. The arrows indicate flow direction and velocity magnitude. Notice the longer arrows in the center of each vessel indicating laminar flow.
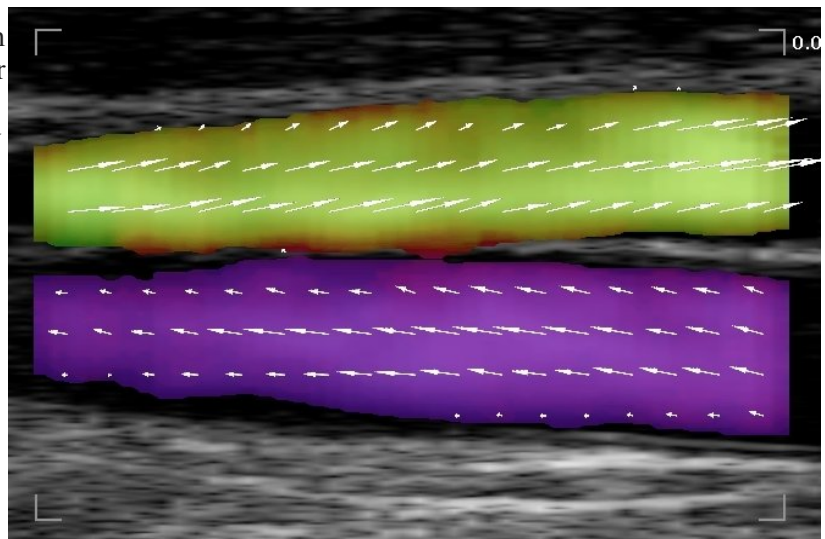
To obtain quantitative measurements of flow velocity with VFI, off-line processing is necessary. The VFI sequences are by default saved as AVI files, and subsequently decoded (Fig. 8), yielding flow velocity and flow direction for each colored pixel in every frame, using in-house coded MATLAB scripts (Mathworks, Natick, MA, USA).
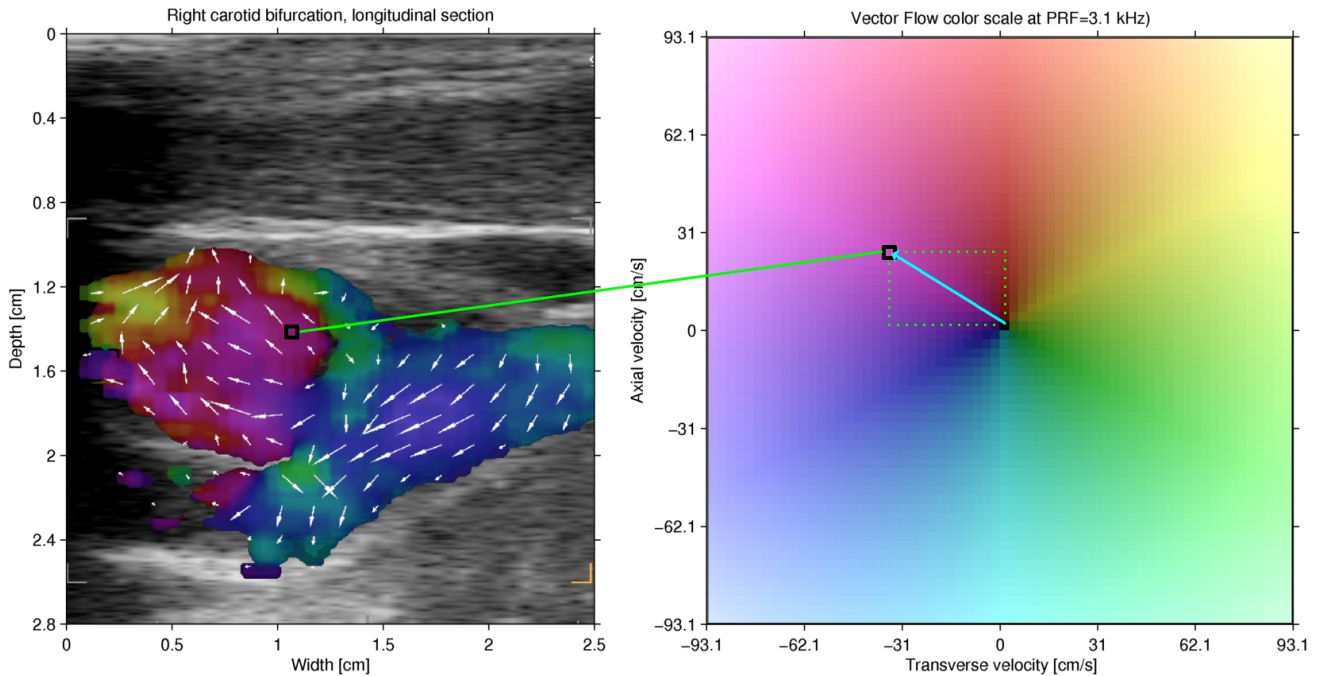


Figure 8: Vector flow image from the carotid bifurcation and the color map used for decoding the vector data. Pythagoras' theorem was used to calculate the true velocity $v$ from the axial velocity $v_z$ and the transversal velocity $v_x$. using $v = \sqrt{(v_z^2 + v_x^2)}$. The flow direction $\theta$ is given by $\theta = arctan(v_z/v_x)$. The image is used by permission (34).

**Clinical possibilities using Vector Flow Imaging**

Due to the limited penetration of VFI, the clinical possibilities are restricted to superficial blood vessels. For the two flow studies in this thesis surgically created arteriovenous fistulas for hemodialysis and arteriosclerotic superficial femoral arteries were chosen for VFI measurements. For both patient groups the intuitive, swift, and quantitative flow estimation provided by VFI combined with the morphological information obtained with B-mode ultrasound could prove to be a valuable diagnostic tool. In the case of the arteriovenous fistulas the clinically interesting parameter is the volumetric flow rate, since an efficient hemodialysis session is completely dependent on a sufficient volume flow in the fistula. The majority of patients will experience some kind of fistula dysfunction during the first 18 months after its creation (35). Regular monitoring of volume flow, as an indication of fistula function is

therefore recommended (36–38). The routine monitoring of fistula function is performed with the ultrasound dilution technique (UDT) (39), which is considered the gold standard (40). In the case of the arteriosclerotic superficial femoral arteries the clinically interesting parameter is the flow velocity change (velocity ratio) related to each flow disturbing lesion in the vessel as an indication of stenosis degree (41–45). The gold standard for diagnosing and grading arterial stenoses is angiography, which provides a measurement of arterial diameter reduction (44).

# Reference techniques used in the flow studies

**Ultrasound dilution technique (UDT)**

UDT is based on the indicator dilution method, where a known quantity of indicator substance is injected into the bloodstream. The indicator concentration is subsequently measured, and the change in indicator concentration downstream is plotted as a function of time, providing a volumetric flow rate. Saline is used as the indicator, and dilutes the protein concentration of the blood, thereby reducing the ultrasound velocity in the blood proportionally. The ultrasound velocity is continuously monitored by a computer with two matched sensors attached to the dialysis blood lines, which must be reversed from normal position to create recirculation between the dialysis needles (46,47). The disadvantages of UDT are the need for the dialysis to be up and running and the exchange of dialysis blood lines before an estimation of flow is obtainable. This process prolongs the dialysis and is uncomfortable for both patient and dialysis nurse.

**Angiography**

The gold standard for diagnosing and evaluating lower extremity arteriosclerosis is digital subtraction angiography. For the remaining part of the thesis, digital subtraction angiography is referred to as angiography. Besides a complete overview of the arteries for diagnostic purposes, angiography allows simultaneous interventional therapy and immediate assessment of the therapy. However, angiography is invasive, associated with risks of both local and systemic complications, and exposes both patients and staff to ionizing radiation (48). The stenosis degree was in each case calculated using the smallest diameter in the stenosis and the diameter in the adjacent disease free segment, and a stenosis degree of 30 % means that the diameter of the vessel is reduced 30 % compared to the normal diameter.

# Study aims

This thesis contains one study regarding B-mode imaging quality and two studies regarding blood flow estimation. An overview of the three studies are provided in table 1.

The following aims and hypotheses are addressed.

**Study I**

*Aim:* To perform a clinical evaluation of image sequences obtained with synthetic aperture sequential beamforming ultrasound from patients with cancer in the liver.

*Hypothesis:* Synthetic aperture sequential beamforming ultrasound and conventional ultrasound imaging generates clinical ultrasound sequences of equal quality.

**Study II**

*Aim:* To investigate the accuracy and variability of Vector Flow Imaging, used for volume flow measurements on arteriovenous fistulas for hemodialysis.

*Hypotheses:* Vector Flow Imaging and ultrasound dilution technique provide equal estimates of volume flow in arteriovenous fistulas, and the standard deviation of the estimates using Vector Flow Imaging is improved compared with ultrasound dilution technique.

**Study III**

*Aim:* To investigate Vector Flow Imaging as a technique for quantitative assessment of peripheral arterial disease.

*Hypothesis:* Velocity ratios derived from Vector Flow Imaging can be used to distinguish significant stenoses (> 50 % diameter reduction) from non-significant stenoses when compared to angiography.

| Study number | I | II | III |
|---|---|---|---|
| Patients | 19 patients with confirmed liver tumors | 20 patients with arteriovenous fistulas for hemodialysis | 11 patients with arteriosclerotic superficial femoral arteries |
| Time for ultrasound scanning | The day before planned liver surgery | Immediately prior to hemodialysis session | Immediately prior to angiography |
| To evaluate | B-mode image quality | Volume flow | Velocity ratios |
| Experimental method | SASB | Vector Flow Imaging | Vector Flow Imaging |
| Reference method | Conventional ultrasound | Ultrasound dilution technique | Angiography |

Table 1: Overview of main contents of the three studies

The same commercial ultrasound scanner (UltraView 800, BK Medical, Herlev, Denmark) was used for all three studies. In study I the scanner was connected to a PC, and the scan sequence was adjusted to alternate between SASB and conventional ultrasound to obtain interleaved real time sequences. In study II and III the scanner was used with factory default settings to record vector flow sequences. These studies are the first to present results from these patient groups using the respective experimental techniques.

# Materials, methods, and results

## Study I

**Clinical Evaluation of Synthetic Aperture Sequential Beamforming Ultrasound in Patients with Liver Tumors**

Published Ultrasound in Medicine and Biology – for details please see appendix 1

**Aim**

The aim of the study was to perform a clinical evaluation of image sequences obtained with SASB from patients with cancer in the liver. The sequences were compared to conventional ultrasound in a side-by-side comparison.
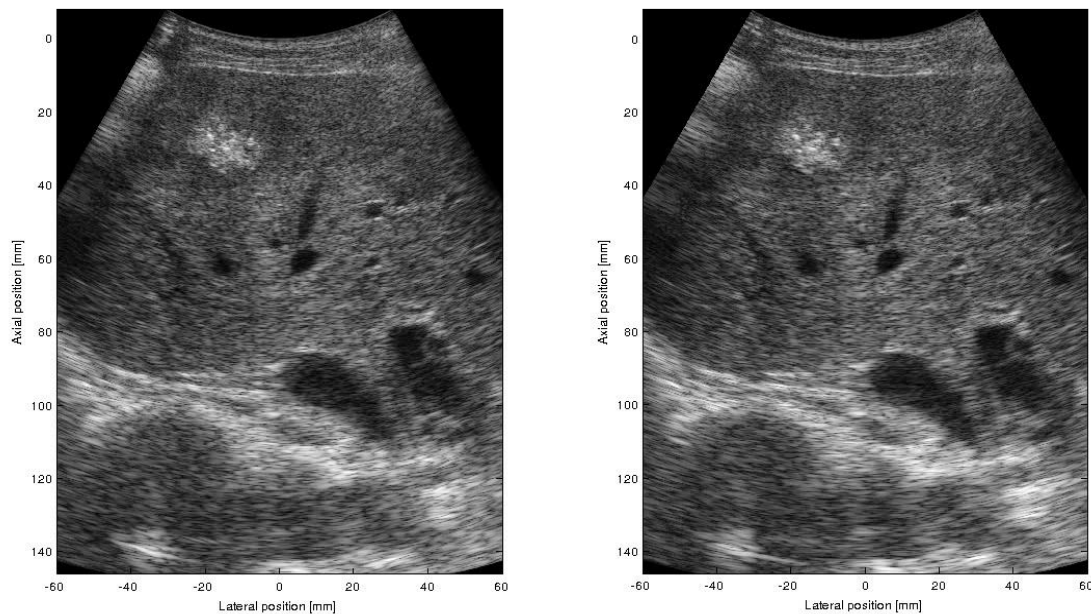


Figure 9: Recording of liver tissue with a tumor. The images are the interleaved recordings with SASB on the left and conventional ultrasound on the right.

**Materials and methods**

Nineteen patients with confirmed malignant liver tumors were ultrasound scanned the day before surgery, using a setup consisting of the scanner (UltraView 800, BK Medical, Herlev, Denmark) equipped with a research interface and connected to a PC. This setup allows images generated with SASB and conventional ultrasound to be recorded interleaved, i.e. one frame generated with SASB follows one frame generated with conventional ultrasound, and ideal real-time sequences for comparison are generated. See Fig. 9. A total of 117 recordings were performed (56 contained the tumor(s) and 61 contained healthy liver tissue).

The sequences were subsequently evaluated from a clinical point of view by five radiologists, using the image quality assessment program IQap. IQap presents the recordings as real time sequences in random order and the radiologist evaluates the image quality with a visual analog scale underneath the displayed sequence. See Fig. 10. All sequences were shown twice with different left-right positioning to avoid bias related to monitor side totaling in 1170 evaluations.



Figure 10: Screen shot from IQap showing a colorectal metastasis. The visual analog scale used for rating the image quality is seen in the bottom, and the control panel for navigating the sequences and the sequence counter is seen in the lower right corner.

**Results**

The visual analog scale ranged from -50 to 50, where positive values favored SASB. The average image evaluation was slightly in favor of SASB with a value of 1.44 (CI: -0.93 to 3.81)(see Fig. 11), but the result was not significant (p = 0.18). 48 % of the evaluations were in favor of SASB, 33 % in favor of conventional ultrasound, and 19 % were rated equal. Evaluations of radiologist four are not included in the analysis due to unconventional use of the scale (when including radiologist number four, the average evaluation score was 1.17 (CI: -0.73 to 3.06), and the conclusion remains the same).
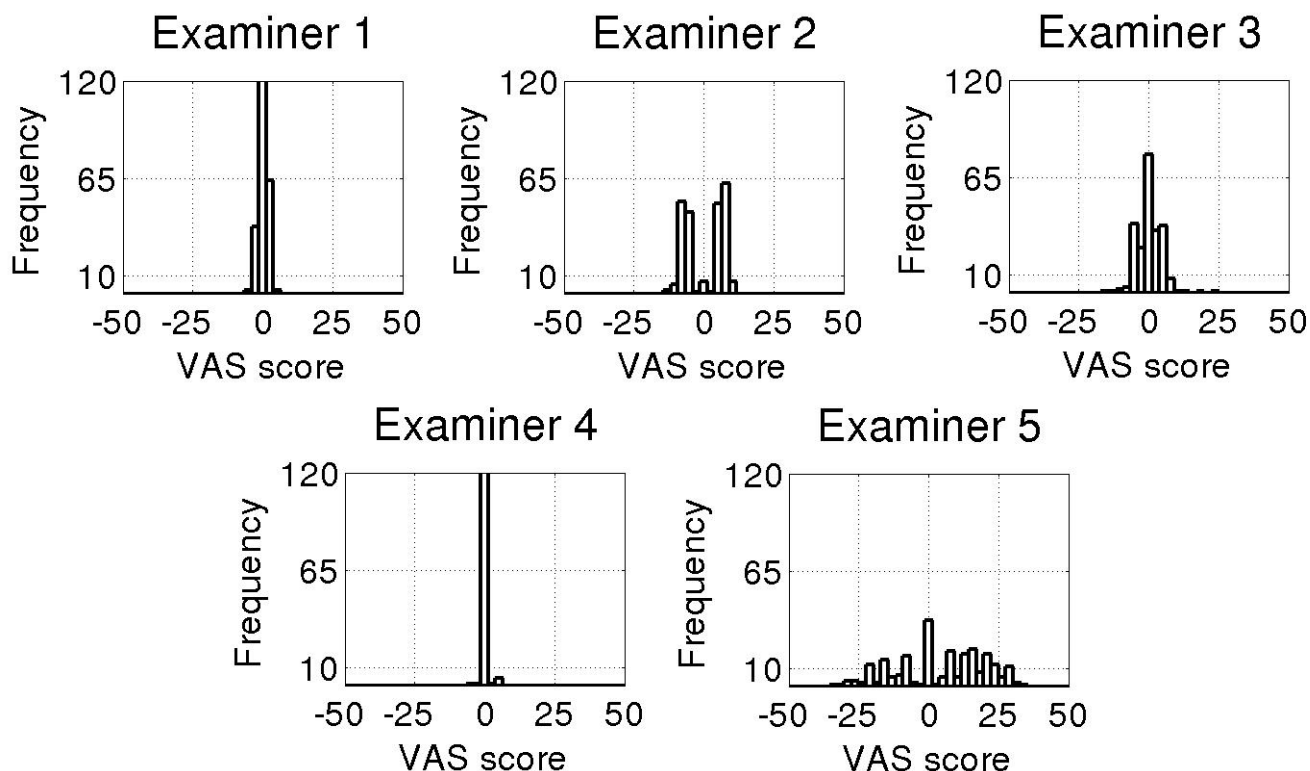


Figure 11: Distribution of pooled answers from each radiologists evaluation of image quality.

**Conclusion**

SASB ultrasound has successfully been tested and evaluated on cancer patients in a true clinical setting. In spite of a data reduction of a factor 64, SASB and conventional ultrasound generates images of at least equal quality.

# Study II

**Volume Flow in Arteriovenous Fistulas using Vector Velocity Ultrasound**

Published Ultrasound in Medicine and Biology – for details please see appendix 2

## Aim

The aim of the study was to investigate the accuracy and variability of Vector Flow Imaging, used for volume flow measurements on arteriovenous fistulas for hemodialysis. The volume flow measurements were compared to volume flow estimations using the gold standard ultrasound dilution technique (see Fig.12).



Figure 12: Flow estimation using the Transonic (ultrasound dilution technique) on a patient in hemodialysis. Notice the red and blue sensors attached to the hemodialysis blood lines, which have been reversed for the flow estimation.

## Materials and methods

Twenty patients with functioning arteriovenous fistulas were scanned with a commercial ultrasound scanner (UltraView 800, BK Medical, Herlev, Denmark) using Vector Flow Imaging directly on the most superficial part of their fistulas. All scans were performed just prior to a hemodialysis session and accompanying UDT volume flow estimation. On each fistula three recordings of vector flow in the longitudinal plane were performed, and the coherent cross sectional diameters of the fistula were measured from transversal B-mode images obtained in the same scan session (see Fig. 13). By multiplying the average flow velocities and the cross sectional areas volume flow estimations were calculated. The average flow velocities were calculated off-line using in-house made MATLAB scripts. Two different approaches were suggested. The first approach (VFImax) estimates the average velocity

by detecting the peak velocity, and then divides this by two. Taking half the peak velocity yields the average velocity assuming the flow profile is parabolic and circular symmetric. The second approach (VFIavg) calculates the mean velocity from all velocities detected across the flow profile. The volume flow estimations from both approaches were compared to three sequential UDT measurements performed during the subsequent dialysis.
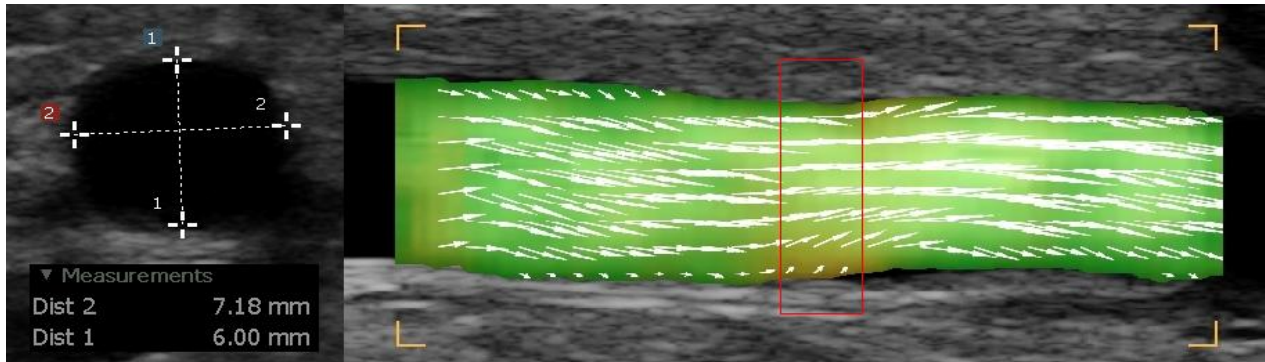


Figure 13: Transversal measurement of cross sectional diameters for calculation of area and longitudinal vector flow recording of a fistula with approximately laminar flow. The red square indicates where the diameters and velocities were measured. Please notice the angle of insonation.

**Results**

Flow results are illustrated in figure 14. Volume flow estimated with vector ultrasound are in most cases lower than the UDT measurements. Patient seven's fistula was difficult to scan due to the anatomical conditions, and it was the only fistula where it was not possible to locate an area with approximately laminar flow. Patient seven is therefore treated as an outlier, and left out of the analysis. The mean values of VFImax and VFIavg are 304 mL/min (CI: 235; 374) and 437 mL/min (CI: 366; 509) lower than UDT, respectively. This corresponds to 31 % and 35 % below the UDT estimations, and the difference is significant ($p < 0.001$ for both VFImax and VFIavg). The observed standard deviations for UDT, VFImax, and VFIavg are 132.9 mL/min, 74.6 mL/min, and 62.3 mL/min, respectively. This corresponds to 9.4 %, 7.4 %, and 6.9 %, respectively.
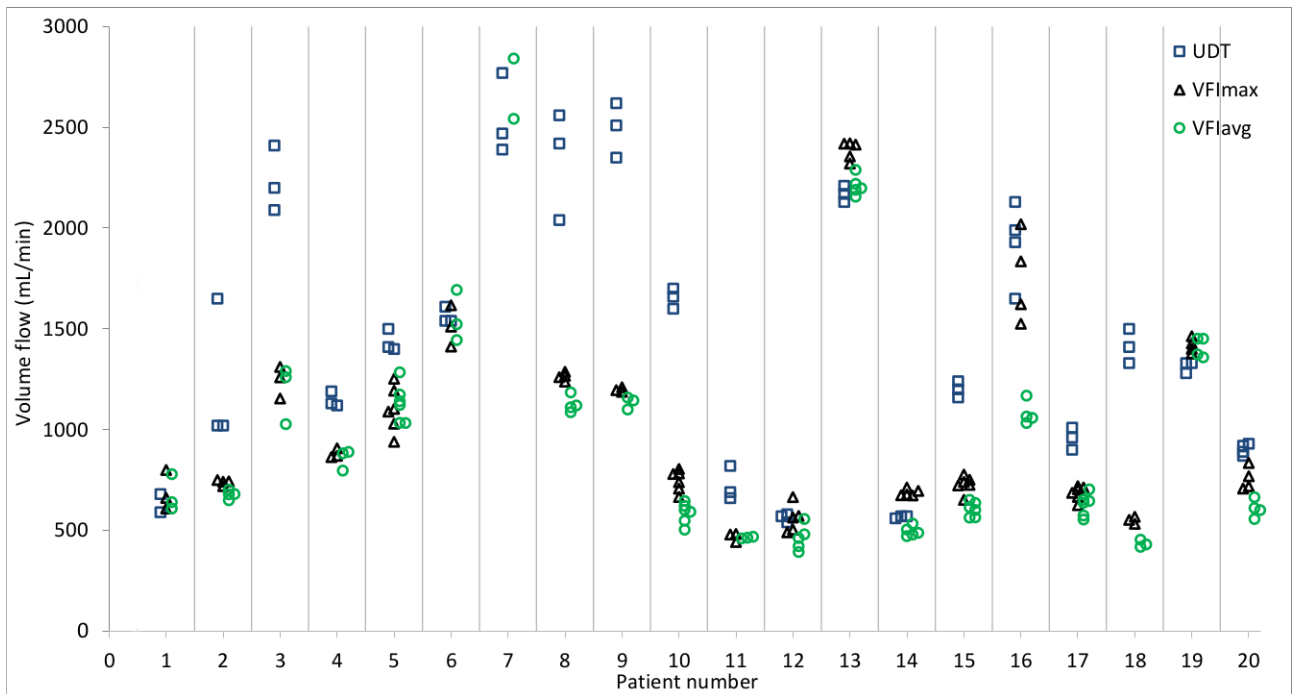
Figure 14: Flow results for all patients. The y-axis have been limited at 3000 mL/min, leaving out the upper VFIavg measurements and all of the VFImax measurements for patient seven. Each symbol indicates one measurement with the given technique.

**Conclusion**

The flow estimations obtained with Vector Flow Imaging were compared to UDT and were on average 31 % and 35 % lower, depending on the approach used, but the standard deviation of Vector Flow Imaging was significantly better than UDT, leading to more stable estimations of volume flow.

# Study III

**Arteriosclerotic Lesions in the Superficial Femoral Artery (SFA) Characterized with Velocity Ratios using Vector Velocity Ultrasound**

Manuscript – for details please see appendix 3

**Aim**

The aim of the study was to investigate Vector Flow Imaging as a technique for quantitative assessment of peripheral arterial disease. The obtained velocity ratios were compared to the diameter reduction of the suspected lesion measured on angiography.

**Materials and methods**

Eleven patients scheduled for angiography of the lower extremities due to suspected peripheral arterial disease were scanned with a commercial ultrasound scanner (UltraView 800, BK Medical, Herlev, Denmark) using Vector Flow Imaging. All patients had their superficial femoral artery scanned, and the scanning was performed in the angiography room just prior to the angiography. The artery was scanned in the transversal and longitudinal plane, and when turbulent/disturbed flow was detected with Vector Flow Imaging, a longitudinal recording, containing flow both in and proximal/distal to the lesion, was made. When turbulent/disturbed flow was detected, a marker was attached to the patients thigh corresponding to the flow disturbance. In the subsequent angiography the marker should then point directly towards the suspected flow disturbing lesion, ensuring matching ultrasound and angiographic recordings. See figure 15. The recordings were analyzed off-line with in-house made MATLAB-scripts. From each recording three frames illustrating flow with the best possible filling of the vessel in both the lesioned and healthy part of the artery were selected. The maximum velocities were located manually in each selected frame from the colored pixels of Vector Flow Imaging, see figure 15. The velocity ratio from each frame was then calculated as the maximum velocity detected in the lesioned segment divided by the maximum velocity detected in the adjacent disease free segment. The average of the three velocity ratios was subsequently calculated and used as the final result.
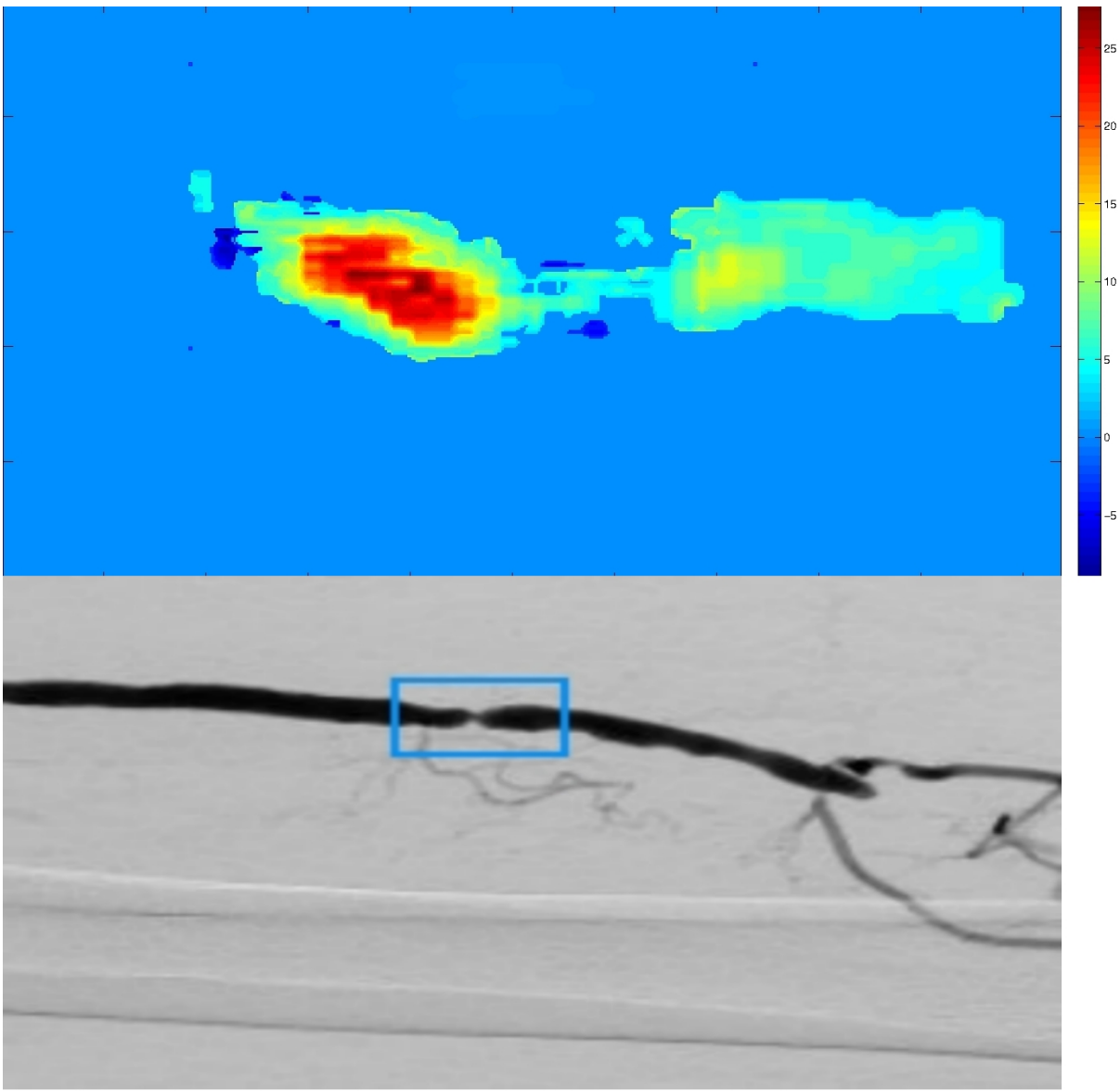
Figure 15: The top image shows the MATLAB processed Vector Flow Imaging recording of the stenosis illustrated by the DSA in the lower image. The blue box illustrates the part of the vessel shown in the top image. Maximum velocities around 25 cm/s are detected in the red area and in the yellow area to the right velocities around 7 cm/s are detected. It appears that peak velocities are detected immediately proximal to the stenosis and not in the stenosis. Possible calcified plaques in the vessel wall disturb the signal, or maybe the angle of insonation is not right for illustrating flow in the most stenotic part of the vessel. The marker is not visible in this projection.

**Results**

From the 11 patients recordings of 16 lesions were performed (thirteen stenoses and three plaques). The calculated velocity ratios, average velocity ratio and angiographic diameter reduction (expressed as percentage reduction) of each lesion are illustrated in table 2. Three lesions are treated as outliers. Patient 6, lesion 1, has a velocity ratio of 2.1 and a stenosis degree of 33 %. Patient 8 has a velocity ratio of 2.5 and a stenosis degree of 11 %, and patient 11 with a velocity ratio of 1 and a stenosis degree of 67 %. No certain factors separate these three patients from the rest. The correlation between the average velocity ratios and stenosis degrees is illustrated in figure 16 with and without outliers. A correlation coefficient $r$ of 0.45 and 0.75 was calculated, respectively. Without outliers, the velocity ratio corresponding to a 50 % stenosis is 2.0, and with all lesions included the velocity ratio is 2.5.

| Patient number | Lesion number | Lesion type | Velocity Ratios | Average Velocity Ratio | Degree of Stenosis (%) |
|---|---|---|---|---|---|
| 1 | 1 | Stenosis | 2.1, 1.9, 2.7 | 2.2 | 78 |
|  | 2 | Plaque | 1.1, 0.9, 1.2 | 1.1 | 0 |
| 2 | 1 | Plaque | 0.9, 1, 1 | 1 | 0 |
|  | 2 | Stenosis | 1.2, 1.2, 1.3 | 1.2 | 19 |
| 3 | 1 | Stenosis | 2.6, 3.6, 2.6 | 2.9 | 68 |
| 4 | 1 | Stenosis | 1.6, 4.4, 1.7 | 2.6 | 65 |
| 5 | 1 | Stenosis | 1.2, 1, 1.3 | 1.2 | 37 |
|  | 2 | Stenosis | 0.7, 0.8, 1.3 | 0.9 | 31 |
| 6 | 1 | Stenosis | 2.4, 1.8, 2.1 | 2.1 | 33 |
|  | 2 | Stenosis | 1.3, 1.6, 1.5 | 1.5 | 15 |
|  | 3 | Stenosis | 1, 1.3, 1.2 | 1.2 | 15 |
| 7 | 1 | Stenosis | 2.1, 2.4, 2.1 | 2.2 | 62 |
| 8 | 1 | Stenosis | 1.9, 2.9, 2.8 | 2.5 | 11 |
| 9 | 1 | Stenosis | 1.2, 1, 1.1 | 1.1 | 47 |
| 10 | 1 | Plaque | 1.3, 1.3, 1.2 | 1.3 | 0 |
| 11 | 1 | Stenosis | 1, 1.1, 1 | 1 | 67 |

Table 2: Velocity ratios based on Vector Flow Imaging recordings from each individual lesion and coherent stenosis degree based on angiographic diameter reduction. A plaque is defined as a flow disturbing lesion with no corresponding angiographic diameter reduction.

f(x) = 30.59 ln(x) + 22.09

**All data**



f(x) = 54.01 ln(x) + 13.73
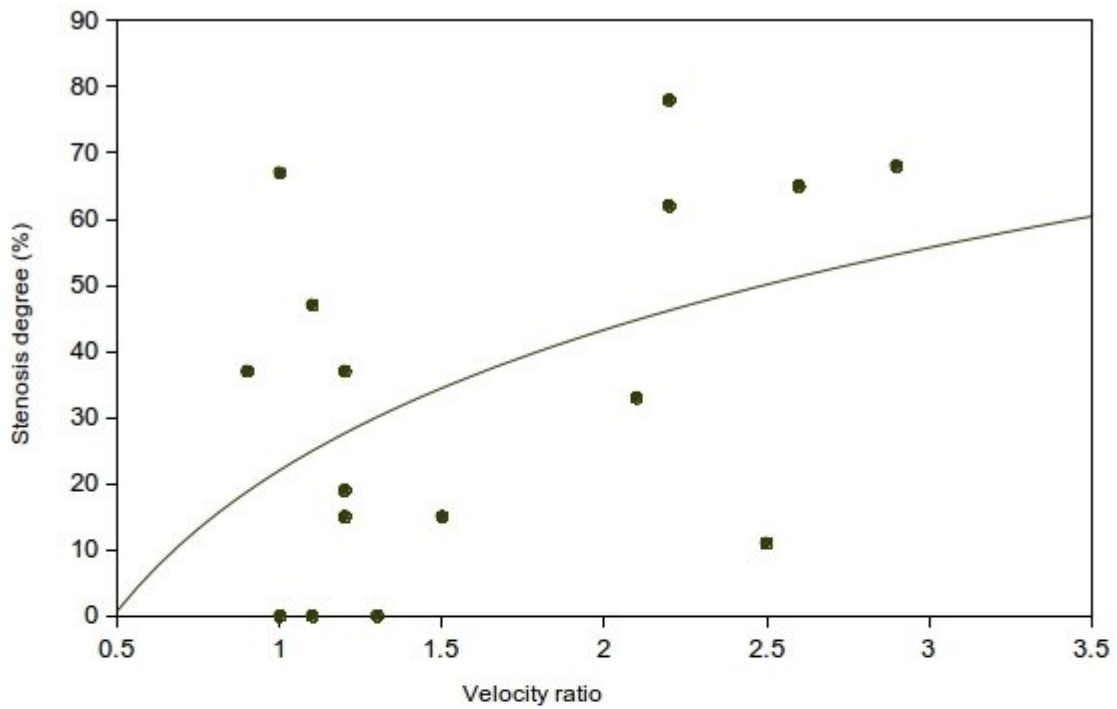
**Without outliers**
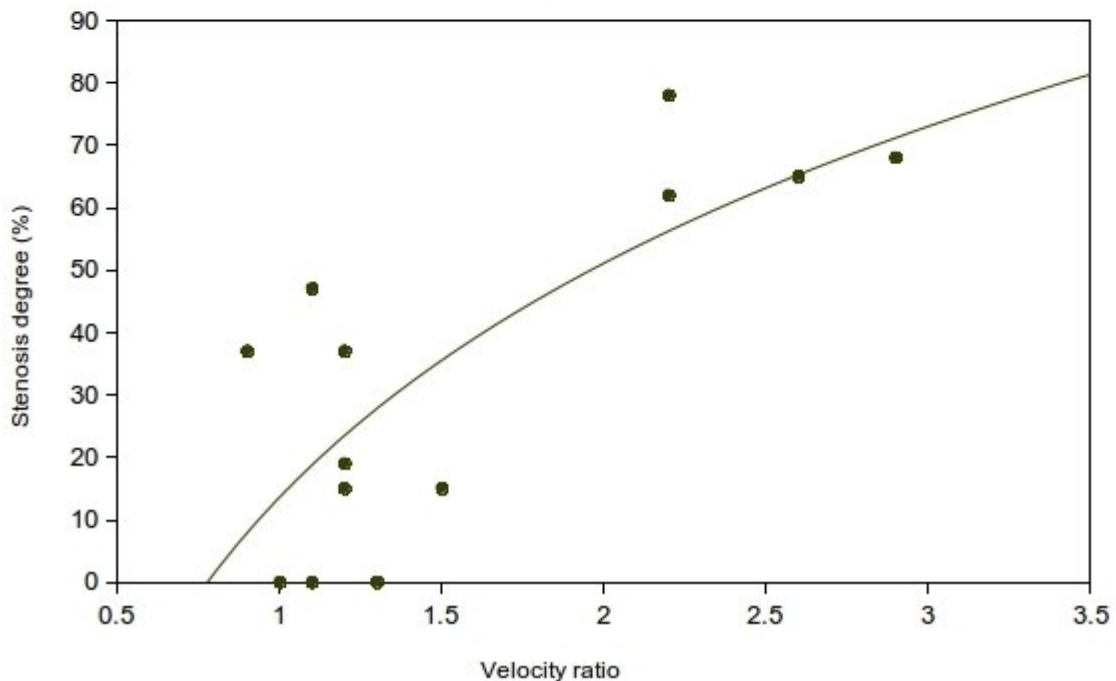


Figure 16: Correlation between calculated average velocity ratios and angiographic diameter reduction expressed as stenosis percentage. The correlation has been illustrated for all data (top) and with the three outliers omitted (bottom). Notice that the ideal correlation line starts in (1, 0) with a velocity ratio of 1 when no stenosis is present. The regression equations are seen in the top of each plot.

**Conclusion**

Arteriosclerotic stenoses and plaques in the superficial femoral artery have for the first time been characterized using velocity ratios obtained with vector ultrasound. A strong correlation ($r = 0.75$) between velocity ratios and angiographic stenosis degrees was found, and a velocity ratio of 2.0 was shown to distinguish between stenoses over and under 50 % angiographic diameter reduction.

# Discussion

## New achievements with synthetic aperture ultrasound and vector flow ultrasound

This thesis presents in study I the first clinical use of synthetic aperture sequential beamforming ultrasound in a hospital setting. SASB has previously been demonstrated on healthy subjects and shown to improve image quality when compared with conventional ultrasound (12). Nineteen patients with liver cancer were now scanned, and SASB still provides better image quality than conventional ultrasound.

In study II and III Vector Flow Imaging was used to obtain volume flow in arteriovenous fistulas for hemodialysis and velocity ratios related to arteriosclerotic stenoses in the SFA, respectively.
In study II volume flow derived from Vector Flow Imaging was on average $31 - 35$ % (depending on the approach) lower than volume flow determined by UDT, but the standard deviation of the measurements was significantly improved.
In Study III a strong correlation ($r = 0.75$) between velocity ratios obtained with Vector Flow Imaging and angiographic stenoses degrees was found. A velocity ratio of 2.0 was shown to distinguish stenoses with clinically relevant angiographic stenoses degrees $> 50$ % from non relevant stenoses $< 50$ %.

The studies in this thesis are the first to present clinically relevant flow results obtained with Vector Flow Imaging from these two patient groups, and in both studies the commercial scanner was used with factory default settings for flow estimation. The recordings were post processed using in-house coded MATLAB scripts, and similar scripts should be implemented in future versions of the scanner software, enabling real-time quantitative angle independent flow estimations.

# Synthetic aperture sequential beamforming

**Previous comparison studies of B-mode techniques**

Several previous studies have performed comparisons of B-mode images obtained with different techniques. Kim et al. (49) performed a study comparing conventional technique, tissue harmonic, compounding, and tissue harmonic compounding in 96 liver lesions. One still image were obtained with each of the four techniques recorded in random order with the transducer held as fixated as possible. The evaluation was performed by two radiologists assessing the ultrasound images one at the time, and rating them on a subjective 4 -5 point scale. Tissue harmonic compounding was overall rated as the technique providing the best image quality. Yen et al. (50) performed very similar studies with comparison of the same four techniques. Fifty one liver lesions were scanned with one technique at the time, and the images were evaluated by two radiologists on a subjective 4 point scale. Once more the combination of compounding and tissue harmonic provided the best overall results. Tanaka et al. (51) had 15 assessors evaluate 100 liver images obtained from 50 patients. Each patient had a conventional image and a tissue harmonic image recorded, and tissue harmonic imaging was found to be more effective for detection of focal lesions. Kim et al. (52) compared images of 31 breast lesions in 24 patients recorded with synthetic aperture ultrasound and conventional imaging. The images were recorded with one technique at the time, and the images were evaluated side-by-side by three radiologists on a 5 point scale. Synthetic aperture were rated better than conventional technique. Another Kim et al. (53) compared images of 10 breast lesions obtained with a synthetic aperture technique and conventional imaging. These images were also acquired sequentially for synthetic aperture and conventional imaging, and the evaluation was performed by two radiologists in a side-by-side comparison. Again the image quality of the synthetic aperture technique was found to be better than conventional ultrasound.

All these comparison studies use consecutive recording of the techniques in question and even with a steady hand and calm patient, the sequences can never be identical. Furthermore the image quality evaluation is performed as a comparison of still images and not sequences, but for evaluation of ultrasound recordings, real time sequences provide substantially more information than still images. The use of radiologists as evaluators is common to all the mentioned studies, and emphasizes the great interest in a clinical approach to the assessment.

**Clinical use of SASB**

SASB is still not developed to the degree, where it can be used for diagnostic purposes. During the actual scanning procedure only images from the first beamforming are shown on the screen, and the quality and frame rate (8 Hz) of these images are only for navigational purposes. The low frame rate is due to the simultaneous use of two techniques. This limits the regions of interest to exposed well defined organs with substantial pathological changes, i.e. liver tumors of a certain size. The images used for the actual evaluation of image quality, are produced off line by the second beamforming, but are still in the most "raw" format the scanner can produce. Application of image enhancing algorithms, i.e. a speckle filter, is therefore needed to evaluate the diagnostic performance of SASB, and to expand the clinical use of SASB.

**Image evaluation setup**

The combination of interleaved recording of the ultrasound techniques in question and the subsequent side-by-side presentation of the real time sequences by IQap, provides a unique image quality evaluation setup. Most of the previously mentioned comparison studies use a side-by-side comparison approach, but are only displaying still images. When using IQap, the sequences are by default shown as real time sequences, and the assessor can chose to view the sequences one frame at the time and skip both forwards and backwards. The displayed sequences are evaluated using a visual analog scale (54) with 100 steps (-50 to +50) to avoid grouping of the results and allow for a more free evaluation, but unfortunately the quality of the recorded sequences were so much alike, that three of the five assessing radiologists simple moved the cursor one or two steps to each side for each evaluation, i.e. an evaluation scale with just five steps would have sufficed. Future studies with other ultrasound techniques or improved versions of SASB will hopefully show expanded use of the visual analog scale.

**Synthetic aperture and tissue motion**

Previous studies have shown a negative effect of tissue motion on synthetic aperture ultrasound images (3,7,55), and this is probably why Kim and Kim chose to perform synthetic aperture ultrasound of breast lesions. The breast is very easy to fixate and is not affected by e.g. breathing. The patients in our study were all asked to lie still and hold their breath during recording of the ultrasound sequence, and the transducer was held in the same position throughout the recording. Few were able to comply completely, and the recordings were therefore marked by movement to a higher extent than the

previous study with healthy volunteers (12). However, the increased movement did not affect the evaluations, and the major limitation for movement in this study was most likely caused by the low frame rate of 8 Hz. If only one technique was used, the frame rate would double. A frame rate of 16 Hz would provide a more objective evaluation of the impact of tissue motion, and would enable the operator to perform a more clinically relevant ultrasound scanning. If tissue motion shows to be a limitation new algorithms for minimizing the limitations are developed (55).

# Volume flow

**Previous studies of volume flow using ultrasound**

Volume flow in hemodialysis fistulas estimated with conventional ultrasound has previously been compared with UDT several times with varying results. Huisman et al. (56) and Schwarz et al. (57) found the Doppler measurements to be approximately 30 % lower than the UDT results, very similar to the results of study II. Lopot et al. (58) found a good correlation ($r = 0.87$) between Doppler and UDT, but with significant scatter, and emphasizes that the Doppler examination of an arteriovenous fistula is a job for skilled and experienced operators. Zanen et al. (59) found volume flow using Doppler to be 1129 mL/min higher than UDT where the average flow estimated by UDT was 752 mL/min. A poor correlation ($r = 0.10$) was found. All of these studies measured volume flow by positioning the transducer directly on the fistula, the same procedure as in study II. Vilkomerson et al. (60) demonstrated an experimental vector ultrasound device, based on Doppler technique, consisting of three receiving ultrasound transducers placed circularly around a central transmitting transducer. The device was simply placed on the fistula, without guidance from a B-mode image (which was not produced), and automatically measured volume flow using the velocity vector provided by each of the three receiving transducers. The device produced impressive flow estimations on a flow rig (average error less than 1 %), and was tested on seven hemodialysis grafts and compared with UDT. For flow rates < 800 mL/min the correlation was good, but when flow exceeded 800 mL/min, the correlation was very poor. One other ultrasonic way of estimating volume flow in an arteriovenous fistula, is by estimating the volume flow in the feeding brachial artery (61). The brachial artery is fairly straight, round, and positioned in a way that allows an angle of insonation less than 60°, and is therefore more accessible for the conventional spectral Doppler examination (62). Heerwagen et al. (63) found the volume flow of the feeding brachial artery to be on average approximately 11 % higher than volume flow in the fistula estimated by UDT.

**Challenges related to conventional Doppler for estimation of volume flow**

The angle dependency of conventional spectral Doppler, and the subsequent operator dependency is one major challenge when quantitative estimations are obtained. This issue is very evident when a vessel as soft and superficial as the arteriovenous fistula is scanned (59,61,64,65) To obtain an acceptable angle of insonation (< 60°) the operator might have to tilt the transducer on the skin, and

almost inevitably deform the vessel, creating disturbed and unpredictable flow, in turn affecting the velocity estimation. The operator is furthermore limited by the manual placement of the Doppler sample volume, which may not be placed in the vessel segment with the highest velocities. When estimating volume flow with conventional Doppler, the time averaged mean flow velocity is normally obtained automatically by the scanner and multiplied with the cross sectional area, calculated from only one diameter, assuming a circular vessel. None of the fistulas in study II were circular, and they all had the shorter diameter in the scan plane. The lateral diameter was on average 7 % larger than the other (66) and this will naturally lead to an underestimation of both cross sectional area and volume flow.

**Benefits and challenges of Vector Flow Imaging for estimation of volume flow**

Compared to other vector velocity ultrasound techniques (27,60,67,68) a major benefit of Vector Flow Imaging is the ability to immediately see the flow patterns (laminar/turbulent flow) real-time at all angles of insonation, and subsequently only perform velocity estimations of vessel segments with predominantly laminar flow. When using Vector Flow Imaging flow information is obtained from the entire vessel visible in the B-mode image (if the colorbox is adjusted correspondingly), and flow in all parts of the visualized vessel can therefore be estimated and quantified at once. The operator is not limited by positioning of the spectral range gate, and can focus completely on a steady and swift scan of the fistula without deforming the vessel walls and create turbulence.

The major challenge of VFI is the need for off line processing to obtain the quantitative velocity estimations. Automated MATLAB scripts were developed for study II, but the processing is time consuming, and knowledge of MATLAB is required by the operator.

Another limitation is the 2-D scan plane and subsequent need to assume circular symmetry of the flow profile, but this of course also applies to conventional spectral Doppler.

The 2-D scan plane leads to another challenge. Correct alignment of ultrasound beam and fistula during the longitudinal recording of flow data was more challenging than expected. Even though great care was taken, Jensen et al. (66) showed that an average misalignment of 28.5 % was present in the study, and this can lead to a 15 % underestimation of volume flow.

**Challenges related to UDT volume flow estimation**

An exact estimation of volume flow with UDT is completely dependent of sufficient mixing of blood and diluting agent (saline) (69). At low flow velocities laminar flow with poor mixing abilities is

present in the fistula, and this affects the performance of UDT in a negative direction. If saline and blood is not sufficiently mixed, the dilution at the proximal/venous hemodialysis needle (where the diluted blood is drawn for the flow estimation) is not uniform and an erroneous flow estimate is provided. High flow velocities generate turbulent flow with better mixing abilities (70), and UDT therefore theoretically performs better at higher flow velocities, as also mentioned by Zanen et al. (59). See Fig. 17.

## Laminar



## Turbulent
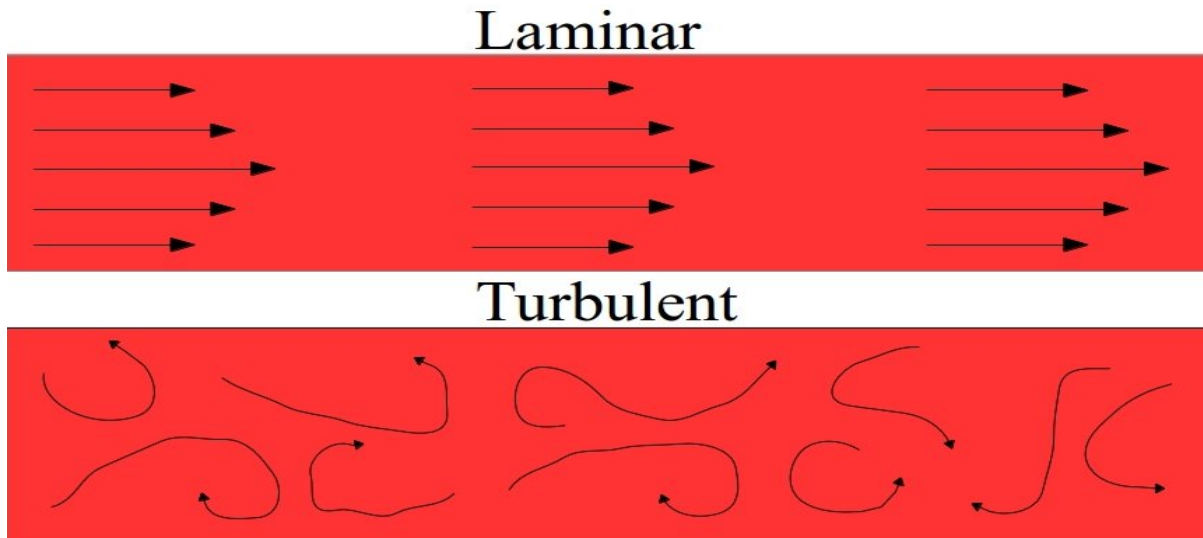
Figure 17: Laminar flow is characterized by flow in parallel layers with no interference between the layers and poor mixing conditions. The uneven blood-saline concentration will lead to erroneous flow estimates by UDT.

This theory was supported by our study, since the group of patients whose average Vector Flow Imaging measurements (based on VFImax) deviated more than 30 % from the UDT estimations had a mean flow velocity of 11.7 cm/s, and the group whose average Vector Flow Imaging measurements deviated less than 30 % had a mean flow velocity of 16.4 cm/s. Vector Flow imaging is not dependent on flow velocity, and a part of the apparent volume flow underestimation by Vector Flow Imaging compared to UDT, could be caused by a relative overestimation of volume flow by UDT.

**Other ultrasound techniques used for estimation of volume flow**

Experimental methods for estimation of volume flow have previously been examined by other research groups. Kripfgans et al. (71) evaluated a 3-D ultrasound method for estimation of volume flow in a flow rig with steady flow rates of 5 and 10 mL/min. The measured flow rates were within +/- 15 % of actual values, but the estimation was angle dependent, since the method was based on Doppler technique. In a later study of the same technique by Richards et al. (72), the angle dependency was

overcome, and the technique had been expanded to 4-D ultrasound scanning. A pulsatile flow phantom was scanned and an average error of 6.4 % was found between the estimated flow results and the true flow output. *In-vivo* studies were also performed on canine carotid and femoral arteries, and an average error of -6.3 % was found.

# Velocity ratios

**Previous studies of velocity ratios**

Several studies of patients with peripheral arterial disease have previously investigated the correlation between velocity ratio and stenosis degree determined by DSA (41–45). All velocities were in these studies estimated with conventional color and spectral Doppler. The peak systolic velocity has also been investigated as a sole indicator of stenosis degree, but the velocity ratio has been shown to provide better estimates of the stenosis degree due to interindividual variations of blood flow (41,43). Even when restenosis of a stent in the SFA occurs, the velocity ratio is the most reliable parameter (73). Velocity ratios in the range of 1.5 to 2.4 have in the previous studies been shown to distinguish between stenoses with < 50 % and > 50 % diameter reduction, which corresponds to the results of study III. Similar studies have been performed on arteriosclerotic carotid arteries, where both peak systolic velocities, end diastolic velocities, and peak systolic velocity ratios are used for grading the stenoses (74). Similar to the SFA, a peak systolic velocity ratio (calculated as peak systolic velocity in the internal carotid artery divided by the peak systolic velocity in the common carotid artery) of approximately 2.0 indicates a 50 % stenosis in the internal carotid artery.

**Challenges and benefits related to conventional Doppler for estimation of velocity ratios**

Conventional spectral Doppler is both angle dependent and operator reliant, and in the presence of stenoses spectral Doppler is even more challenging to use (64,75). Because of the angle dependency of conventional spectral Doppler, substantial errors in estimation of peak velocities can occur due to operator misjudgment, and these potential errors can lead to calculation of even more erroneous velocity ratios if one peak velocity is overestimated and the other underestimated. The angle dependency is furthermore a problem if an acceptable angle of insonation (< 60°) cannot be achieved by electronically steering of the ultrasound beam. The operator then has to tilt the transducer on the skin, and risk to compress the vessel of interest, thereby creating disturbed and unpredictable flow. This is not a major problem with regard to the SFA, but when e.g. a femoral *in-situ bypass* (a superficial vein left in place and used as a bypass) is scanned, the vessel is very easy to deform when the transducer is tilted.

One of the benefits of conventional Doppler is the automated detection of peak systolic (and end diastolic) velocities. This allows for direct comparison of velocities from either end of a vessel, because

the operator knows the velocities are from the same part of the cardiac cycle. This feature is used in all the previous studies of velocity ratios obtained with spectral Doppler. Furthermore the possibility of using continuous wave Doppler (as opposed to pulsed wave Doppler) offers independence of the PRF when quantitative flow measurements are performed. The range of measurable velocities is not limited, and both very high and low velocities are measured simultaneously. Unfortunately continuous wave ultrasound cannot produce a B-mode image, and provides therefore no anatomical information.

**Challenges and benefits related to vector ultrasound for estimation of velocity ratios**

The major challenge with VFI in its current implementation, is the manual acquisition of quantitative flow estimations from each generated vector velocity map through off-line processing. This process requires knowledge of MATLAB, is very time consuming, and limits the number of possible velocity estimations used for each velocity ratio calculation. Furthermore is VFI dependent on the PRF, and with the major flow fluctuations taking place in a stenotic artery (41), numerous frames are affected by either aliasing or too little velocity information. The calculation of velocity ratios is therefore rather fragile and compromises the process. Since no velocities are detected automatically, as opposed to Doppler, both velocities used for calculation of a velocity ratio, must be from the same frame, to ensure they are from the same part of the cardiac cycle. This limits the size of the examined region to the width of the transducer (approximately 4 cm), whereas conventional Doppler can directly compare peak systolic velocities obtained in either end of the vessel. The detection of both velocities from the same frame can on the other hand be an advantage, allowing velocities throughout the entire cardiac cycle to be directly compared and used for velocity ratio calculation. The generation of a vector velocity map of each single frame is also a major advantage, providing substantial amounts of flow information. The map illustrates the different flow phenomena occurring in relation to the stenosis, and provides the precise location of the maximum velocities both in the stenosis and in the adjacent normal vessel segment. This eliminates the need to assume and potentially misjudge where in the vessel the Doppler range gate should be positioned.

**Challenges related to DSA**

DSA provides 2-D images of the arteries and are routinely recorded in two planes. The image yielding the most severe stenosis degree is used for diagnostic purposes, as well as calculation of the exact stenosis degree in this study. There is however no guarantee that the selected angiographic image

depicts the true stenosis degree, since the stenoses seldom are concentric, and underestimation of stenosis degree can therefore occur. Measurements of vessel diameter and the resulting calculation of stenosis degree is evaluator dependent, and precise and uniform measurement of diameters is challenging. Some previous studies of angiographic assessment of arterial stenoses simply divides stenoses in two groups, less and more than 50 %, instead of providing an exact stenoses degree (76,77). Van Jarsveld et al. (78) divided renal artery stenoses in 10 % sections, and found general agreement about the degree between three assessors, however 50 – 60 % and 60 – 70 % stenoses could not be separated. It might therefore seem reasonable to think of a given stenosis degree as a +/- 10 % estimate, and keep in mind that the primary task is to identify the clinically relevant stenoses with more than 50 % diameter reduction.

**Other ultrasound techniques potentially used for evaluation of stenoses**

Other vector ultrasound techniques have previously been demonstrated on both healthy volunteers and patients. Hansen et al. (79) demonstrated the Plane Wave Excitation method on four volunteers and visualized complex flow patterns in various arteries and veins using an experimental ultrasound scanner. However, no quantitative estimations were performed. Ekroll et al. (28) demonstrated a combination of plane waves and spectral Doppler using a research scanner. Twelve patients suffering from carotid artery disease were scanned, and spatial maps showing the peak systolic velocity in every image point, were generated. These maps could be used to calculate velocity ratios similar to the approach in study III. Hoskins (80) used two independent beam directions and produced a vector method for quantitative estimation of peak velocities. The method was tested under ideal circumstances on a flow phantom with simulated stenoses, and a positive correlation of velocity and stenosis grade was found at angles of insonation from 50 – 80º.  Another approach to vector velocity ultrasound is synthetic aperture. Jensen and Oddershede used a research scanner and a flow rig to obtain flow velocity and direction with approximately 2 % standard deviation. An in-vivo example from a common carotid artery of a healthy volunteer was also produced (68). Synthetic aperture in a dual beamforming setup for flow estimation has been presented by Li and Jensen (27). The main motivation is again the ambition to implement synthetic aperture on a commercial scanner. The study was conducted on a research scanner, and the amount of data was reduced by a factor 64. The flow velocity was estimated with an average standard deviation of  6.4 %, and a frame rate of 100 Hz and a penetration depth of 15 cm was obtainable using this setup.

# Conclusion

The overall aim of the thesis was to perform true clinical patient studies of two new ultrasound techniques.

SASB has previously been demonstrated *in-vivo* on healthy volunteers and compared to conventional ultrasound technique, and in study I, the first patients were scanned using SASB. SASB continues to produce ultrasound sequences with at least the same image quality as conventional ultrasound and therefore has potential for further development. The data reduction of SASB enables wireless transfer of the data using existing wireless protocols, and facilitates implementation of the technique on conventional ultrasound scanners.

Besides a clinical evaluation of a new ultrasound technique, study I is just as much the conclusion of the developmental process leading to study I. Furthermore it is a final trial of the unique scan sequence allowing interleaved recording of two ultrasound techniques, and of the assessment program IQap allowing evaluation of real time sequences. Both the scan sequence and the use of IQap worked without any kind of malfunction.

The clinical use of Vector Flow Imaging has so far been tested in limited clinical applications. Previous clinical use concerns epicardial ultrasound scanning during transthoracic cardiac surgery (31,81). Study II and III were attempts to discover new clinical purposes with the technique.

Study II presented volume flow measurements obtained from arteriovenous fistulas for hemodialysis. Focus was to develop an easy, intuitive, and fast way of estimating volume flow in the fistulas. I believe that the most intuitive and direct way to measure the flow is to simply measure directly on the fistula. Another major benefit of this, is the possibility to immediately visualize the anatomy and possible pathology of the fistula, and its effect on the flow. It was possible to derive a reasonable volume flow by scanning directly on the most superficial part of the fistula, and the measurements had an improved standard deviation when compared to the UDT.

In study III arteriosclerotic stenoses in the SFA were assessed and quantified using velocity ratios derived from the VFI scans. When compared to angiography a moderate to strong correlation was found between velocity ratio and stenosis degree, and a velocity ratio of 2.0 was shown to distinguish clinically relevant stenoses from non relevant stenoses. These results too indicate the major potential of Vector Flow Imaging as an intuitive technique capable of providing quantitative flow results used for numerous clinical purposes. When algorithms similar to the MATLAB scripts used in study II and III at

some point are implemented in the scanner, and real time quantitative flow estimations are made possible, the clinical usability will expand substantially and benefit both patients and healthcare practioners.

# Perspectives

Numerous future studies are possible with both synthetic aperture sequential beamforming ultrasound and Vector Flow Imaging

*SASB:*

The recordings already obtained can be post processed using different image enhancing algorithms, e.g. a speckle filter, and the effect on the image quality can be evaluated similar to study I.

Letting an experienced sonographer/radiologist perform scans of the same healthy subject or patient with one technique at the time (blinded), allowing a frame rate of 16 Hz, and decide which technique provides the better image.

Develop wireless transfer between the two beamformers and repeat study I. Could also be done with healthy subjects.

*Vector Flow Imaging:*

Investigate the diagnostic performance of Vector Flow Imaging on deep venous thrombosis. Compare to conventional Doppler.

Volume flow in hemodialysis fistulas obtained with MR compared to volume flow obtained with Vector Flow Imaging immediately before or after the MR.

Compare volume flow in the brachial artery of patients with hemodialysis fistula obtained with Vector Flow Imaging and conventional spectral Doppler.

Compare flow velocities obtained with Vector Flow Imaging and conventional spectral Doppler in patients with arteriosclerotic carotid arteries.

Expand patient number in study III and supplement with interobserver study of velocity ratio calculation.

Implement real time flow quantification and repeat all the above proposals, incl. study II and III.

# Bibliography

1.  Jensen JA. Medical ultrasound imaging. Prog Biophys Mol Biol. 2007 Jan;93(1–3):153–65.

2.  Sherwin CW, Ruina JP, Rawcliffe RD. Some Early Developments in Synthetic Aperture Radar Systems. IRE Trans Mil Electron. 1962 Apr;MIL-6(2):111–5.

3.  Jensen JA, Nikolov SI, Gammelmark KL, Pedersen MH. Synthetic aperture ultrasound imaging. Ultrasonics. 2006 Dec 22;44, Supplement:e5–15.

4.  Nikolov SI. Synthetic aperture tissue and flow ultrasound imaging. Technical University of Denmark; 2001.

5.  Thomson RN. Transverse and longitudinal resolution of the synthetic aperture focusing technique. Ultrasonics. 1984 Jan;22(1):9–15.

6.  Gammelmark KL, Jensen JA. Multielement synthetic transmit aperture imaging using temporal encoding. IEEE Trans Med Imaging. 2003;22(4):552–63.

7.  Pedersen MH, Gammelmark KL, Jensen JA. In-vivo evaluation of convex array synthetic aperture imaging. Ultrasound Med Biol. 2007 Jan;33(1):37–47.

8.  Daher NM, Yen JT. 2-D array for 3-D Ultrasound Imaging Using Synthetic Aperture Techniques. IEEE Trans Ultrason Ferroelectr Freq Control. 2006 May;53(5):912–24.

9.  Nikolov SI, Jensen JA. Investigation of the feasibility of 3D synthetic aperture imaging. 2003 IEEE Symposium on Ultrasonics. 2003. p. 1903–6 Vol.2.

10. Kortbek J, Jensen JA, Gammelmark KL. Sequential beamforming for synthetic aperture imaging. Ultrasonics. 2013 Jan;53(1):1–16.

11. Karaman M, Li P-C, O'donnell M. Synthetic aperture imaging for small scale systems. IEEE Trans Ultrason Ferroelectr Freq Control. 1995;42(3):429–42.

12. Hemmsen MC, Hansen PM, Lange T, Hansen JM, Hansen KL, Nielsen MB, et al. In Vivo Evaluation of Synthetic Aperture Sequential Beamforming. Ultrasound Med Biol. 2012 Apr;38(4):708–16.

13. Hemmsen MC. Image processing in medical ultrasound. Technical University of Denmark; 2011.

14. Hemmsen MC, Petersen MM, Nikolov SI, Nielsen MB, Jensen JA. Ultrasound image quality assessment: a framework for evaluation of clinical image quality. Proceedings of SPIE. 2010 p. 76290C – 76290C – 12.

15. Hemmsen MC, Nikolov SI, Pedersen MM, Pihl MJ, Enevoldsen MS, Hansen JM, et al. Implementation of a versatile research data acquisition system using a commercially available

medical ultrasound scanner. IEEE Trans Ultrason Ferroelectr Freq Control. 2012;59(7):1487–99.

16.  Hansen JM, Hemmsen MC, Jensen JA. An object-oriented multi-threaded software beamformation toolbox. Proceedings of SPIE [Internet]. 2011 [cited 2013 Nov 27]. p. 79680Y – 79680Y – 9. Available from: http://dx.doi.org/10.1117/12.878178

17.  Engholm G, Ferlay J, Christensen N, Bray F, Gjerstorff ML, Klint A, et al. NORDCAN--a Nordic tool for cancer information, planning, quality control and research. Acta Oncol Stockh Swed. 2010 Jun;49(5):725–36.

18.  Razaak M, Martini M, Savino K. A Study on Quality Assessment for Medical Ultrasound Video Compressed via HEVC. IEEE J Biomed Health Inform. 2014 May 30;

19.  Radermacher J, Chavan A, Bleck J, Vitzthum A, Stoess B, Gebel MJ, et al. Use of Doppler Ultrasonography to Predict the Outcome of Therapy for Renal-Artery Stenosis. N Engl J Med. 2001 Feb 8;344(6):410–7.

20.  Krumme B, Hollenbeck M. Doppler sonography in renal artery stenosis—does the Resistive Index predict the success of intervention? Nephrol Dial Transplant. 2007 Mar 1;22(3):692–6.

21.  Lanzarini L, Fontana A, Campana C, Klersy C. Two Simple Echo-Doppler Measurements Can Accurately Identify Pulmonary Hypertension in the Large Majority of Patients With Chronic Heart Failure. J Heart Lung Transplant. 2005 Jun 1;24(6):745–54.

22.  Ameloot K, Palmers P-J, Vande Bruaene A, Gerits A, Budts W, Voigt J-U, et al. Clinical value of echocardiographic Doppler-derived right ventricular dp/dt in patients with pulmonary arterial hypertension. Eur Heart J Cardiovasc Imaging. 2014 Sep 8;

23.  Shastri M, Kulkarni S, Patell R, Jasdanwala S. Portal Vein Doppler: A Tool for Non-Invasive Prediction of Esophageal Varices in Cirrhosis. J Clin Diagn Res JCDR. 2014 Jul;8(7):MC12–5.

24.  Bohs LN, Geiman BJ, Anderson ME, Gebhart SC, Trahey GE. Speckle tracking for multi-dimensional flow estimation. Ultrasonics. 2000 Mar;38(1–8):369–75.

25.  Trahey GE, Allison JW, von Ramm OT. Angle independent ultrasonic detection of blood flow. IEEE Trans Biomed Eng. 1987 Dec;34(12):965–7.

26.  Dunmire B, Beach KW, Labs K-H, Plett M, Strandness DE. Cross-beam vector Doppler ultrasound for angle-independent velocity measurements. Ultrasound Med Biol. 2000 Oct 1;26(8):1213–35.

27.  Li Y, Jensen JA. Synthetic aperture flow imaging using dual stage beamforming: Simulations and experiments. J Acoust Soc Am. 2013 Apr 3;133(4):2014–24.

28.  Ekroll IK, Dahl T, Torp H, Løvstakken L. Combined Vector Velocity and Spectral Doppler Imaging for Improved Imaging of Complex Blood Flow in the Carotid Arteries. Ultrasound Med Biol. 2014 Jul;40(7):1629–40.

29. Jensen JA, Munk P. A new method for estimation of velocity vectors. IEEE Trans Ultrason Ferroelectr Freq Control. 1998;45(3):837–51.

30. Udesen J, Jensen JA. Investigation of transverse oscillation method. IEEE Trans Ultrason Ferroelectr Freq Control. 2006 May;53(5):959–71.

31. Hansen KL, Pedersen MM, Møller-Sørensen H, Kjaergaard J, Nilsson JC, Lund JT, et al. Intraoperative Cardiac Ultrasound Examination Using Vector Flow Imaging. Ultrason Imaging. 2013 Oct 1;35(4):318–32.

32. Udesen J, Nielsen MB, Nielsen KR, Jensen JA. Examples of In Vivo Blood Vector Velocity Estimation. Ultrasound Med Biol. 2007 Apr;33(4):541–8.

33. Jensen JA. Optimization of Transverse Oscillating Fields for Vector Velocity Estimation with Convex Arrays. Proc IEEE Int Ultrason Symp. 2013;1753–6.

34. Pedersen MM. Quantification of In Vivo 2D Vector Flow Ultrasound. University of Copenhagen; 2011.

35. Huijbregts HJT, Bots ML, Wittens CHA, Schrama YC, Moll FL, Blankestijn PJ, et al. Hemodialysis arteriovenous fistula patency revisited: results of a prospective, multicenter initiative. Clin J Am Soc Nephrol CJASN. 2008 May;3(3):714–9.

36. Shetty A, Whittier WL. Does regular surveillance improve the long-term survival of arteriovenous fistulas? Int J Nephrol. 2012;2012:539608.

37. Soule JL, Henry ML. Noninvasive methods to identify early vascular access dysfunction. Semin Vasc Surg. 2007 Sep;20(3):164–6.

38. Whittier WL. Surveillance of hemodialysis vascular access. Semin Interv Radiol. 2009 Jun;26(2):130–8.

39. Bosman PJ, Boereboom FT, Bakker CJ, Mali WP, Eikelboom BC, Blankestijn PJ, et al. Access flow measurements in hemodialysis patients: in vivo validation of an ultrasound dilution technique. J Am Soc Nephrol. 1996 Jun 1;7(6):966–9.

40. Wijnen E, Essers S, van Meijel G, Kooman JP, Tordoir J, Leunissen KML, et al. Comparison between two on-line reversed line position hemodialysis vascular access flow measurement techniques: saline dilution and thermodilution. ASAIO J Am Soc Artif Intern Organs 1992. 2006 Aug;52(4):410–5.

41. Ranke C, Creutzig A, Alexander K. Duplex scanning of the peripheral arteries: Correlation of the peak velocity ratio with angiographic diameter reduction. Ultrasound Med Biol. 1992;18(5):433–40.

42. Schlager O, Francesconi M, Haumer M, Dick P, Sabeti S, Amighi J, et al. Duplex Sonography Versus Angiography for Assessment of Femoropopliteal Arterial Disease in A "Real-World" Setting. J Endovasc Ther. 2007 Aug;14(4):452–9.

43. Khan SZ, Khan MA, Bradley B, Dayal R, McKinsey JF, Morrissey NJ. Utility of duplex ultrasound in detecting and grading de novo femoropopliteal lesions. J Vasc Surg. 2011 Oct;54(4):1067–73.

44. Baxter GM, Polak JF. Lower limb colour flow imaging: A comparison with ankle: Brachial measurements and angiography. Clin Radiol. 1993 Feb;47(2):91–5.

45. Flanigan DP, Ballard JL, Robinson D, Galliano M, Blecker G, Harward TRS. Duplex ultrasound of the superficial femoral artery is a better screening tool than ankle-brachial index to identify at risk patients with lower extremity atherosclerosis. J Vasc Surg. 2008 Apr;47(4):789–93.

46. Krivitski NM. Theory and validation of access flow measurement by dilution technique during hemodialysis. Kidney Int. 1995 Jul;48(1):244–50.

47. Krivitski NM. Novel method to measure access flow during hemodialysis by ultrasound velocity dilution technique. ASAIO J Am Soc Artif Intern Organs 1992. 1995 Sep;41(3):M741–5.

48. Egglin TKP, O'Moore PV, Feinstein AR, Waltman AC. Complications of peripheral arteriography:A new system to identify patients at increased risk. J Vasc Surg. 1995 Dec;22(6):787–94.

49. Kim SH, Lee JM, Kim KG, Kim JH, Han JK, Lee JY, et al. Comparison of fundamental sonography, tissue-harmonic sonography, fundamental compound sonography, and tissue-harmonic compound sonography for focal hepatic lesions. Eur Radiol. 2006 Nov 1;16(11):2444–53.

50. Yen C-L, Jeng C-M, Yang S-S. The benefits of comparing conventional sonography, real-time spatial compound sonography, tissue harmonic sonography, and tissue harmonic compound sonography of hepatic lesions. Clin Imaging. 2008 Jan;32(1):11–5.

51. Tanaka S, Oshikawa O, Sasaki T, Ioka T, Tsukuma H. Evaluation of tissue harmonic imaging for the diagnosis of focal liver lesions. Ultrasound Med Biol. 2000 Feb;26(2):183–7.

52. Kim WH, Chang JM, Kim C, Park J, Yoo Y, Moon WK, et al. Synthetic Aperture Imaging in Breast Ultrasound: A Preliminary Clinical Study. Acad Radiol. 2012 Aug;19(8):923–9.

53. Kim C, Yoon C, Park J-H, Lee Y, Kim WH, Chang JM, et al. Evaluation of Ultrasound Synthetic Aperture Imaging Using Bidirectional Pixel-Based Focusing: Preliminary Phantom and In Vivo Breast Study. IEEE Trans Biomed Eng. 2013;60(10):2716–24.

54. Freyd M. The Graphic Rating Scale. J Educ Psychol. 1923;14(2):83–102.

55. Gammelmark KL, Jensen JA. 2-D Tissue Motion Compensation of Synthetic Transmit Aperture Images. IEEE Trans Ultrason Ferroelectr Freq Control. 2014;

56. Huisman RM, Dijk M van, Bruin C de, Loonstra J, Sluiter WJ, Zeebregts CJ, et al. Within-session and between-session variability of haemodialysis shunt flow measurements. Nephrol Dial Transplant. 2005 Dec 1;20(12):2842–7.

57. Schwarz C, Mitterbauer C, Boczula M, Maca T, Funovics M, Heinze G, et al. Flow monitoring: performance characteristics of ultrasound dilution versus color Doppler ultrasound compared with fistulography. Am J Kidney Dis Off J Natl Kidney Found. 2003 Sep;42(3):539–45.

58. Lopot F, Nejedlý B, Sulková S, Bláha J. Comparison of different techniques of hemodialysis vascular access flow evaluation. J Vasc Access. 2004 Mar;5(1):25–32.

59. Zanen AL, Toonder IM, Korten E, Wittens CH, Diderich PN. Flow measurements in dialysis shunts: lack of agreement between conventional Doppler, CVI-Q, and ultrasound dilution. Nephrol Dial Transplant Off Publ Eur Dial Transpl Assoc - Eur Ren Assoc. 2001 Feb;16(2):395–9.

60. Vilkomerson D, Chilipka T, Nazarov A, Kuhlmann M, Levin NW. Non-Specialist Ultrasound Measuring of Access Flow: New Technology. Blood Purif. 2004;22(1):78–83.

61. Wiese P, Nonnast-Daniel B. Colour Doppler ultrasound in dialysis access. Nephrol Dial Transplant Off Publ Eur Dial Transpl Assoc - Eur Ren Assoc. 2004 Aug;19(8):1956–63.

62. Zierler BK, Kirkman TR, Kraiss LW, Reiss WG, Horn JR, Bauer LA, et al. Accuracy of duplex scanning for measurement of arterial volume flow. J Vasc Surg. 1992 Oct 1;16(4):520–6.

63. Heerwagen ST, Hansen MA, Schroeder TV, Ladefoged SD, Lönn L. Blood flow measurements during hemodialysis vascular access interventions - Catheter-based thermodilution or Doppler ultrasound? J Vasc Access. 2012;13(2):145–51.

64. Lui EYL, Steinman AH, Cobbold RSC, Johnston KW. Human factors as a source of error in peak Doppler velocity measurement. J Vasc Surg. 2005 Nov;42(5):972–9.

65. Teodorescu V, Gustavson S, Schanzer H. Duplex ultrasound evaluation of hemodialysis access: a detailed protocol. Int J Nephrol. 2012;2012:508956.

66. Jensen J, Olesen JB, Hansen PM, Nielsen MB, Jensen JA. In vivo evaluation of an angle independent flow rate estimator. Proc IEEE Int Ultrason Symp. 2014;

67. Oddershede N, Lovstakken L, Torp H, Jensen J. Estimating 2-D vector velocities using multidimensional spectrum analysis. IEEE Trans Ultrason Ferroelectr Freq Control. 2008 Aug;55(8):1744–54.

68. Jensen JA, Oddershede N. Estimation of Velocity Vectors in Synthetic Aperture Ultrasound Imaging. IEEE Trans Med Imaging. 2006 Dec;25(12):1637–44.

69. Depner TA, Krivitski NM. Clinical measurement of blood flow in hemodialysis access fistulae and grafts by ultrasound dilution. ASAIO J Am Soc Artif Intern Organs 1992. 1995 Sep;41(3):M745–9.

70. Avila K, Moxey D, Lozar A de, Avila M, Barkley D, Hof B. The Onset of Turbulence in Pipe Flow. Science. 2011 Jul 8;333(6039):192–6.

71. Kripfgans OD, Rubin JM, Hall AL, Gordon MB, Fowlkes JB. Measurement of Volumetric Flow. J Ultrasound Med. 2006 Oct 1;25(10):1305–11.

72. Richards MS, Kripfgans OD, Rubin JM, Hall AL, Fowlkes JB. Mean Volume Flow Estimation in Pulsatile Flow Conditions. Ultrasound Med Biol. 2009 Nov;35(11):1880–91.

73. Kawarada O, Higashimori A, Noguchi M, Waratani N, Yoshida M, Fujihara M, et al. Duplex criteria for in-stent restenosis in the superficial femoral artery. Catheter Cardiovasc Interv. 2013;81(4):E199–205.

74. Quirk K, Bandyk DF. Interpretation of carotid duplex testing. Semin Vasc Surg. 2013 Jun;26(2–3):72–85.

75. Gill RW. Measurement of blood flow by ultrasound: Accuracy and sources of error. Ultrasound Med Biol. 1985 Jul;11(4):625–41.

76. Ar  de V, Ph E, Tt O, Tp S, Bg G. Iobserver variability in assessing renal artery stenosis by digital subtraction angiography. Diagn Imaging Clin Med. 1983 Dec;53(6):277–81.

77. Cossman DV, Ellison JE, Wagner WH, Carroll RM, Treiman RL, Foran RF, et al. Comparison of contrast arteriography to arterial mapping with color-flow duplex imaging in the lower extremities. J Vasc Surg. 1989 Nov;10(5):522–9.

78. Van Jaarsveld BC, Pieterman H, van Dijk LC, van Seijen AJ, Krijnen P, Derkx FH, et al. Inter-observer variability in the angiographic assessment of renal artery stenosis. DRASTIC study group. Dutch Renal Artery Stenosis Intervention Cooperative. J Hypertens. 1999 Dec;17(12 Pt 1):1731–6.

79. Hansen K, Udesen J, Gran F, Jensen J, Bachmann Nielsen M. In-vivo Examples of Flow Patterns With The Fast Vector Velocity Ultrasound Method. Ultraschall Med - Eur J Ultrasound. 2009 Oct;30(05):471–7.

80. Hoskins PR. Peak velocity estimation in arterial stenosis models using colour vector Doppler. Ultrasound Med Biol. 1997;23(6):889–97.

81. Hansen KL, Møller-Sørensen H, Pedersen MM, Hansen PM, Kjaergaard J, Lund JT, et al. First report on intraoperative vector flow imaging of the heart among patients with healthy and diseased aortic valves. Ultrasonics

# Appendix 1

http://dx.doi.org/10.1016/j.ultrasmedbio.2014.07.008

● *Original Contribution*

# CLINICAL EVALUATION OF SYNTHETIC APERTURE SEQUENTIAL BEAMFORMING ULTRASOUND IN PATIENTS WITH LIVER TUMORS

PETER MØLLER HANSEN,* MARTIN HEMMSEN,[†] ANDREAS BRANDT,* JOACHIM RASMUSSEN,[†]
THEIS LANGE,[‡] PAUL SUNO KROHN,[§] LARS LÖNN,*[¶] JØRGEN ARENDT JENSEN,[†]
and MICHAEL BACHMANN NIELSEN*

*Department of Radiology, Copenhagen University Hospital, Rigshospitalet, Copenhagen, Denmark; [†]Center for Fast
Ultrasound Imaging, Department of Electrical Engineering, Technical University of Denmark, Lyngby, Denmark; [‡]Department
of Biostatistics, University of Copenhagen, Copenhagen, Denmark; [§]Department of Surgical Gastroenterology, Copenhagen
University Hospital, Rigshospitalet, Copenhagen, Denmark; and [¶]Department of Vascular Surgery, Copenhagen University
Hospital, Rigshospitalet, Copenhagen, Denmark

**Abstract**—Medical ultrasound imaging using synthetic aperture sequential beamforming (SASB) has for the first time been used for clinical patient scanning. Nineteen patients with cancer of the liver (hepatocellular carcinoma or colorectal liver metastases) were scanned simultaneously with conventional ultrasound and SASB using a commercial ultrasound scanner and abdominal transducer. SASB allows implementation of the synthetic aperture technique on systems with restricted data handling capabilities due to a reduction in the data rate in the scanner by a factor of 64. The image quality is potentially maintained despite the data reduction. A total of 117 sequences were recorded and evaluated blinded by five radiologists from a clinical perspective. Forty-eight percent of the evaluations were in favor of SASB, 33% in favor of conventional ultrasound and 19 % were equal, that is, a clear, but non-significant trend favoring SASB over conventional ultrasound ($p = 0.18$), despite the substantial data reduction. (E-mail: pdmhansen@gmail.com)    © 2014 World Federation for Ultrasound in Medicine & Biology.

*Key Words:* Ultrasound imaging, Synthetic aperture sequential beamforming, Clinical evaluation, Liver tumors.

## INTRODUCTION

Medical ultrasound scanning is a versatile and widely used diagnostic tool. It is used for prenatal screening; diagnosis and assessment of cardiovascular, musculo-skeletal and urogenital disease; traumatic organ damage; numerous cancer types; and so on. Ultrasound scanners are highly mobile, inexpensive compared with other medical imaging modalities (computed tomography, magnetic resonance) and free from cancer-inducing radiation (X-ray, computed tomography), and ultrasound scanning is performed by medical personnel at all levels. Improvement of the technique will therefore benefit large groups of patients and health care practitioners.

A conventional ultrasound image is generated by a number of adjacent ultrasound beams emitted and received consecutively and converted to image lines.

The frame rate is therefore limited by the speed of sound in tissue, the scanning depth and the number of image lines. Visualization of deep structures and organs and generation of high-resolution ultrasound images, which require a larger number of image lines, are thus performed at the expense of frame rate. Image generation is further affected by the single focus during transmit, causing the final image to be optimally focused in one depth only. This can be alleviated by using multiple transmit foci, but the frame rate is then reduced by the number of foci. These conditions limit the possibilities of performing high-resolution dynamic examinations of, for example, the beating heart, a joint in motion, or internal organs moving as a result of breathing.

One way to obtain both high resolution and high frame rate is to apply a synthetic aperture technique (Jensen et al. 2006; Sherwin et al. 1962). The basic idea is to synthesize a large aperture by stepwise moving a smaller active aperture through the complete array. For each step, a low-resolution image of the entire desired

---

Address correspondence to: Peter Møller Hansen, Department of Radiology, Rigshospitalet, Blegdamsvej 9, DK - 2100, Copenhagen OE, Denmark. E-mail: pdmhansen@gmail.com

region is generated from a single unfocused ultrasound wave, and these low-resolution images are summed to produce a high-resolution image with focus throughout the image. Several different implementations of synthetic aperture exist. The most simple version uses one array element at a time in both transmit and receive (Thomson 1984), and the most demanding versions use one or a small group of elements for transmitting and all of the elements for receiving (full synthetic aperture) (Gammelmark and Jensen 2003; Jensen et al. 2006). To implement full synthetic aperture, the scanner must have one channel for each element and be able to control all channels individually. Synthetic aperture has previously been tested *in vivo* with convincing results using an experimental ultrasound scanner (Pedersen et al. 2007). The disadvantage of synthetic aperture is high system requirements, because of the large number of low-resolution images the scanner has to produce and process. The desire to test synthetic aperture in a true clinical setting, that is, in a hospital, requires implementation on a conventional ultrasound scanner. The consequent limitations of the conventional scanner necessitate implementation of synthetic aperture as multi-element synthetic aperture, where a group of elements transmits and receives (Karaman et al. 1995). Multi-element synthetic aperture has previously been tested clinically on both benign and malignant breast changes. Image quality was significantly improved using synthetic aperture, but in those studies, only still images were produced (Kim et al. 2012, 2013). To further reduce the computational demands on the ultrasound scanner, the data-reducing concept of synthetic aperture sequential beamforming (SASB) was introduced (Fig. 1) (Kortbek et al. 2013). A dual-stage procedure for beamforming, using two separate beamformers, leads to a substantial data reduction. In the current setup, the amount of data is reduced by a factor of 64. This reduction makes it possible to implement SASB in conventional ultrasound scanners and, in the future, to construct, for example, wireless ultrasound transducers and tablet-based ultrasound scanners based on the technique. The technique is described in detail by Hemmsen et al. (2012a) and Kortbek et al. (2013) and has previously been tested preclinically on healthy volunteers, where improvement of image quality compared with conventional imaging was seen (Hemmsen et al. 2012a).

The purpose of this study was to perform a clinical evaluation of image sequences obtained with SASB from patients with cancer of the liver. The sequences were compared with conventional dynamic receive focus ultrasound and evaluated by radiologists. The hypothesis was that SASB and conventional ultrasound imaging generate clinical ultrasound sequences of equal image quality, despite the substantial reduction in data volume.
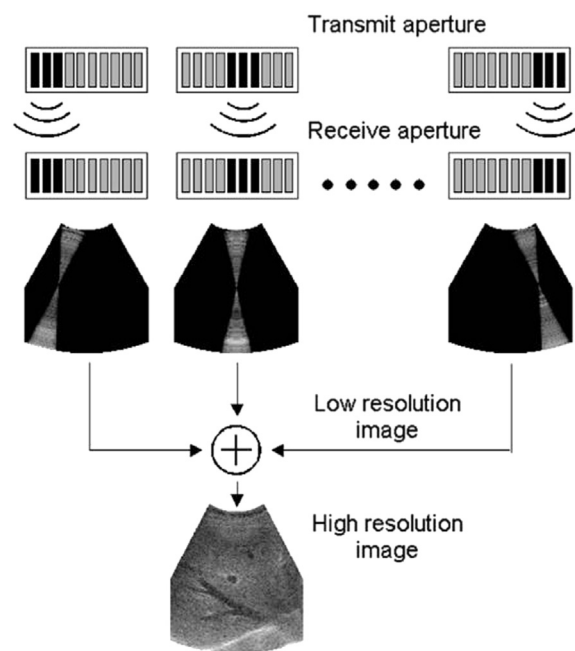


Fig. 1. Schematic of ultrasound imaging using synthetic aperture sequential beamforming. A number of fixed-focus beams are emitted and received to generate the basic data. Each beam is seen as a virtual ultrasound source emitting from the beam focal point. All received beams are then combined in a second-stage beamformer to yield a dynamically focused image in both transmit and receive from the second-stage focusing. More details on the second-stage focusing are given by Kortbek et al. (2013)

## METHODS

### Patients

Twenty-five patients diagnosed with hepatocellular carcinoma or colorectal liver metastases and planned for surgical resection were asked to participate in the study. The day before surgery, all patients were ultrasound scanned with a conventional scanner in factory default mode for abdominal scanning. If the tumor(s) could be located, the patient would proceed to the experimental scanning. If not, the patient was excluded from the study. Nineteen patients proceeded to experimental scanning. The 6 women and 13 men ranged in age from 37 to 82 y (mean = 65 y) and in body mass index from 16.8 to 33.0 $kg/m^2$ (mean = 24.8 $kg/m^2$). In all there were 3 cases of hepatocellular carcinoma and 16 cases of colorectal liver metastases in the group. The study was approved by the local ethics committee, and all patients entered the study after submitting written informed consent.

### Scanning

All scans, both factory mode and experimental, were performed by the same experienced physician. The 19 patients who proceeded to experimental scanning

underwent a total of 117 different recordings of both pathologic and healthy liver tissue regions. Fifty-six distinct recordings contained the tumor(s), and another 61 contained only healthy liver tissue (Fig. 2). The aim was to record six sequences from each patient, but because of technical challenges, this was possible for only 15 patients. One patient had five recordings (one recording was not saved properly), one patient had 8 and two patients had 7 recordings (because of misleading "error" messages from the system during the save process, additional recordings were made. Because these extra recordings were clinically useful, they were not deleted afterward.) The transducer was repositioned between recordings to avoid identical recordings.

*Equipment and data processing*

The same conventional ultrasound scanner and transducer were used for both the initial factory mode scanning and the subsequent experimental scanning. An UltraView 800 ultrasound scanner (BK Medical, Herlev, Denmark) equipped with a research interface and an abdominal 3.5-MHz 3.5 CL192-3 ML transducer (Sound Technology, State College, PA, USA) was used. The scanner was connected to a standard PC via the research interface. By use of the experimental setup, images generated with SASB and conventional ultrasound were recorded interleaved; that is, one frame generated with SASB followed one frame generated with conventional ultrasound (Hemmsen et al. 2010, 2012b). Hereby images from the same anatomic location were recorded almost simultaneously with both techniques, and ideal sequences for comparison were generated. Data generated with conventional ultrasound were

beamformed with the UltraView 800 scanner and recorded on the PC via the research interface. The first beamforming of the data generated with SASB was also performed with the UltraView 800 scanner and then recorded on the PC. By use of MATLAB (The MathWorks, Natick, MA, USA) and the beamformation toolbox BFT3 (Hansen et al. 2011), the second beamforming was performed on the PC subsequently. During the actual recording, only images for navigational purposes from the first beamforming were visualized on the scanner. All recorded sequences were automatically corrected with respect to the time gain compensation to obtain homogeneous images for comparison, and palindromic sequences of 3 s were generated to avoid temporal discontinuities. The scan depth in all recordings was set to 14.6 cm, and the frame rate was 8 frames/s. Before the actual scans, the acoustic outputs of the ultrasound scanner were measured. Intensity levels are listed in Table 1 and are considerably lower than the Food and Drug Administration (FDA) limits for abdominal ultrasound scanning (FDA 2008).

*Image evaluation*

Five ultrasound experts (radiologists) evaluated the sequences. None of the five radiologists had participated in the recording procedure or had seen any of the sequences before. Each radiologist evaluated the sequences isolated from collegial influences, and each evaluation was performed as a subjective assessment of image quality in terms of spatial resolution, contrast, penetration depth, unwanted artifacts and other factors.

The evaluation process was handled with the in-house coded program IQap (Hemmsen et al. 2010).
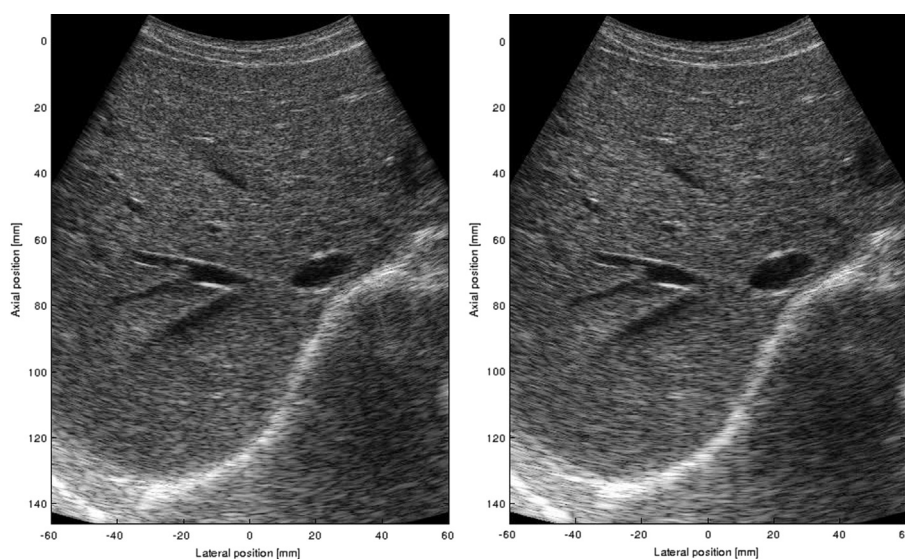


Fig. 2. Recording of healthy liver tissue with liver veins. The images are the interleaved recordings, with synthetic aperture sequential beamforming on the left and conventional ultrasound on the right.

Table 1. Ultrasound intensities and mechanical index

|  | FDA limits | Conventional | SASB |
|---|---|---|---|
| $I_{SPTA.3}$ (mW/cm$^2$) | 94 | 0.21 | 0.66 |
| $I_{SPPA.3}$ (W/cm$^2$) | 190 | 28.49 | 69.74 |
| Mechanical index | 1.9 | 0.51 | 0.80 |

FDA = Food and Drug Administration; SASB = synthetic aperture sequential beamforming.

With this program, evaluations were performed as double-blinded, side-by-side comparisons of matching real-time sequence pairs in random order. Each sequence pair consisted of the interleaved frames recorded with the two different techniques. In this way, the radiologists evaluated the two techniques by directly comparing two ultrasound sequences displaying the same anatomic location. During the evaluation, it was possible to view the recordings both as real-time sequences and as single frames. Before the actual evaluation, five trial examples were displayed to show the radiologists what to expect and how to use the program. All 117 sequences were evaluated twice with different left–right positioning, to avoid bias related to uneven monitor quality, monitor side preferred by the evaluator, light conditions in the office and other factors. A total of 234 sequence pairs were therefore evaluated by each of the five radiologists, resulting in 1170 evaluations. Each evaluation of image quality was performed with a visual analogue scale (Freyd 1923) underneath the displayed sequence (Fig. 3). If the evaluator found no difference between the two sequences, the indicator on the scale would be left in the middle; otherwise it would be drawn toward the side with better image quality. How far to the side the indicator was drawn corresponded to the degree to which that sequence was rated better than the other.

*Statistical analysis*

The results of the evaluations were analyzed with a mixed-effect linear model with a random effect for each sequence pair and each radiologist, thereby accounting for the dependence induced by repeatedly scoring the same sequence pair and collecting multiple scores from the same radiologist. The parameter of interest was the intercept, which captured the average score. Positive values indicate that SASB was preferred over conventional ultrasound. The mixed-effect model was used solely to account for dependencies induced by sequence pair and radiologist and thereby provided a valid confidence interval for the intercept.

**RESULTS**

The distribution of all evaluations from each radiologist is illustrated in Figure 4. The scale ranges from -50 to 50, where positive values favor SASB.
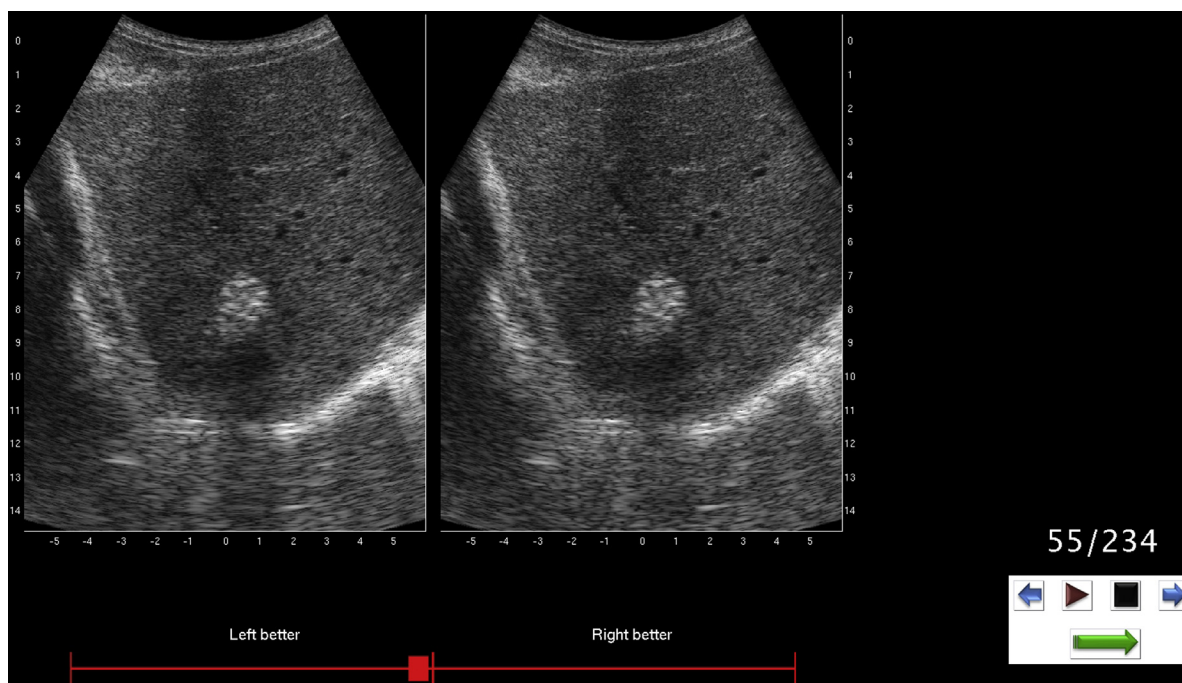


Fig. 3. Screen shot from the image quality assessment program IQap. A hyper-echoic colorectal metastasis is seen in the center of the image. The visual analogue scale used for rating image quality is seen in the bottom (the indicator is drawn a little to the left side), and the control panel for navigating the sequences and the sequence counter is seen in the lower right corner.
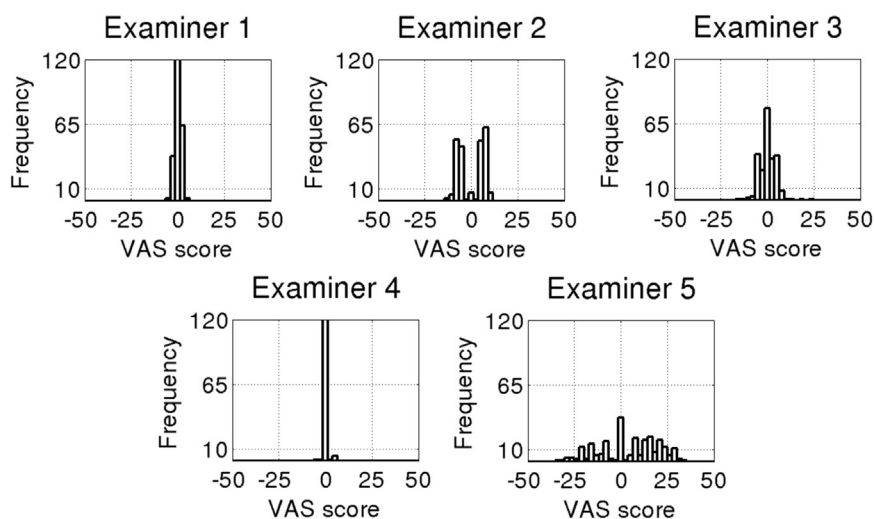
Fig. 4. Distribution of pooled answers from each radiologist's evaluation of image quality. Positive values favor synthetic aperture sequential beamforming. VAS = visual analogue scale.

The average image quality evaluation was in favor of SASB, with an average score of 1.44 (confidence interval [CI]: $-0.93$ to 3.81), but the result was not significant ($p = 0.18$).

Radiologist 4 rated all except seven (five positive, two negative) sequences to be of equal quality. This evaluation differed so much from those of the other radiologists that it was treated as an outlier and not included in the main analysis. Of the remaining 936 image quality evaluations, 451 (48%) favored SASB, 307 (33 %) favored conventional ultrasound, and 178 (19 %) rated the two as equal. Radiologists 1–5 spent 48.9, 49.4, 57.8, 25.8 and 31.6 min on the evaluation, respectively.

There was no significant difference between the left–right and right–left evaluations, meaning that it did not matter on what side of the monitor either of the two techniques was presented ($p = 0.23$). This covariate was therefore omitted.

As a check on robustness, the analysis was redone including radiologist 4; this did not change the conclusions of the analysis (new average evaluation score = 1.17, CI: $-0.73$ to 3.06), but as expected, the model fit was poorer because of radiologist 4's unconventional use of the scale.

## DISCUSSION

Our study indicates that SASB is suitable for true clinical ultrasound scanning. The evaluations performed by the radiologists indicate a clear, but non-significant, trend favoring SASB.

Synthetic aperture sequential beamforming has never previously been used for patient scanning. In the previous *in vivo* study comparing SASB with conventional ultrasound, the image quality using SASB was found to be slightly, but significantly better when healthy volunteers were scanned (Hemmsen et al. 2012a). The difference between scanning young, slim, healthy individuals and severely diseased cancer patients is substantial. Several patients had undergone previous surgery on the liver, altering the anatomic layout; some patients had thicker abdominal fat layers, higher heart rates leading to more movement around the left liver lobe or gas-filled intestines ruining the view, and typically could not cooperate as well as healthy subjects because of pain and discomfort. The small, but significant improvement, SASB previously has had on image quality could very well be blurred by these circumstances. Despite these scanning challenges and the substantial data reduction, SASB provides clinical ultrasound images with a quality at least as high as that of conventional ultrasound. The hypothesis of this study is therefore accepted.

Tissue motion has in previous reports been reported to degrade the quality of synthetic aperture images (Gammelmark and Jensen 2014; Jensen et al. 2006; Pedersen et al. 2007). All patients were asked to lie still and hold their breath during the recording of the ultrasound sequences, but only a few were able to comply completely with our request. Compared with the study by Hemmsen et al. (2012a) more movement artifacts were therefore present in the recordings, but this still did not affect the image quality evaluations, further confirming the suitability of SASB for clinical use.

The major limitation of the evaluation setup and SASB in its current form is that the generated sequences are displayed only in the most "raw" format the scanner can produce. There is no application of image-enhancing algorithms, for example, a speckle

filter, and the sequences are therefore not truly suited for evaluation of pathologic changes from a diagnostic perspective. The radiologists were therefore told not to consider differential diagnoses, but rather to treat the pathologic changes as a general part of the visual clinical evaluation of image quality. Future studies are in progress in which specific image-improving algorithms will supplement the technique and presumably reveal the diagnostic efficacy of SASB.

The major advantage of the evaluation setup is the interleaved recording of the different techniques in question. This ensures the most simultaneous recording possible, even if the organ/structure of interest moves. Furthermore, the setup allows recording and subsequent visualization of real-time sequences and not only still images, as several other image quality evaluation studies do (Kim et al. 2006; Sodhi et al. 2005; Tanaka et al. 2000; Yen et al. 2008).

## CONCLUSIONS

Ultrasound imaging using SASB has successfully been illustrated and evaluated in a true clinical setting, that is, a hospital. Patients with cancer of the liver were scanned simultaneously with conventional ultrasound and SASB, and the sequences were subsequently compared and evaluated in a double-blinded setup by radiologists. The primary advantage of SASB is data reduction by a factor of 64 compared with conventional ultrasound, and despite this, the evaluations revealed an insignificant advantage for SASB.

## REFERENCES

Food and Drug Administration (FDA). Guidance for industry and FDA staff—Information for manufacturers seeking marketing clearance of diagnostic ultrasound systems and transducers. Tech Rep. 2008. U.S. Department of Health and Human Services, FDA, Center for Devices and Radiologic Health.

Freyd M. The graphic rating scale. J Educ Psychol 1923;14:83–102.

Gammelmark KL, Jensen JA. Multielement synthetic transmit aperture imaging using temporal encoding. IEEE Trans Med Imaging 2003; 22:552–563.

Gammelmark KL, Jensen JA. 2-D tissue motion compensation of synthetic transmit aperture images. IEEE Trans Ultrason Ferroelectr Freq Control 2014;61:594–610.

Hansen JM, Hemmsen MC, Jensen JA. An object-oriented multi-threaded software beamformation toolbox. Proc SPIE 2011;7968.

Hemmsen MC, Hansen PM, Lange T, Hansen JM, Hansen KL, Nielsen MB, Jensen JA. In vivo evaluation of synthetic aperture sequential beamforming. Ultrasound Med Biol 2012a;38:708–716.

Hemmsen MC, Nikolov SI, Pedersen MM, Pihl MJ, Enevoldsen MS, Hansen JM, Jensen JA. Implementation of a versatile research data acquisition system using a commercially available medical ultrasound scanner. IEEE Trans Ultrason Ferroelectr Freq Control 2012b;59:1487–1499.

Hemmsen MC, Petersen MM, Nikolov SI, Nielsen MB, Jensen JA. Ultrasound image quality assessment: A framework for evaluation of clinical image quality. Proc SPIE 2010;7629.

Jensen JA, Nikolov SI, Gammelmark KL, Pedersen MH. Synthetic aperture ultrasound imaging. Ultrasonics 2006;44(Suppl.):e5–e15.

Karaman M, Li PC, O'Donnell M. Synthetic aperture imaging for small scale systems. IEEE Trans Ultrason Ferroelectr Freq Control 1995; 42:429–442.

Kim C, Yoon C, Park JH, Lee Y, Kim WH, Chang JM, Choi BI, Song TK, Yoo YM. Evaluation of ultrasound synthetic aperture imaging using bidirectional pixel-based focusing: Preliminary phantom and in vivo breast study. IEEE Trans Biomed Eng 2013;60: 2716–2724.

Kim SH, Lee JM, Kim KG, Kim JH, Han JK, Lee JY, Choi BI. Comparison of fundamental sonography, tissue-harmonic sonography, fundamental compound sonography, and tissue-harmonic compound sonography for focal hepatic lesions. Eur Radiol 2006;16: 2444–2453.

Kim WH, Chang JM, Kim C, Park J, Yoo Y, Moon WK, Cho N, Choi BI. Synthetic aperture imaging in breast ultrasound: A preliminary clinical study. Acad Radiol 2012;19:923–929.

Kortbek J, Jensen JA, Gammelmark KL. Sequential beamforming for synthetic aperture imaging. Ultrasonics 2013;53:1–16.

Pedersen MH, Gammelmark KL, Jensen JA. In-vivo evaluation of convex array synthetic aperture imaging. Ultrasound Med Biol 2007;33:37–47.

Sherwin CW, Ruina JP, Rawcliffe RD. Some early developments in synthetic aperture radar systems. IRE Trans Mil Elect 1962;MIL-6: 111–115.

Sodhi KS, Sidhu R, Gulati M, Saxena A, Suri S, Chawla Y. Role of Tissue harmonic imaging in focal hepatic lesions: Comparison with conventional sonography. J Gastroenterol Hepatol 2005;20: 1488–1493.

Tanaka S, Oshikawa O, Sasaki T, Ioka T, Tsukuma H. Evaluation of tissue harmonic imaging for the diagnosis of focal liver lesions. Ultrasound Med Biol 2000;26:183–187.

Thomson RN. Transverse and longitudinal resolution of the synthetic aperture focusing technique. Ultrasonics 1984;22:9–15.

Yen CL, Jeng CM, Yang SS. The benefits of comparing conventional sonography, real-time spatial compound sonography, tissue harmonic sonography, and tissue harmonic compound sonography of hepatic lesions. Clin Imaging 2008;32:11–15.

# Appendix 2

http://dx.doi.org/10.1016/j.ultrasmedbio.2014.06.004

● *Original Contribution*

# VOLUME FLOW IN ARTERIOVENOUS FISTULAS USING VECTOR VELOCITY ULTRASOUND

PETER MØLLER HANSEN,* JACOB BJERRING OLESEN,[†] MICHAEL JOHANNES PIHL,[†] THEIS LANGE,[‡]
SØREN HEERWAGEN,* MADS MØLLER PEDERSEN,* MARIANNE RIX,[§] LARS LÖNN,*[∥]
JØRGEN ARENDT JENSEN,[†] and MICHAEL BACHMANN NIELSEN*

*Department of Radiology, Copenhagen University Hospital, Copenhagen, Denmark; [†]Center for Fast Ultrasound Imaging,
Department of Elec. Eng., Technical University of Denmark, Lyngby, Denmark; [‡]Department of Biostatistics, University of
Copenhagen, Copenhagen, Denmark; [§]Department of Nephrology, Copenhagen University Hospital, Copenhagen, Denmark;
and [∥]Department of Vascular Surgery, Copenhagen University Hospital, Copenhagen, Denmark

**Abstract**—Volume flow in arteriovenous fistulas for hemodialysis was measured using the angle-independent ultrasound technique Vector Flow Imaging and compared with flow measurements using the ultrasound dilution technique during dialysis. Using an UltraView 800 ultrasound scanner (BK Medical, Herlev, Denmark) with a linear transducer, 20 arteriovenous fistulas were scanned directly on the most superficial part of the fistula just before dialysis. Vector Flow Imaging volume flow was estimated with two different approaches, using the maximum and the average flow velocities detected in the fistula. Flow was estimated to be 242 mL/min and 404 mL/min lower than the ultrasound dilution technique estimate, depending on the approach. The standard deviations of the two Vector Flow Imaging approaches were 175.9 mL/min and 164.8 mL/min compared with a standard deviation of 136.9 mL/min using the ultrasound dilution technique. The study supports that Vector Flow Imaging is applicable for volume flow measurements. (E-mail: pdmhansen@gmail.com)    © 2014 World Federation for Ultrasound in Medicine & Biology.

*Key Words:* Vector Flow Imaging, Arteriovenous fistula, Ultrasound, Volume flow estimation, Flow velocity estimation, Hemodialysis, Ultrasound dilution technique.

## INTRODUCTION

Patients with severe renal insufficiency and end-stage renal disease require renal replacement therapy (*i.e.,* peritoneal dialysis, hemofiltration, or hemodialysis). Eighty percent of the patients with end-stage renal disease in Denmark receive hemodialysis, the predominant form of renal replacement therapy (Heaf 2012). The preferred access for long-term hemodialysis is the surgically created communication between a native artery and superficial vein in the upper extremity (*i.e.,* the arteriovenous fistula) (Besarab and Work 2006; Bittl 2010; Konner et al. 2003). Up to 60% of patients will experience some degree of dysfunction during the first 18 mo after its creation. Dysfunction mainly is due to incomplete maturation of the shunt, stenosis, or thrombosis (Huijbregts et al. 2008).

To preserve arteriovenous fistula patency, regular clinical assessment and monitoring of blood flow is recommended (Shetty and Whittier 2012; Soule and Henry 2007; Whittier 2009). Flow measurements can be performed using both direct and indirect techniques, including, among others, conventional Doppler ultrasound (direct) and ultrasound dilution technique (UDT) (indirect). The latter is considered the reference method for volume flow estimation in arteriovenous fistulas (Wijnen et al. 2006). The technique is based on the indicator dilution method, where a known quantity of indicator substance is injected into the bloodstream. The indicator concentration is subsequently measured, and the change in indicator concentration downstream is plotted as a function of time. In UDT saline is used as the indicator. Saline dilutes the protein concentration of the blood and reduces the ultrasound velocity in the blood proportionally. The ultrasound velocity is continuously monitored by a computer with two matched sensors attached to the dialysis blood lines, which must be reversed from normal position to create recirculation between the dialysis needles (Krivitski 1995a, 1995b).

Address correspondence to: Peter Møller Hansen, Rigshospitalet, Radiologisk Klinik, Blegdamsvej 9, 2100 Copenhagen OE, Denmark. E-mail: pdmhansen@gmail.com

The disadvantages of UDT are the need for the dialysis to be up and running and the exchange of dialysis blood lines before an estimation of flow is obtainable. This process prolongs the dialysis and is uncomfortable for both patient and dialysis nurse.

A direct method for estimating volume flow is using conventional Doppler. This technique provides real-time quantitative velocity estimations along with morphologic information and has been used to obtain volumetric flow rates for decades (Gill 1979, 1985; Lewis et al. 1986). However, Doppler ultrasound is angle dependent, highly operator reliant, and challenging to use directly on the irregular superficial fistula (Lui et al. 2005; Teodorescu et al. 2012; Wiese and Nonnast-Daniel 2004; Zanen et al. 2001).

To circumvent the angle dependency of conventional Doppler, the angle-independent ultrasound technique Vector Flow Imaging was proposed by Jensen and Munk (1998). Vector Flow Imaging provides simultaneously the axial and transverse velocity components of the blood flow. The technique creates a double-oscillating pulse-echo field by manipulating the apodization function during receive beamforming. A conventional ultrasound pulse for flow estimation is transmitted, and the received echoes are beamformed to yield three beams in parallel. One uses conventional beamforming for estimating the axial velocity, and the other two beams are used for estimating the transverse velocity component. By combining the velocity components along the two axes, two-dimensional (2-D) vector velocities are obtained. These velocities are subsequently multiplied by the cross-sectional area of the fistula to calculate volume flow.

Vector Flow Imaging and its clinical application is described further by Jensen and Munk (1998), Udesen and Jensen (2006), and Udesen et al. (2007), and the clinical use by Hansen et al. (2011), Pedersen et al. (2012) and Hansen et al. (2013). Volume flow measurements, using Vector Flow Imaging on an experimental scanner, has previously been validated *in vivo* against magnetic resonance angiography with a high correlation (Hansen et al. 2009a, 2009b).

The purpose of the study was to investigate the accuracy and variability of Vector Flow Imaging for volume flow measurements on arteriovenous fistulas. The hypotheses are that Vector Flow Imaging and UDT provide equal estimates of volume flow in arteriovenous fistulas, and the standard deviation of the estimates using Vector Flow Imaging is improved compared with UDT.

## MATERIALS AND METHODS

### Patients

Twenty-two patients with mature (>3 mo since creation) and functional arteriovenous fistulas from the hospital dialysis center were asked to participate and 20 were included. One patient declined, and one more could not participate because of logistics during hospitalization. The inclusion criteria was possession of a well-functioning arteriovenous fistula, defined as a fistula that was not in imminent risk of referral to intervention, and where the last intervention was at least 6 mo ago. Of the 20 fistulas, 13 were lower and 7 were upper arm fistulas. Written informed consent was obtained. The local Ethics Committee waived approval because ultrasound scanning of arteriovenous fistulas is considered a routine procedure.

### Scan setup

A commercial scanner (UltraView 800, BK Medical, Herlev, Denmark) was used with a linear transducer with a center frequency of 9 MHz (8670, BK Medical, Herlev, Denmark).

Before scanning blood pressure and heart rate were confirmed to be in habitual pre-dialysis level compared with the two previous dialysis sessions ($\pm$ 20 mm Hg systolic, $\pm$ 10 mm Hg diastolic).

Initial B-mode scanning transversely and longitudinally directly on the fistula was performed for orientation purposes. Because UDT measures flow between the dialysis needles, the section between the two puncture sites was scanned using Vector Flow Imaging. At the same time, the part of the fistula in this section was inspected for branching because deviation of flow would necessitate estimation and summation of flow in the individual branches to ensure correct comparison with UDT.

Vector Flow Imaging provides 2-D images of the blood flow velocity where each pixel contains quantitative information about direction and velocity magnitude. To facilitate visualization of the flow, the scanner can superimpose arrows in real-time on the color-coded pixels. The arrows indicate flow direction and the length of the arrows indicate velocity magnitude. It is therefore feasible to immediately determine whether the flow is laminar or disturbed (Fig. 1). The presence of laminar flow can be judged using the arrows of Vector Flow Imaging. Starting with a pulse repetition frequency where no aliasing is present, the flow in the center of the vessel can be evaluated. Lowering the pulse repetition frequency stepwise and ignoring the increasing aliasing in the middle of the vessel where the flow velocities peak, the slower flow along the vessel walls can be evaluated. The assessment of laminar flow was confirmed off line in Matlab (MathWorks, Natick, MA, USA) using streamlines. It is important to emphasize that this assessment of flow only can be performed in the 2-D scan plane. The color box was adjusted to cover as much of the fistula as possible to obtain a maximum amount of flow data.
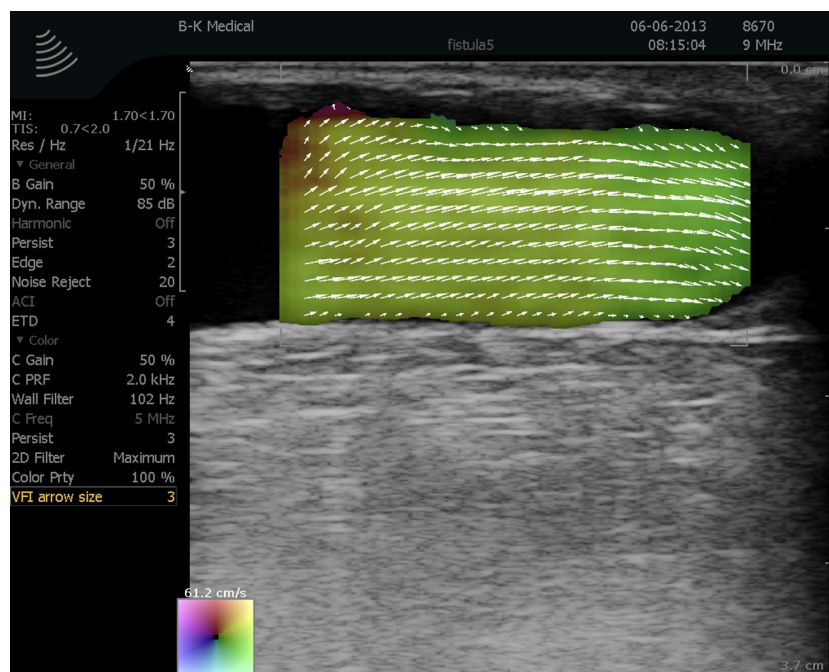
Fig. 1. Longitudinal scan of an arteriovenous fistula with Vector Flow Imaging. The *arrows* illustrate flow direction and velocity magnitude. Notice the longer arrows toward the middle of the fistula, indicating higher flow velocities. Also notice the angle of insonation.

To estimate the most reliable volume flow, a part of the fistula with approximately laminar flow and regular diameter was located. If not achievable between the puncture sites, it was typically necessary to move the transducer beyond the proximal puncture site. The fistula was then rescanned transversely to measure two perpendicular diameters of the vessel. The built-in length gauge of the scanner was used to manually measure the diameter from the superficial to the deep tunica intima and the corresponding mediolateral diameter (Fig. 2). The diameters were measured three times, and the mean values were used for area calculation. To obtain cohesive measurements of cross-sectional area and flow velocity, a small mark was made on the skin next to the transducer.

The transducer was then rotated back to record blood flow longitudinally, making sure the mark on the skin corresponded to the center of the transducer. To ensure that the longitudinal Vector Flow Imaging recording was from the center of the fistula, the transducer was positioned where the fistula had its widest diameter, and the tunica intima was visible in both the superficial and deep vessel wall. Fifteen seconds of recording was made.

The transducer was raised and repositioned between each recording, and all scans were performed with a very light touch of the transducer on the skin to avoid deformation of the fistula. In 19 of the fistulas the angle of insonation was approximately 90 degrees, and one fistula's position necessitated an angle of insonation of 70
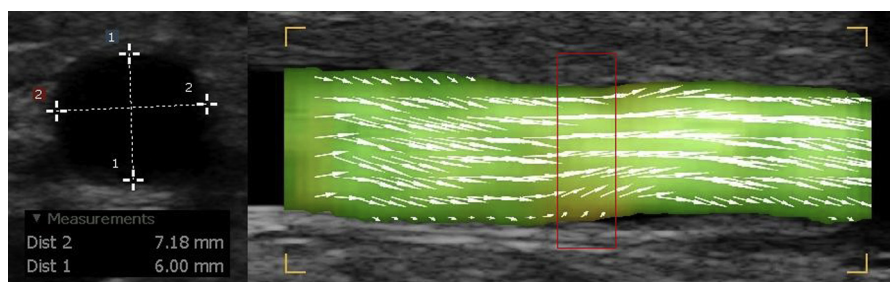


Fig. 2. Cohesive measurements of cross-sectional diameters and longitudinal Vector Flow Imaging. Notice the arrows overlapping in several places indicating approximately laminar flow in the scan plane. The *red box* illustrates where the flow velocities were measured and corresponds to the part of the fistula, where the cross-sectional diameters were measured.

degrees. The pulse repetition frequency was adjusted for each fistula to the lowest level where no aliasing was seen. Seventeen of the fistulas were scanned with a pulse repetition frequency of either 2.0, 3.0 or 4.1 kHz. The remaining three were scanned with a pulse repetition frequency of 5.0, 7.0 and 11.9 kHz, respectively. Wall filter and color gain was in each case adjusted to the level providing optimal filling of the fistula without flow being visualized outside the fistula. All other settings remained in default mode.

In the interest of comparing UDT with intra-observer variability of Vector Flow Imaging, enough recordings were made to ensure at least three uninterrupted 15-s recordings. The scans were performed before insertion of the hemodialysis needles and start of the dialysis, and the flow measurements with UDT were made as soon as possible after the final recording with Vector Flow Imaging to minimize dialysis-induced alterations of the flow. Based on the Vector Flow Imaging recordings and the measured geometry of the vessel, volume flow in the fistula was calculated.

*Vector Flow Imaging*

Vector Flow Imaging is approved by the U.S. Food and Drug Administration for clinical scanning. This approval does not include quantitative measurements using the approach because the Food and Drug Administration demands a large, quantitative study for such an approval. The investigations previously performed on a flow rig and in clinical studies indicate a negative bias around −10% for volume flow measurements (Hansen et al. 2013; Udesen et al. 2007). This is due to a bias in the estimation scheme, which can be compensated for in an optimized setup as demonstrated by Jensen (2013). Such a scheme could be implemented in the commercial scanner.

The scanner was set to record 15-s sequences with Vector Flow Imaging at a frame rate of 15 frames/s (*i.e.,* each sequence consists of 225 2-D vector velocity maps).

*Ultrasound dilution technique*

The UDT measurements were made using Transonic HD03 Flow-QC hemodialysis monitor (Transonic Systems Inc., Ithaca, NY, USA) and performed by dialysis nurses with a minimum 5 y of experience with UDT.

The hemodialysis monitor provides on-screen instructions for all steps of the flow measurement. First step is to reverse the blood lines and attach the sensors. The dialysis flow rate is then reduced to 250–300 mL/min, and ultrafiltration is turned off. Ten mL saline is injected with a slow steady flow into the circuit, and the monitor then provides a flow estimate.

A minimum of three UDT measurements were made per patient for comparison of volume flow and intra-observer variability.

*Calculation of volume flow from Vector Flow Imaging*

Two approaches are suggested for calculating the volumetric flow rate. Both techniques are tested off-line using in-house–made Matlab scripts. The scripts were developed through scanning of a flow phantom and four patients with arteriovenous fistulas in a pilot study. Based on these initial scans the two suggested approaches were implemented in Matlab.

The basic idea of the implemented methods is to calculate the cross-sectional area of the fistula and then use the Vector Flow Imaging measurement for estimating an average velocity through this area. Multiplying the cross-sectional area by the average velocity yields the flow rate. The difference between the two suggested methods is the estimation of the average velocity as the calculation of the area is the same. The first approach (VFImax) estimates the average velocity by detecting the peak velocity in each 2-D map of vector velocities and then divides this by two. Taking half the peak velocity yields the average velocity under the assumption that the flow profile is parabolic and circular symmetric. The second approach (VFIavg) calculates the mean velocity across the flow profile and uses this as input for estimating the flow rate. The latter approach still requires the flow to be circular symmetric, but the assumption of having a parabolic profile is not necessary. Intuitively, VFIavg should produce a more robust estimate compared with VFImax because it requires fewer assumptions.

Both methods use all 225 successive maps of vector velocities as input to the flow rate estimator. This corresponds to the 15 s of data acquisition. The average flow velocity was calculated from the 2-D velocity maps assuming circular symmetric flow, even though all of the fistulas were more or less elliptical with the smaller diameter going from superficial to deep (*i.e.,* the scan plane). To reduce the risk of underrating the volume flow because of improper underestimated area, the area was in each case calculated as an ellipse from the perpendicular diameters measured in the transversal scan. To ensure a constant diameter throughout the investigated flow region, only a fraction of the examined area was used in the volume flow estimations. The selected region accounts for approximately 15% of the examined area, which corresponds to roughly 4 mm of the fistula (see Fig. 2).

*Statistical analysis*

All flow measurements were analyzed using two-way ANOVA with a person-specific factor and a type of measurement factor. We allowed for different standard

deviations of the error terms for each of the three types of measurements by stratification. Thus the reported standard deviations reflect the variation between consecutive measurements made on the same person. Differences between measurements types are reported using mean differences and relative differences. The assumption of normality was confirmed using probability plots (QQ-plots).

## RESULTS

Flow results are visualized in Figures 3 and 4, which indicate that volume flow measured with Vector Flow Imaging is lower than volume flow measured with UDT in most cases.

The mean values of VFImax and VFIavg are 242 mL/min (CI: 161; 323) and 404 mL/min (CI: 325; 483) lower than UDT, respectively. This corresponds to 39% and 31% below the UDT estimations, and the difference is significant ($p < 0.001$ for both VFImax and VFIavg). The observed standard deviations for UDT, VFImax, and VFIavg are 136.9 mL/min, 175.9 mL/min and 164.8 mL/min, respectively. This corresponds to 9.4%, 13.4% and 15.8%, respectively.

The flow measurements for patient 7 differ substantially from the rest of the patients. The measurements using VFImax and VFIavg range from 4871 mL/min to 6557 mL/min and 2671 mL/min to 3806 mL/min, respectively (see Fig. 4). The measurements using VFImax are unrealistically high for an unaffected patient at rest, and the flow ranges are remarkable compared with the rest of the patients. The second largest flow ranges in the

study are observed for patients 16 (VFImax, range 1525 mL/min to 2020 mL/min) and 5 (VFIavg, range 1033 mL/min to 1285 mL/min). Patient 7's fistula was difficult to scan because of the anatomic conditions of the vessel with a very tortuous path, branching, and alternating diameter. It was the only fistula necessitating an angle of insonation other than 90 degrees, and where flow required a PRF setting of 11.9 kHz (maximum) to avoid aliasing. Furthermore it was the only fistula where it was not possible to locate a section of the fistula with approximately laminar blood flow (Fig. 5). It is worth mentioning that for patient 7 VFIavg by far provides the best flow estimate compared with UDT, and it is the only fistula where the two Vector Flow Imaging approaches provide very different results. If the measurements for patient 7 are considered as outliers and left out of the analysis, the flow results change substantially.

Without patient 7 the mean values of VFImax and VFIavg are 304 mL/min (CI: 235; 374) and 437 mL/min (CI: 366; 509) lower than UDT, respectively. This corresponds to 31% and 35% below the UDT estimations, and the difference is significant ($p < 0.001$ for both VFImax and VFIavg). The observed standard deviations for UDT, VFImax, and VFIavg are 132.9 mL/min, 74.6 mL/min and 62.3 mL/min, respectively. This corresponds to 9.4%, 7.4% and 6.9%, respectively.

Except for patient 7, none of the patients had any branching of the fistula in the section where the measurements were performed. Unfortunately, the anatomy of patient 7's fistula made it impossible to perform an estimation of the individual branches with Vector Flow Imaging.
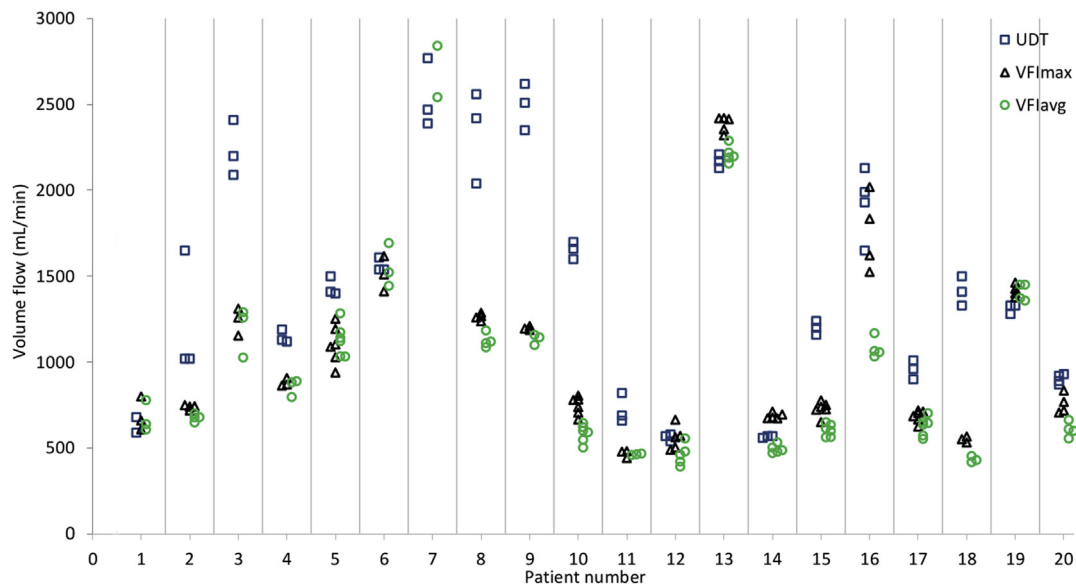


Fig. 3. Flow results for all patients. The y axis have been limited at 3000 mL/min, leaving out the upper VFIavg measurements and all of the VFImax measurements for patient 7. Each symbol indicates one measurement with the given technique.
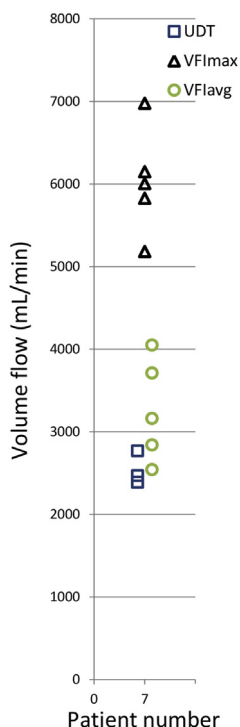
Fig. 4. Flow results for patient 7. Each symbol indicates one measurement with the given technique.

The time between the last Vector Flow Imaging recording and the first UDT measurement varied between 11 and 90 min (mean 47 min, median 39 min). This includes the time to insert dialysis needles and start the dialysis.

## DISCUSSION

### Summary and comparison of results

The flow results calculated from the Vector Flow Imaging recordings are on average substantially lower than the corresponding UDT results. The repeatability of the flow measurements using Vector Flow Imaging is improved significantly when patient 7 is excluded. Based on the absolute numbers of the standard deviations, VFImax and VFIavg replicate themselves approximately twice as well as UDT. Previous studies comparing duplex ultrasound flow measurements with UDT measurements found the duplex measurements to be 30% lower on average (Huisman et al. 2005; Schwarz et al. 2003), similar to our results using Vector Flow Imaging. Huisman et al. (2005) found the within-session variation of duplex flow measurements to be 11.6% compared with 7.4% (VFImax) and 6.9% (VFIavg) in our study.

### Difficulties with UDT comparison

Because of constant changes in mean arterial pressure, central venous pressure, and vascular resistance of the access circuit during each dialysis session, the volume flow varies correspondingly. Previous studies using several UDT measurements during the first 3 h of a single dialysis session, show flow variations up to 40%–50%, and these variations could be more substantial from session to session. It is therefore proposed that a change in volume flow between dialysis sessions must be greater than 25%–33% to be significantly different from background variation (Huisman et al. 2005; Paulson et al. 2012). To ensure the best comparison of volume flow from session to session, the flow measurements should each time be made in the very beginning of the dialysis session (Huisman et al. 2005; Paulson et al. 2012). The flow measurements obtained from Vector Flow Imaging (or any other flow measurement technique) just before start of dialysis can therefore not necessarily be directly compared with flow measurements obtained during the dialysis. However, it should not lead to a systematic error, because the flow both increases and decreases
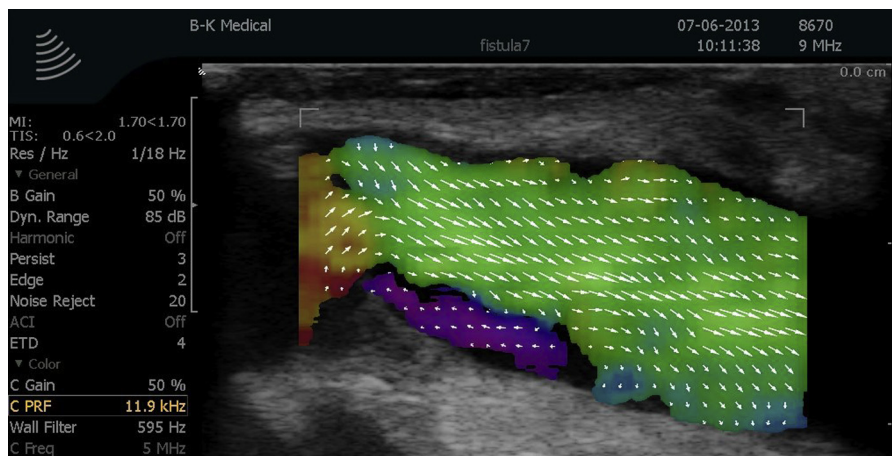


Fig. 5. Fistula of patient 7. Notice the retrograde *(purple)* flow in the deep part of the fistula. This was the only fistula, where an area with approximately laminar flow could not be found.

during dialysis. To minimize the hemodynamic variations during dialysis, time between ultrasound scanning and UDT measurement was reduced as much as possible.

Insufficient mixing of the diluting agent (saline) in the blood when using UDT, will also lead to erroneous and unstable flow estimations (Depner and Krivitski 1995). The performance of UDT therefore improves when the blood flow velocity increases, because better mixing conditions of saline and blood occurs at high flow velocities. This is vaguely supported by our findings. The group of patients whose average Vector Flow Imaging measurements (based on VFImax) deviate the most from their average UDT measurements (more than 30%, patients 3, 8-11, 15 and 18) have a mean flow velocity of 11.7 cm/s (median velocity 11.3 cm/s). The group whose average Vector Flow Imaging measurements deviate less than 30% (patients 1, 2, 4–6, 12–14, 16, 17, 19 and 20) have a mean flow velocity of 16.4 cm/s (median velocity 11.7 cm/s). This difference is not statistically significant but suggests that Vector Flow Imaging and UDT correlates better at higher flow velocities. The average UDT measurements are calculated according to the manufacturers guidelines.

*Advantages of Vector Flow Imaging*

One of the strengths of Vector Flow Imaging is the ability to immediately assess whether the flow is laminar or disturbed and where in the scan plane the highest flow velocities are detected. This is done at all angles of insonation because of the angle independence. In all fistulas, except number 7, it was possible to locate an area with laminar flow in the scan plane, and a more or less parabolic flow profile at the mea-
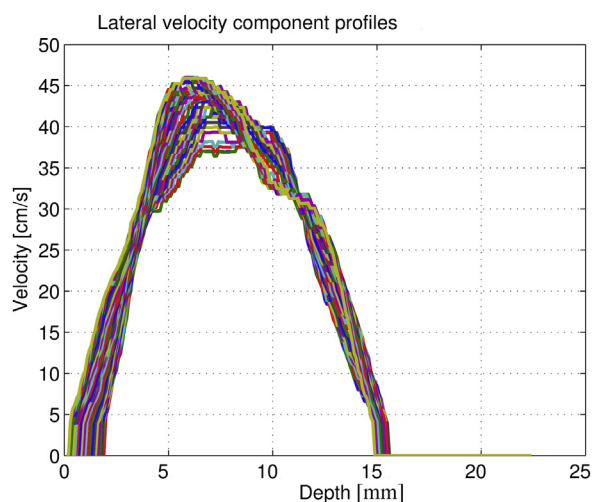


Fig. 6. Parabolic flow profile from patient 12. The center of the fistula is approximately 7.5 mm from the skin surface. Velocities are between 45 cm/s in the middle of the vessel and 0 cm/s at the vessel wall (with a PRF of 3.0 kHz).

surement site (Fig. 6). The ability to immediately locate these areas during the scans eliminates the need to assume and potentially misjudge these flow circumstances when using conventional spectral Doppler ultrasound. Furthermore the operator is not limited by size or placement of the Doppler sample volume. The angle independence is also an advantage when holding the transducer against the skin. Just the weight of the transducer is enough to compress and deform the fistula, thereby creating disturbed and unpredictable flow, and it is therefore a challenge to obtain the recommended angle of insonation less than 60 degrees for conventional spectral estimation (Teodorescu et al. 2012). Using Vector Flow Imaging the operator can focus on scanning with a very light touch without deforming the fistula. The accuracy of Vector Flow Imaging will most likely improve when the bias of the velocity estimation is resolved.

*Disadvantages of Vector Flow Imaging*

One of the limitations of Vector Flow Imaging compared with UDT is the 2-D visualization of the flow direction and velocities. This makes Vector Flow Imaging most suited for calculation of volume flow in a circular blood vessel, because it is only possible to obtain data from the longitudinal scan plane going from top to bottom of the vessel. All cross-sectional areas were calculated as ellipses to avoid underestimation of volume flow from improper underestimated area, but it is still only an approximation, because no flow data is obtained from the transversal scan plane. The recording of cohesive measurements of longitudinal flow and cross-sectional diameters is also a major challenge but should not lead to systematic error.

**CONCLUSIONS**

Using the commercially available ultrasound technique Vector Flow Imaging, volume flow has been estimated by scanning directly on 20 arteriovenous fistulas. The flow estimations were compared with UDT and were on average 31% and 35% lower, depending on the approach used, but the standard deviation of Vector Flow Imaging was significantly better than UDT, leading to more stable estimations of volume flow. A single outlier was excluded from the analysis. The best coherence between Vector Flow Imaging and UDT was found in the fistulas with the highest flow velocities. As opposed to UDT, the performance of Vector Flow Imaging is not dependent on any minimum flow velocity to achieve sufficient mixing of diluting agent and blood. Vector Flow Imaging could therefore theoretically perform better than UDT in fistulas with lower flow velocities. Vector Flow Imaging has the potential to be a useful tool to obtain both

morphologic information and quantitative information about volume flow in arteriovenous fistulas, and the angle independence of Vector Flow Imaging makes the flow estimation intuitive and less operator dependent. Future studies will reveal the ability of Vector Flow Imaging to predict developing stenoses in arteriovenous fistulas.

## REFERENCES

Clinical practice guidelines for vascular access. In: Besarab A, Work J, (eds). Am J Kidney Dis 2006;48(Suppl 1):S176–S247.

Bittl JA. Catheter interventions for hemodialysis fistulas and grafts. JACC Cardiovasc Interv 2010;3:1–11.

Depner TA, Krivitski NM. Clinical measurement of blood flow in hemodialysis access fistulae and grafts by ultrasound dilution. ASAIO J 1995;41:M745–749.

Gill RW. Pulsed Doppler with B-mode imaging for quantitative blood flow measurement. Ultrasound Med Biol 1979;5:223–235.

Gill RW. Measurement of blood flow by ultrasound: Accuracy and sources of error. Ultrasound Med Biol 1985;11:625–641.

Hansen KL, Udesen J, Oddershede N, Henze L, Thomsen C, Jensen JA, Nielsen MB. In vivo comparison of three ultrasound vector velocity techniques to MR phase contrast angiography. Ultrasonics 2009a; 49:659–667.

Hansen KL, Udesen J, Thomsen C, Jensen JA, Nielsen MB. In Vivo Validation of a Blood Vector Velocity Estimator with MR Angiography. IEEE Trans Ultrason Ferroelectr Freq Control 2009b;56:91–100.

Hansen KL, Pedersen MM, Møller-Sørensen H, Kjaergaard J, Nilsson JC, Lund JT, Jensen JA, Nielsen MB. Intraoperative cardiac ultrasound examination using vector flow imaging. Ultrason Imaging 2013;35:318–332.

Hansen PM, Pedersen MM, Hansen KL, Nielsen MB, Jensen JA. New technology: Demonstration of a vector velocity technique. Ultraschall Med 2011;32:213–215.

Heaf J, (ed). Danish Nephrology Registry (DNR) annual report 2012. Herlev: Danish Society of Nephrology; 2013.

Huijbregts HJT, Bots ML, Wittens CHA, Schrama YC, Moll FL, Blankestijn PJ. CIMINO study group. Hemodialysis arteriovenous fistula patency revisited: Results of a prospective, multicenter initiative. Clin J Am Soc Nephrol 2008;3:714–719.

Huisman RM, van Dijk M, de Bruin C, Loonstra J, Sluiter WJ, Zeebregts CJ, van den Dungen JAM. Within-session and between-session variability of haemodialysis shunt flow measurements. Nephrol Dial Transplant 2005;20:2842–2847.

Jensen JA, Munk P. A new method for estimation of velocity vectors. IEEE Trans Ultrason Ferroelectr Freq Control 1998;45:837–851.

Jensen JA. Optimization of transverse oscillating fields for vector velocity estimation with convex arrays. Proceedings of IEEE International Ultrasonics Symposium 2013;1753–1756.

Konner K, Nonnast-Daniel B, Ritz E. The arteriovenous fistula. J Am Soc Nephrol 2003;14:1669–1680.

Krivitski NM. Theory and validation of access flow measurement by dilution technique during hemodialysis. Kidney Int 1995a;48: 244–250.

Krivitski NM. Novel method to measure access flow during hemodialysis by ultrasound velocity dilution technique. ASAIO J 1995b;41: M741–745.

Lewis P, Psaila JV, Davies WT, McCarty K, Woodcock JP. Measurement of volume flow in the human common femoral artery using a duplex ultrasound system. Ultrasound Med Biol 1986;12: 777–784.

Lui EYL, Steinman AH, Cobbold RSC, Johnston KW. Human factors as a source of error in peak Doppler velocity measurement. J Vasc Surg 2005;42:972–979.

Paulson WD, Moist L, Lok CE. Vascular access surveillance: An ongoing controversy. Kidney Int 2012;81:132–142.

Pedersen MM, Pihl MJ, Haugaard P, Hansen JM, Hansen KL, Nielsen MB, Jensen JA. Comparison of real-time in vivo spectral and vector velocity estimation. Ultrasound Med Biol 2012;38: 145–151.

Schwarz C, Mitterbauer C, Boczula M, Maca T, Funovics M, Heinze G, Lorenz M, Kovarik J, Oberbauer R. Flow monitoring: Performance characteristics of ultrasound dilution versus color Doppler ultrasound compared with fistulography. Am J Kidney Dis 2003;42: 539–545.

Shetty A, Whittier WL. Does regular surveillance improve the long-term survival of arteriovenous fistulas? Int J Nephrol 2012;539608.

Soule JL, Henry ML. Noninvasive methods to identify early vascular access dysfunction. Semin Vasc Surg 2007;20:164–166.

Teodorescu V, Gustavson S, Schanzer H. Duplex Ultrasound evaluation of hemodialysis access: A detailed protocol. Int J Nephrol 2012;508956.

Udesen J, Nielsen MB, Nielsen KR, Jensen JA. Examples of in vivo blood vector velocity estimation. Ultrasound Med Biol 2007;33: 541–548.

Udesen J, Jensen JA. Investigation of transverse oscillation method. IEEE Trans Ultrason Ferroelectr Freq Control 2006;53:959–971.

Whittier WL. Surveillance of hemodialysis vascular access. Semin Intervent Radiol 2009;26:130–138.

Wiese P, Nonnast-Daniel B. Colour Doppler ultrasound in dialysis access. Nephrol Dial Transplant 2004;19:1956–1963.

Wijnen E, Essers S, van Meijel G, Kooman JP, Tordoir J, Leunissen KML, van der Sande FM. Comparison between two on-line reversed line position hemodialysis vascular access flow measurement techniques: Saline dilution and thermodilution. ASAIO J 2006;52:410–415.

Zanen AL, Toonder IM, Korten E, Wittens CH, Diderich PN. Flow measurements in dialysis shunts: Lack of agreement between conventional Doppler, CVI-Q, and ultrasound dilution. Nephrol Dial Transplant 2001;16:395–399.

# Appendix 3

# Arteriosclerotic Lesions in the Superficial Femoral Artery (SFA) Characterized with Velocity Ratios using Vector Velocity Ultrasound

Peter Møller Hansen[1], Kristoffer Lindskov Hansen[1], Mads Møller Pedersen[1], Lars Lönn[1, 3], Jørgen Arendt Jensen[2], Michael Bachmann Nielsen[1]

[1]Dept. of Radiology, Copenhagen University Hospital, Rigshospitalet,

DK-2100 Copenhagen, Denmark

[2]Center for Fast Ultrasound Imaging, Dept. of Elec. Eng., Bldg. 349,

Technical University of Denmark, DK-2800 Lyngby, Denmark

[3]Dept. of Vascular Surgery, Copenhagen University Hospital, Rigshospitalet,

DK-2100 Copenhagen, Denmark


Corresponding author: Peter Møller Hansen

Address: Blegdamsvej 9, 2100 Copenhagen OE, Denmark

Phone: 004526830107

Email: pdmhansen@gmail.com

**Abstract**

Velocity ratios (intrastenotic blood flow velocity divided by prestenotic velocity) from arteriosclerotic stenoses and plaques in the superficial femoral artery of 11 patients were obtained using the commercially available vector velocity ultrasound technique Vector Flow Imaging. The stenosis degree, expressed as percentage diameter reduction of the artery, was determined from digital subtraction angiography and compared to the velocity ratios. A correlation coefficient $r$ of 0.45 was calculated and a velocity ratio of 2.5 was found to distinguish clinically relevant stenoses with > 50 % diameter reduction from stenoses with < 50 % diameter reduction. The study supports that Vector Flow Imaging is applicable for evaluation of arterial stenoses based on velocity ratios.

Key words: Vector Flow Imaging, ultrasound, flow velocity estimation, angiography, velocity ratio, arteriosclerotic stenosis, peripheral arterial disease.

**Introduction**

Doppler ultrasound mapping is a morphologic and functional method providing information of vessel wall and hemodynamics commonly used for evaluation of peripheral arterial disease. Color and spectral Doppler can be used to localize and assess the severity of possible stenoses using the increase of blood flow velocity through the stenoses. The flow velocity correlates with lumen diameter, but due to interindividual variations of blood flow, velocity ratios i.e. the intrastenotic velocity divided by the prestenotic velocity, provide better estimates of the stenoses (Ranke, Creutzig, and Alexander 1992; Khan et al. 2011). Velocity ratios are calculated on the basis of peak systolic velocities, measured in the stenosis and in a proximal vessel segment with normal lumen. In previous studies, velocity ratios varying from 1.5 to 2.4 have been shown to distinguish < 50 % stenoses from > 50 % stenoses, where the stenosis degree was based on angiographic diameter reduction (Ranke, Creutzig, and Alexander 1992; Schlager et al. 2007; Khan et al. 2011; Baxter and Polak 1993; Flanigan et al. 2008). The conventional Doppler technique is angle-dependent and operator reliant, in particular in the presence of stenoses (Gill 1985; Lui et al. 2005). Operator errors can therefore lead to substantial deviations in peak velocity estimation, further aggravated by the fact that two flow velocities need to be estimated to provide a velocity ratio.

Digital Subtraction Angiography (DSA) is by tradition the golden standard for vessel analysis.

Besides a complete overview of the blood vessels for diagnostic purposes, it allows simultaneous endovascular therapy. However, DSA is invasive, associated with risks of both local and systemic complications, and exposes both patients and staff to ionizing radiation (Egglin et al. 1995). Moreover, traditional DSA is a two dimensional (2-D) image modality, limiting the stenosis assessment to the imaged projection plane.

To circumvent the angle dependency of conventional Doppler, the angle independent ultrasound technique Vector Flow Imaging was proposed by (J A Jensen and Munk 1998). Vector Flow Imaging provides simultaneously the axial and transverse velocity components of the blood flow. The technique creates a double oscillating pulse-echo field by manipulating the apodization function during receive beamforming. A conventional ultrasound pulse for flow estimation is transmitted, and the received echoes are beamformed to yield three beams in parallel. One uses conventional beamforming for estimating the axial velocity, and the other two beams are used for estimating the transverse velocity component. By combining the velocity components along the two axes, 2-D vector velocities are obtained. Vector Flow Imaging is currently only operational with linear arrays and has a tissue penetration of 5 centimeters. It is therefore only applicable for use on superficial blood vessels. The technique is described further by J A Jensen and Munk 1998; J. Udesen and Jensen 2006; Jesper Udesen et al. 2007, and the clinical use by P. M. Hansen et al. 2011; Pedersen et al. 2012; K. L. Hansen et al. 2013;  P.M. Hansen et al. 2014; K. L. Hansen et al. 2014.

The aim of the study was to investigate Vector Flow Imaging as a technique for quantitative assessment of peripheral arterial disease. The technique was tested in a small population of patients with peripheral arterial disease and clinical indication of stenosis in the superficial femoral artery (SFA). The hypothesis is that velocity ratios derived from Vector Flow Imaging can be used to distinguish significant stenoses (> 50 % diameter reduction) from non-significant stenoses when compared to DSA.


**Materials and Methods**

*Patients*

Thirty consecutive patients scheduled for DSA of the lower extremities due to suspected peripheral arterial disease were scanned during a one-month period. Patients were eligible for inclusion

if they had one or more previously untreated arteriosclerotic lesions (stenosis or plaque) in the SFA. Nineteen patients with previous by-pass surgery, endovascular surgery, occlusion, no lesions (judged by both ultrasound and DSA), or widespread arteriosclerotic disease according to The Trans-Atlantic Inter-Society Consensus Document on Management of Peripheral Arterial Disease (TASC II, (Norgren et al. 2007)) were excluded. Eleven of the 30 patients were included providing a total of 16 lesions consisting of 13 stenoses and three plaques.

Written informed consent was obtained. The local Ethics Committee waived approval, since ultrasound scanning of arteriosclerotic extremities is considered a routine procedure (protocol number: H-4-2013-001).

*Scan setup*

A commercial scanner (UltraView 800, BK Medical, Herlev, Denmark) was used with a linear transducer with a center frequency of 9 MHz (8670, BK Medical, Herlev, Denmark).

All patients were ultrasound scanned in the angiography room just prior to the DSA, and all were scanned in a supine position after at least 15 minutes of rest. Due to the limited penetration of Vector Flow Imaging, the SFA was chosen for scanning. The patients were scanned from the bifurcation of the common femoral artery to the point where the SFA enters the adductor canal. The SFA was scanned both in the transversal and longitudinal plane, and when turbulent/disturbed flow was detected with Vector Flow Imaging, a longitudinal recording of 15 seconds length was made. The recording contained flow both in the lesion and proximal/distal to the lesion. Turbulent/disturbed flow was defined as presence of vortices and/or suddenly occurring aliasing indicating increasing blood flow velocities (Fig. 1).
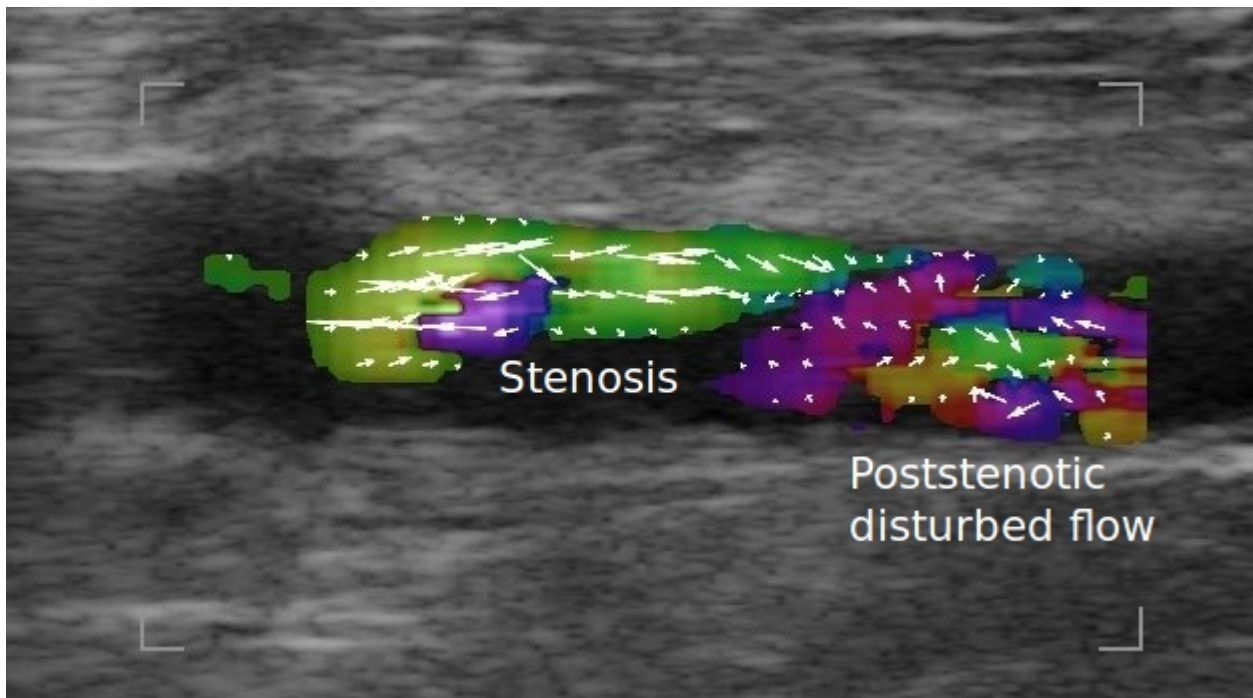
Figure 1: Scanning of a stenosis (patient 4) using Vector Flow Imaging. The arrows illustrate flow direction and velocity magnitude. The blood flows from left to right as indicated by the arrows in the green area. Aliasing indicating higher flow velocities is seen in the purple area to the left and poststenotic turbulence/disturbed flow is seen to the right. Notice the angle of insonation of 90º.

The color box is operated similar to color Doppler and was adjusted to cover all of the blood vessel including the vessel walls, and the pulse repetition frequency (PRF) was in each case adjusted to the level providing optimal filling of the vessel, even if aliasing still was present in peak systole. If the PRF was adjusted to the level where no aliasing was present, too much data containing the lower blood flow velocities would be neglected. Wall filter and color gain was also adjusted to the level providing optimal filling of the vessel without flow being visualized outside the vessel. All other settings remained in default mode. The angle of insonation was in all cases 70 - 90 degrees. When turbulent/disturbed flow was detected in the SFA, a marker was attached to the patient's thigh corresponding to the flow disturbance. In the subsequent DSA, the marker should then point directly towards the suspected flow disturbing lesion, ensuring matching ultrasound and angiographic recordings (Fig. 2).

Figure 2: DSA with marker indicating the stenosis (patient 7)

*Vector Flow Imaging*

Vector Flow Imaging is FDA-approved for clinical scanning. This approval does not include quantitative measurements using the approach, as FDA demands a large, quantitative study for such an approval. The investigations previously performed on a flow rig and in clinical studies indicate a negative bias around -10 % for velocity estimations (K. L. Hansen et al. 2013; Jesper Udesen et al. 2007). This is due to a bias in the estimation scheme, which can be compensated for in an optimized setup as demonstrated by Jørgen Arendt Jensen 2013. Such a scheme could be implemented in the commercial scanner. However, in this study determination of the exact velocities is not relevant, since the velocity estimations are only used to calculate velocity ratios and thus, the systematic error is left out of the estimation.

The scanner was set to record 15 seconds long sequences with Vector Flow Imaging at a frame rate of 15 frames per second, i.e. each sequence consists of 225 2-D vector velocity maps.

*Angiography*

An Infinix-i system (model INFX-8000V, Toshiba Medical Systems Corporation, Tochigi-ken, Japan) was used for the DSA. After local anesthesia an arterial puncture in the common femoral artery was performed followed by placement of an 11 cm long 5 French sheath into the vessel. A 4 or 5 French catheter was used when needed for contrast injections. DSA of the femoral arteries was performed using 2 frames/second and a 6-10 ml. contrast injection (Visipaque 270 mgI/ml). Routine anteroposterior images in two planes were recorded and subsequent measurements were performed on a standard workstation. The image yielding the most severe diameter reduction was used for calculation of the stenosis degree percentage. This was calculated using the smallest diameter in the stenosis versus the diameter in an adjacent normal arterial segment. A stenosis degree of 40 % corresponds to a vessel diameter reduced by 40 % compared to the normal vessel. Disturbed/turbulent flow detected with Vector Flow Imaging without corresponding diameter reduction in the DSA was defined as an arteriosclerotic plaque. Stenosis degree percentage was calculated independently of the ultrasound scanning by a radiologist not otherwise involved in the study.

*Velocity ratios calculated from Vector Flow Imaging*

The ultrasound recordings of the flow disturbances were analyzed off-line with in-house made MATLAB-scripts (MathWorks, Natick, MA, USA). From each recording three frames illustrating flow with the best possible filling of the vessel in both the lesioned and healthy part of the SFA were selected. Only frames without aliasing were chosen, since no reliable velocity estimate can be derived during aliasing. The velocity ratio was then calculated as the maximum velocity detected centrally in the lesioned segment divided by the maximum velocity detected centrally in the adjacent disease free segment. Both velocities were obtained from the same frame. The maximum velocities were located manually in each selected frame from the colored pixels of Vector Flow Imaging (Fig. 3). The final velocity ratio was calculated as the average of the velocity ratios from the three frames. If shadowing from a calcified plaque in the superficial vessel wall was present, maximum velocities were obtained from either side of the shadow, and the velocity obtained distal to the lesion was divided with the velocity obtained proximal to the lesion. Assuming a high level of arterial stiffness due to arteriosclerosis throughout the SFA, the relationship between the cross sectional areas in the diseased vs. the non-diseased vessel segments remains constant. The relationship between the velocities, i.e. the

velocity ratio, remains constant too, as long as the obtained velocities are from the same point of the cardiac cycle. This is ensured by the velocities being from the same frame, and it is therefore not necessary to obtain peak systolic velocities only. All velocity ratios were calculated blinded to the estimation of angiographic stenosis degree.
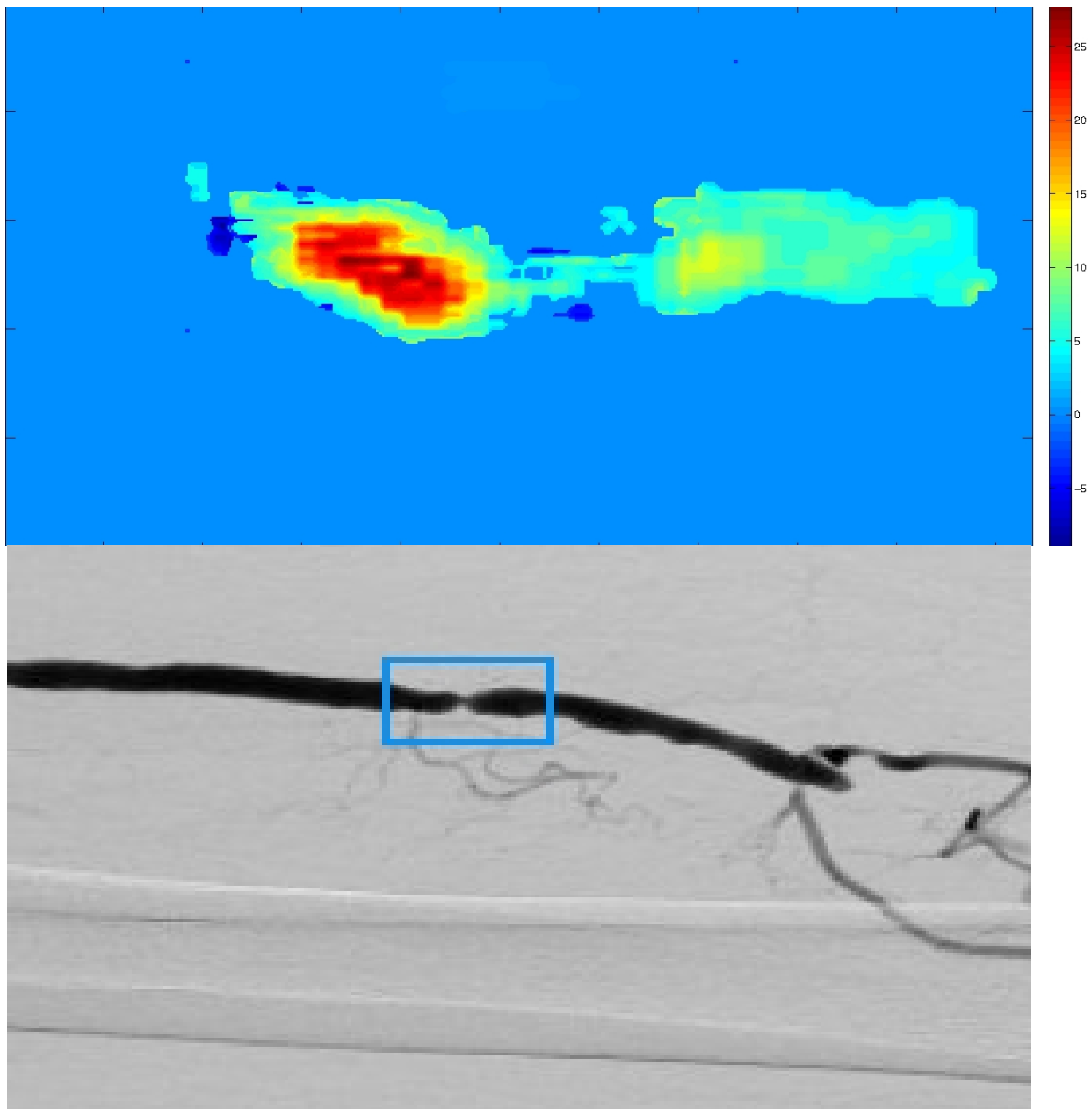


Figure 3: The top image shows the MATLAB processed Vector Flow Imaging recording of the stenosis illustrated by the DSA in the lower image (patient 3). The blue box illustrates the part of the vessel shown in the

top image. Maximum velocities around 25 cm/s are detected in the red area and in the yellow area to the right velocities around 7 cm/s are detected. It appears that peak velocities are detected immediately proximal to the stenosis and not in the stenosis. Possible calcified plaques in the vessel wall disturb the signal, or maybe the angle of insonation is not right for illustrating flow in the most stenotic part of the vessel. The marker is not visible in this projection.

*Statistical analysis*

Correlation of average velocity ratios and angiographic stenosis degree was estimated by nonlinear regression analysis. The correlation coefficient *r* and the velocity ratio corresponding to a 50 % stenosis were calculated. Stenoses > 50 % and < 50 % were treated as two different groups, and mean velocity ratios including standard deviations were calculated for each group and compared. An unpaired t-test was performed and $p < 0.05$ was considered significant. All calculations were performed both with and without outliers. All statistical calculations were performed in LibreOffice Calc.

**Results**

All calculated velocity ratios, the average velocity ratio and the angiographic stenosis degree (expressed as percentage reduction) of each lesion are shown in Table 1. Three lesions are outliers. Patient 6, lesion 1, has a velocity ratio of 2.1 and a stenosis degree of 33 %. Patient 8 has a velocity ratio of 2.5 and a stenosis degree of 11 %, and finally patient 11 with a velocity ratio of 1 and a stenosis degree of 67 %. In the case of patient 6 and 8, the error could be caused by an angiographic underestimation of the stenosis, and for patient 11 the error could be caused by flaws in the scanning process or errors in the calculation of the velocity ratio. However, no certain factors separate these three patients from the rest. The correlation between the average velocity ratios and stenosis degrees is illustrated in figure 4 with and without the outliers. A correlation coefficient *r* of 0.45 and 0.75 was calculated, respectively. The regression equations are seen in figure 4 as well. Without the outliers, the velocity ratio corresponding to a 50 % stenosis is 2.0, and with all lesions included the velocity ratio is 2.5.

With patient 6, lesion 1, patient 8 and patient 11 excluded from the analysis, the mean velocity ratio (based on the average velocity ratios) for an angiographic stenosis degree < 50 % is 1.2 (standard deviation (SD) 0.17) and mean velocity ratio for an angiographic stenosis degree > 50 % is 2.5 (SD

0.34). The difference between the two groups is significant ($p < 0.01$). With all patients included in the analysis the mean velocity ratios for stenosis degrees < 50 % and > 50 % are 1.4 (SD 0.49) and 2.2 (SD 0.72), respectively. The difference is still significant ($p = 0.02$).

| Patient number | Lesion number | Lesion type | Velocity Ratios | Average Velocity Ratio | Degree of Stenosis (%) |
|---|---|---|---|---|---|
| 1 | 1 | Stenosis | 2.1, 1.9, 2.7 | 2.2 | 78 |
|   | 2 | Plaque | 1.1, 0.9, 1.2 | 1.1 | 0 |
| 2 | 1 | Plaque | 0.9, 1, 1 | 1 | 0 |
|   | 2 | Stenosis | 1.2, 1.2, 1.3 | 1.2 | 19 |
| 3 | 1 | Stenosis | 2.6, 3.6, 2.6 | 2.9 | 68 |
| 4 | 1 | Stenosis | 1.6, 4.4, 1.7 | 2.6 | 65 |
| 5 | 1 | Stenosis | 1.2, 1, 1.3 | 1.2 | 37 |
|   | 2 | Stenosis | 0.7, 0.8, 1.3 | 0.9 | 31 |
| 6 | 1 | Stenosis | 2.4, 1.8, 2.1 | 2.1 | 33 |
|   | 2 | Stenosis | 1.3, 1.6, 1.5 | 1.5 | 15 |
|   | 3 | Stenosis | 1, 1.3, 1.2 | 1.2 | 15 |
| 7 | 1 | Stenosis | 2.1, 2.4, 2.1 | 2.2 | 62 |
| 8 | 1 | Stenosis | 1.9, 2.9, 2.8 | 2.5 | 11 |
| 9 | 1 | Stenosis | 1.2, 1, 1.1 | 1.1 | 47 |
| 10 | 1 | Plaque | 1.3, 1.3, 1.2 | 1.3 | 0 |
| 11 | 1 | Stenosis | 1, 1.1, 1 | 1 | 67 |

Table 1: Velocity ratios based on Vector Flow Imaging recordings from each individual lesion and coherent stenosis degree based on angiographic diameter reduction. A plaque is defined as a flow disturbing lesion with no corresponding angiographic diameter reduction.

f(x) = 30.59 ln(x) + 22.09

## All data



f(x) = 54.01 ln(x) + 13.73
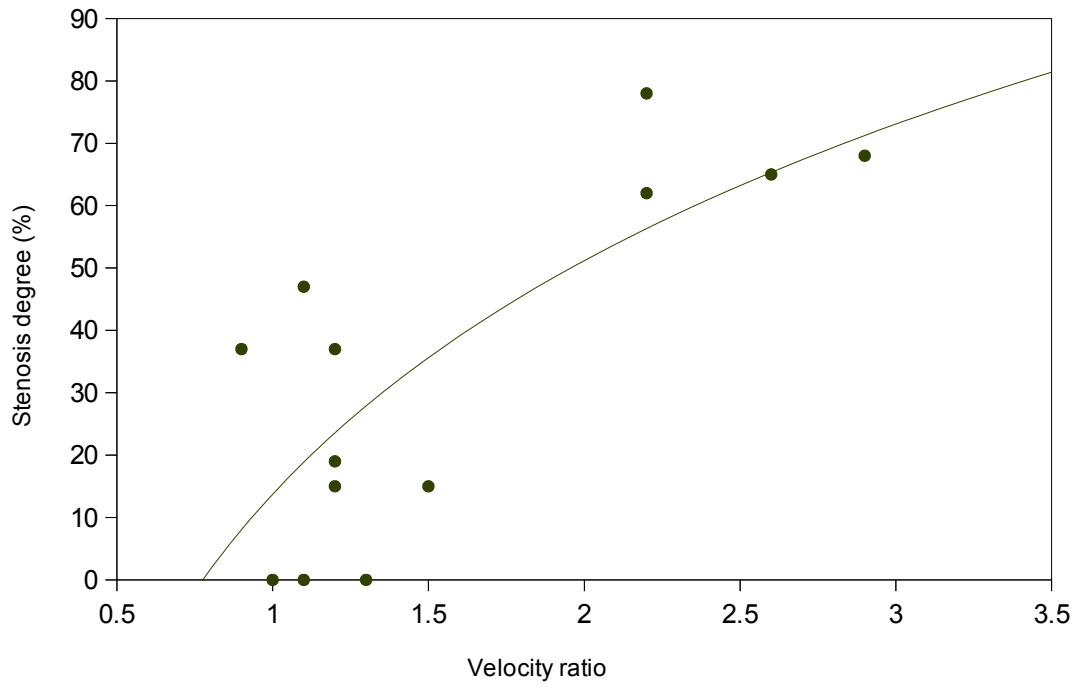
## Without outliers



11
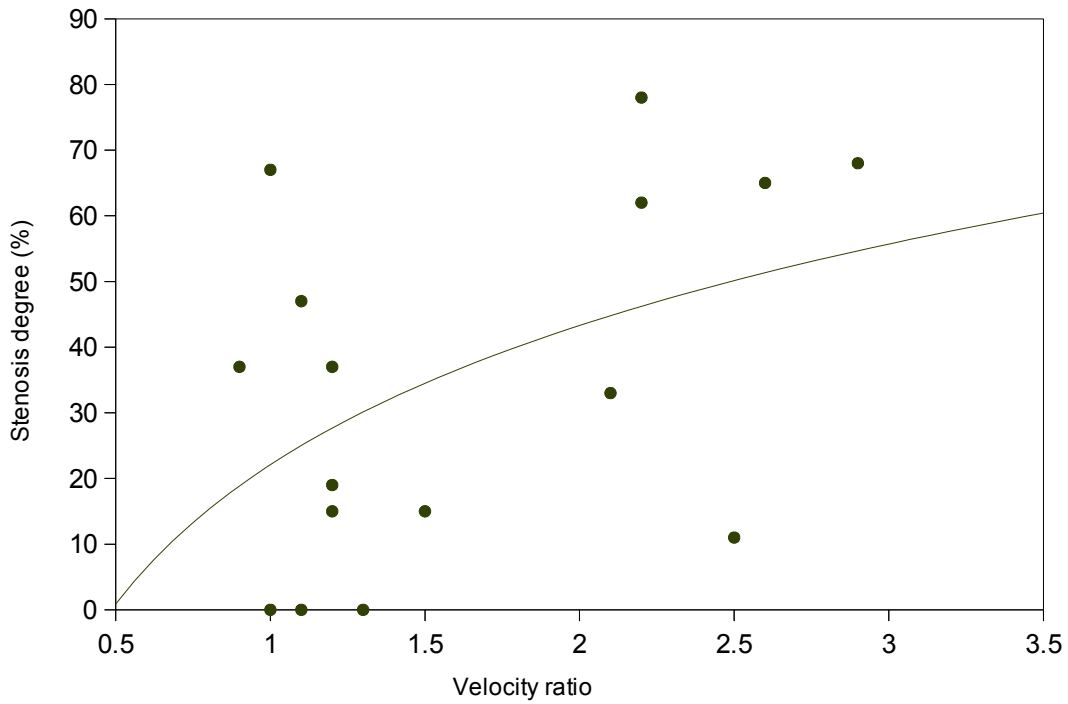
Figure 4: Correlation between calculated average velocity ratios and angiographic diameter reduction expressed as stenosis percentage. The correlation has been illustrated for all data (top) and with the three outliers omitted (bottom). Notice that the ideal correlation line starts in (1, 0) with a velocity ratio of 1 when no stenosis is present. The regression equations are seen in the top of each plot.

**Discussion**

To the authors' knowledge, this study is the first to characterize and grade arterial stenoses in the superficial femoral artery using vector velocity ultrasound. The obtained velocity ratios of 2.0 (without outliers) and 2.5 (all data) corresponding to a 50 % stenosis match previous larger studies based on spectral Doppler as mentioned in the introduction, and the difference between the two patient groups (< 50 % and > 50 % stenosis) is statistically significant, both with and without the outliers. The correlation coefficient for all data ($r = 0.45$) is modest, but when the outliers are omitted, a strong correlation ($r = 0.75$) is seen. The hypothesis of the study is therefore partly accepted.

Use of Vector Flow Imaging is more intuitive than conventional Doppler and provides major amounts of quantitative blood flow information to help assess the flow conditions and diagnose the causative factors in the vessels. This can potentially help physicians diagnose peripheral arterial disease more effective, spare patients for potential unnecessary examinations, and save time in the daily clinical practice. Further development of Vector Flow Imaging is, however, necessary, before the technique provides all results in real-time during the scanning procedure, and the full potential is exploited.

The use of Vector Flow Imaging in this study is among other things limited by the manual acquisition of all velocities. This limits the number of velocity measurements used for each velocity ratio calculation and makes the process more vulnerable for erroneous measurements. This could be one reason for the three outliers, and the process should be automatized in future studies. The velocity ratios were calculated by one radiologist only, and inter-observer variation was therefore not found.

Vector Flow Imaging is dependent on the PRF, and in a stenotic artery with major velocity fluctuations between the normally calibrated segments and the stenotic segments (the velocity increases more than five times when the stenosis exceeds 80 % (Ranke, Creutzig, and Alexander 1992)), numerous frames will be affected by either aliasing when the PRF is set too low or no velocity information when the PRF is set too high. This further limits the number of usable frames from each

Vector Flow Imaging recording. The lack of automation leads to a spatial problem as well. To ensure that the velocities measured with Vector Flow Imaging are from the same point in the cardiac cycle (and therefore comparable) the velocities must be obtained from the same frame, limiting the size of the region of interest to the width of the transducer (approximately 4 cm). When using conventional Doppler the peak systolic velocity is automatically detected, and velocities obtained in either end of an artery are therefore directly comparable. Another limitation of ultrasonic grading of stenoses is the 2-D visualization of the region of interest, which can affect the positioning of the transducer relative to the artery, and in turn affect the velocity estimation (J. Jensen et al. 2014), but this limitation of course applies to both Vector Flow Imaging and conventional spectral Doppler.

The major advantage of Vector Flow Imaging in this study is the generation of a complete map of velocities for each single frame. It is therefore not necessary to assume where in the stenotic vessel the peak velocities are found as is would be with spectral Doppler when positioning the range gate. All detected velocities are illustrated immediately independently of the angle of insonation. The SFA is a superficial vessel running parallel to the skin surface. In conventional Doppler, the transducer is often slightly tilted on the skin to ensure an acceptable angle of insonation of the vessel, with the risk of altering the investigated flow because of pressure from the transducer. This is less likely with the angle independent Vector Flow Imaging as reliable estimates are obtained at all angles of insonation, including 90°.

DSA is the gold standard for diagnosing and grading peripheral arterial disease, but is, just as ultrasound, a 2-D visualization of the vessels, and underestimation of stenoses can therefore occur, if the smallest diameter of the vessel is not visible in the present angiographic projection. The DSA is occasionally supplemented by oblique projections if any doubt about a stenosis is raised, but that is no guarantee for a projection illustrating the most severe stenosis degree. This fact could be the reason for the two first outliers.


**Conclusion**

Arteriosclerotic stenoses and plaques in the superficial femoral artery have for the first time been characterized using velocity ratios obtained with a commercially available vector velocity ultrasound technique. A moderate correlation ($r = 0.45$) was found between the DSA derived stenosis degrees and the velocity ratios obtained with Vector Flow Imaging, and a velocity ratio of 2.5 has been

shown to distinguish between stenoses over and under 50 % angiographic diameter reduction. If three outliers are omitted, a strong correlation ($r = 0.75$) is seen, and a velocity ratio of 2.0 is shown to distinguish stenoses over 50 % from stenoses less than 50 %. The technique has potential to be used for monitoring of arteriosclerotic patients and to support the indication of referral to DSA. The patient number in this study is small, but the results are in line with previous larger studies. Future studies including more patients and determination of inter-observer variability of Vector Flow Imaging will hopefully support the use of the technique.

# References

Baxter, G. M., and J. F. Polak. 1993. "Lower Limb Colour Flow Imaging: A Comparison with Ankle: Brachial Measurements and Angiography." *Clinical Radiology* 47 (2): 91–95. doi:10.1016/S0009-9260(05)81179-1.

Egglin, Thomas K. P., Paul V. O'Moore, Alvan R. Feinstein, and Arthur C. Waltman. 1995. "Complications of Peripheral arteriography:A New System to Identify Patients at Increased Risk." *Journal of Vascular Surgery* 22 (6): 787–94. doi:10.1016/S0741-5214(95)70070-6.

Flanigan, D. Preston, Jeffrey L. Ballard, Doreen Robinson, Mark Galliano, Gina Blecker, and Timothy R. S. Harward. 2008. "Duplex Ultrasound of the Superficial Femoral Artery Is a Better Screening Tool than Ankle-Brachial Index to Identify at Risk Patients with Lower Extremity Atherosclerosis." *Journal of Vascular Surgery* 47 (4): 789–93. doi:10.1016/j.jvs.2007.11.023.

Gill, Robert W. 1985. "Measurement of Blood Flow by Ultrasound: Accuracy and Sources of Error." *Ultrasound in Medicine & Biology* 11 (4): 625–41. doi:10.1016/0301-5629(85)90035-3.

Hansen, Kristoffer Lindskov, Hasse Møller-Sørensen, Mads Møller Pedersen, Peter Møller Hansen, Jesper Kjaergaard, Jens Teglgaard Lund, Jens Christian Nilsson, Jørgen Arendt Jensen, and Michael Bachmann Nielsen. 2014. "First Report on Intraoperative Vector Flow Imaging of the Heart among Patients with Healthy and Diseased Aortic Valves." *Ultrasonics*. Accessed September 6. doi:10.1016/j.ultras.2014.07.015.

Hansen, Kristoffer Lindskov, Mads Møller Pedersen, Hasse Møller-Sørensen, Jesper Kjaergaard, Jens Christian Nilsson, Jens Teglgaard Lund, Jørgen Arendt Jensen, and Michael Bachmann Nielsen. 2013. "Intraoperative Cardiac Ultrasound Examination Using Vector Flow Imaging." *Ultrasonic Imaging* 35 (4): 318–32. doi:10.1177/0161734613505552.

Hansen, Peter Møller, Jacob Bjerring Olesen, Michael Johannes Pihl, Theis Lange, Søren T. Heerwagen, Mads Møller Pedersen, Marianne Rix, Lars Lönn, Jørgen Arendt Jensen, and Michael Bachmann Nielsen. 2014. "Volume Flow In Arteriovenous Fistulas Using Vector Velocity Ultrasound." *Accepted for Publication*.

Hansen, Peter M, Mads M Pedersen, Kristoffer L Hansen, Michael Bachmann Nielsen, and Jørgen A Jensen. 2011. "New Technology - Demonstration of a Vector Velocity Technique." *Ultraschall in Der Medizin (Stuttgart, Germany: 1980)* 32 (2): 213–15. doi:10.1055/s-0031-1274628.

Jensen, J A, and P Munk. 1998. "A New Method for Estimation of Velocity Vectors." *IEEE Transactions on Ultrasonics, Ferroelectrics, and Frequency Control* 45 (3): 837–51. doi:10.1109/58.677749.

Jensen, Jonas, Jacob Bjerring Olesen, Peter Møller Hansen, Michael Bachmann Nielsen, and Jørgen Arendt Jensen. 2014. "In Vivo Evaluation of an Angle Independent Flow Rate Estimator." *Proceedings of IEEE International Ultrasonics Symposium*.

Jensen, Jørgen Arendt. 2013. "Optimization of Transverse Oscillating Fields for Vector Velocity Estimation with Convex Arrays." *Proceedings of IEEE International Ultrasonics Symposium*, 1753–56. doi:10.1109/ULTSYM.2013.0447.

Khan, Sikandar Z., Muhammad A. Khan, Benjamin Bradley, Rajeev Dayal, James F. McKinsey, and Nicholas J. Morrissey. 2011. "Utility of Duplex Ultrasound in Detecting and Grading de Novo Femoropopliteal Lesions." *Journal of Vascular Surgery* 54 (4): 1067–73. doi:10.1016/j.jvs.2011.03.282.

Lui, Elaine Y L, Aaron H Steinman, Richard S C Cobbold, and K Wayne Johnston. 2005. "Human Factors as a Source of Error in Peak Doppler Velocity Measurement." *Journal of Vascular*

*Surgery* 42 (5): 972–79. doi:10.1016/j.jvs.2005.07.014.

Norgren, L., W. R. Hiatt, J. A. Dormandy, M. R. Nehler, K. A. Harris, F. G. R. Fowkes, and on behalf of the TASC II Working Group. 2007. "Inter-Society Consensus for the Management of Peripheral Arterial Disease (TASC II)." *Journal of Vascular Surgery* 45 (1): S5–67. doi:10.1016/j.jvs.2006.12.037.

Pedersen, Mads Møller, Michael Johannes Pihl, Per Haugaard, Jens Munk Hansen, Kristoffer Lindskov Hansen, Michael Bachmann Nielsen, and Jørgen Arendt Jensen. 2012. "Comparison of Real-Time In Vivo Spectral and Vector Velocity Estimation." *Ultrasound in Medicine & Biology* 38 (1): 145–51. doi:10.1016/j.ultrasmedbio.2011.10.003.

Ranke, Carsten, Andreas Creutzig, and Klaus Alexander. 1992. "Duplex Scanning of the Peripheral Arteries: Correlation of the Peak Velocity Ratio with Angiographic Diameter Reduction." *Ultrasound in Medicine & Biology* 18 (5): 433–40. doi:10.1016/0301-5629(92)90082-L.

Schlager, Oliver, Marcel Francesconi, Markus Haumer, Petra Dick, Schila Sabeti, Jasmin Amighi, Wolfgang Mlekusch, Renate Koppensteiner, Erich Minar, and Martin Schillinger. 2007. "Duplex Sonography Versus Angiography for Assessment of Femoropopliteal Arterial Disease in A 'Real-World' Setting." *Journal of Endovascular Therapy* 14 (4): 452–59. doi:10.1583/1545-1550(2007)14[452:DSVAFA]2.0.CO;2.

Udesen, Jesper, Michael Bachmann Nielsen, Kristina Rue Nielsen, and Jorgen Arendt Jensen. 2007. "Examples of In Vivo Blood Vector Velocity Estimation." *Ultrasound in Medicine & Biology* 33 (4): 541–48. doi:10.1016/j.ultrasmedbio.2006.10.014.

Udesen, J., and J.A. Jensen. 2006. "Investigation of Transverse Oscillation Method." *IEEE Transactions on Ultrasonics, Ferroelectrics and Frequency Control* 53 (5): 959–71. doi:10.1109/TUFFC.2006.1632686.